UNIVERSITY OF OKLAHOMA

GRADUATE COLLEGE

INDUSTRIAL BYPRODUCTS AS A TREATMENT FOR BIORETENTION UNDERDRAIN EFFLUENT: A BENCHTOP PROOF OF CONCEPT

A THESIS

SUBMITTED TO THE GRADUATE FACULTY

in partial fulfillment of the requirements for the

Degree of

MASTER OF SCIENCE

By

KYLE MATTHEW MATTINGLY

Norman, Oklahoma

2022

INDUSTRIAL BYPRODUCTS AS A TREATMENT FOR BIORETENTION UNDERDRAIN EFFLUENT: A BENCHTOP PROOF OF CONCEPT

A THESIS APPROVED FOR THE
SCHOOL OF GEOSCIENCES

BY THE COMMITTEE CONSISTING OF

Dr. Kato T. Dee, Co-Chair
Dr. Jason Vogel, Co-Chair
Dr. Caitlin Hodges

Dedication

I would like to dedicate this thesis to those in my life who have encouraged me to pursue my goals and to persevere through all the challenges.

First to Becky and Jade, for serving as the example and helping me chart the course towards graduate school. I'm not sure how I got so lucky to have met you both and it's with no doubt in my mind that I would not be the scientist I am today if it weren't for you two. Long live the quad!

To my parents. I know my academic and professional pursuits have been a far stray away from the world you both know of instructional education and music. Despite my pursuits being uncharted territory for you both, I always felt supported in my ambitions and always knew I could achieve anything I wanted if by nothing else but by your encouragement and support alone.

And finally, to Juan, my bubby. It takes a special kind of person to put up with me in general, but it takes a special kind of person to put up with me when I'm at maximum capacity. The nonstop support you've shown me over this two year journey has given me the space to achieve something I've always dreamed of. You've cooked. You've cleaned. You've baked. You've hugged. You've consoled. You've poured yourself out time and time again to help me achieve my goals. I'm not sure I can put into words what that has meant to me, so all I can do is support you in return so that you can aim high and achieve.

I love you all, and from the deepest depths of my heart, thank you.

Contents

Abstract xvii

1 Introduction 1

1.1 Pollutants 4

1.1.1 Neonicotinoid Pesticides 4

1.1.2 Metals 11

1.1.3 Phosphorus 18

1.2 Treatment Media 21

1.2.1 Fly Ash 21

1.2.2 Steel Slag 25

1.2.3 Biochar 30

2 Methods and Materials 37

2.1 Methods 37

2.1.1 Synthetic Stormwater 37

2.1.1.1 Nutrients and General Rainwater Chemistry 38

2.1.1.2 Metals 39

2.1.1.3 Neonicotinoids 40

2.1.1.4 pH 41

2.2 Materials: Industrial Byproducts 41

2.2.1.1 Aggregated Fly Ash 44
2.2.1.2 Steel Slag 45
2.2.1.3 Biochar 46
2.2.2 Vertical Columns 47
2.2.3 Horizontal Columns 49
2.2.4 Sample Preparation and Analysis 51
2.2.4.1 General Chemistry 51
2.2.4.2 Metals 52
2.2.4.3 Phosphorus 52
2.2.4.4 Neonicotinoids 52
2.3 Data Analysis 53
2.3.1 Influent-Effluent Ratio Analysis 53
2.3.2 Modeling Results 54
2.3.3 Statistical Analysis 56
2.3.4 Mass Removal Rate Analysis 57
2.4 Quality Assurance/Quality Control (QA/QC) 58
2.5 General Contaminant Removal Mechanisms 60
3 Results 61
3.1 Influent 63
3.2 QA/QC 69

3.3 Vertical Columns 69
3.3.1 General Chemistry 70
3.3.2 Metals 73
3.3.2.1 Aluminum (Al) 73
3.3.2.2 Arsenic (As) 75
3.3.2.3 Beryllium (Be) 77
3.3.2.4 Manganese (Mn) 79
3.3.3 Neonicotinoids 81
3.3.3.1 Acetamiprid 81
3.3.3.2 Dinotefuran 84
3.3.3.3 Imidacloprid 86
3.3.4 Phosphorus 88
3.4 Horizontal Columns 90
3.4.1 General Chemistry 90
3.4.2 Metals 94
3.4.2.1 Arsenic (As) 94
3.4.3 Neonicotinoids 97
3.4.4 Phosphorus (P) 101
3.4.5 Mass Removal Rate 103
3.4.5.1 Arsenic 103

3.4.5.2 Phosphorus 109

4 Discussion 115

4.1 Media Dissolution Impacts on pH and Specific Conductivity 115

4.2 Leaching 116

4.3 Below Detection Limits (BDLs) and Control-Experimental Separation 117

4.4 Metals 118

4.5 Phosphorus 121

4.6 Neonicotinoids 122

4.7 Mass Removal Rate 124

5 Considerations 127

5.1 Gompertz Function and Influent-Effluent Graphs 127

5.2 Study Design: Proof of Concept 129

5.3 Environmental Safety Considerations 130

6 Future Studies 132

7 Conclusions 134

8 Acknowledgements 137

9 Sources 138

10 Appendix 162

Table of Figures

Figure 3-1 Photograph of vertical column setup. Pictured from left to right is the sample bottles (collection point), vertical columns containing the media of interest, the peristaltic pumps, and the synthetic stormwater influent tank. 49

Figure 3-2 Photograph of the horizontal column setup. Pictured from left to right are the experimental columns, peristaltic pumps, and the synthetic stormwater influent tank. Experimental columns each demonstrate 6 inches of ponding in the upper portion of the vertical tube followed by 12 inches of bioretention simulation sand, a 90 degree elbow, 12 inches of a media packed tube, and lastly a cap with a 1/16 inch orifice outlet. 51

Figure 4-1 Influent pH in vertical column experiments 64

Figure 4-2 Influent pH in horizontal column experiments 65

Figure 4-3 Influent specific conductivity in vertical column experiments (run 2 only due to calibration issues during run 1) 67

Figure 4-4 Influent specific conductivity in horizontal column experiments 68

Figure 4-5 Effluent pH results from vertical column experiments 71

Figure 4-6 Effluent specific conductivity results from vertical column experiments (run 2 only due to calibration issues in run 1) 72

Figure 4-7 Dissolved Al^{+3} removal in vertical column experiments as demonstrated by the influent-effluent ratio as defined by effluent concentration (C_{eff}) divided by influent concentration (C_{in}) and plotted against pore volumes passed. Aggregated fly ash and steel slag is not shown due to Al^{+3} leaching which places IE ratio values outside the range of 0.0 – 2.0. 74

Figure 4-8 Dissolved As^{+5} removal in vertical column experiments as demonstrated by the influent-effluent ratio as defined by effluent concentration (C_{eff}) divided by influent concentration (C_{in}) and plotted against pore volumes passed. 76
Figure 4-9 Be^{+2} removal in vertical column experiments as demonstrated by the influent-effluent ratio as defined by effluent concentration (C_{eff}) divided by influent concentration (C_{in}) and plotted against pore volumes passed. 78
Figure 4-10 Mn^{+2} removal in vertical column experiments as demonstrated by the influent-effluent ratio as defined by effluent concentration (C_{eff}) divided by influent concentration (C_{in}) and plotted against pore volumes passed. 80
Figure 4-11 Acetamiprid removal in vertical column experiments as demonstrated by the influent-effluent ratio as defined by effluent concentration (C_{eff}) divided by influent concentration (C_{in}) and plotted against pore volumes passed. 83
Figure 4-12 Dinotefuran removal in vertical column experiments as demonstrated by the influent-effluent ratio as defined by effluent concentration (C_{eff}) divided by influent concentration (C_{in}) and plotted against pore volumes passed. 85
Figure 4-13 Imidacloprid removal in vertical column experiments as demonstrated by the influent-effluent ratio as defined by effluent concentration (C_{eff}) divided by influent concentration (C_{in}) and plotted against pore volumes passed. 87
Figure 4-14 Phosphorus removal in vertical column experiments as demonstrated by the influent-effluent ratio as defined by effluent concentration (C_{eff}) divided by influent concentration (C_{in}) and plotted against pore volumes passed. 89
Figure 4-15 Effluent pH results from horizontal column experiments. 92
Figure 4-16 Effluent specific conductivity results in horizontal column experiments....93

Figure 4-17 Dissolved As^{+5} removal in horizontal column experiments as demonstrated by the influent-effluent ratio as defined by effluent concentration (C_{eff}) divided by influent concentration (C_{in}) and plotted against volume passed. 96
Figure 4-18 Acetamiprid removal in horizontal column experiments as demonstrated by the influent-effluent ratio as defined by effluent concentration (C_{eff}) divided by influent concentration (C_{in}) and plotted against volume passed. 98
Figure 4-19 Dinotefuran removal in horizontal column experiments as demonstrated by the influent-effluent ratio as defined by effluent concentration (C_{eff}) divided by influent concentration (C_{in}) and plotted against volume passed. 99
Figure 4-20 Imidacloprid removal in horizontal column experiments as demonstrated by the influent-effluent ratio as defined by effluent concentration (C_{eff}) divided by influent concentration (C_{in}) and plotted against volume passed. 100
Figure 4-21 Phosphorus removal in horizontal column experiments as demonstrated by the influent-effluent ratio as defined by effluent concentration (C_{eff}) divided by influent concentration (C_{in}) and plotted against volume passed. 102
Figure 4-22 Comparison of column orientation on the mass removal rate (MRR) of As^{+5} per media volume (MV) of small steel slag against cumulative As^{+5} input. 104
Figure 4-23 Comparison of column orientation on the mass removal rate (MRR) of As^{+5} per media volume (MV) of small aggregated fly ash against cumulative As^{+5} input. 106
Figure 4-24 Comparison of column orientation on the mass removal rate (MRR) of As^{+5} per media volume (MV) of small biochar against cumulative As^{+5} input. 108
Figure 4-25 Comparison of column orientation on the mass removal rate (MRR) of P per media volume (MV) of small steel slag against cumulative P input. 110

Figure 4-26 Comparison of column orientation on the mass removal rate (MRR) of P per media volume (MV) of small aggregated fly ash against cumulative P input. 112
Figure 4-27 Comparison of column orientation on the mass removal rate (MRR) of P per media volume (MV) of small biochar against cumulative P input. 114

Table of Tables

Table 1-1 Soil sorptive coefficients (log Koc) values for three subspecies of neonicotinoids which are the focus of this study. 6

Table 1-2 Summary of acute and/or chronic values suggested for aquatic neonicotinoids (amended from Morrissey et al., 2015 and US EPA (2015a)). 9

Table 1-3 Median influent and effluent values for metals in various BMP devices (grass swale, infiltration basin, percolation trench, bioretention, high rate biofiltration, and multi-chambered treatment train) for available studies nationwide. (BMP Statistical Analysis Tool, n.d.) 16

Table 1-4 EPA National Recommended Aquatic Life Criteria for freshwater (US EPA, 2015b). 17

Table 1-5 Selected literature of heavy metal removal capacities of fly ash. **Error! Bookmark not defined.**

Table 1-6 General composition of iron and steel slags (X. Zhang et al., 2020). 27

Table 1-7 Comparison of biochar and activated carbon properties and performance (Mohanty et al., 2018). 36

Table 2-1 List of basic rainwater chemistry and chemicals used to create a synthetic rainwater (Ricci et al., 2010). 38

Table 2-2 Target metals concentrations in the synthetic stormwater. 40

Table 2-3 Composition of media used in this study. Fly ash is converted from % metal-oxide to % metal composition. Biochar is converted from mass/mass to % composition. BDL refers to a value being reported below the detection limit. 43

Table 2-4 - Composition of the fly ash used in this study as reported by W. Zhang et al. (2008). 45

Table 2-5 Elemental composition of the steel slag used in this study (Bowen, 2021). Elements measured at levels below the detection limits of the instrument are reported as BDL. 46
Table 2-6 Reported compositions of the biochar used in this study (J. Gaspard, personal communication, October 10, 2022) 47
Table 3-1 Categories of results. 1: results below detection limits or did not resemble a breakthrough curve, or were too scattered; 2: media had no effect either generally or compared to the control column; 3: the media leached the contaminant; 4: media/contaminant combination of interest ..62
Table 4-1 Media-contaminant-orientation combinations that yielded results below detection limit (BDL). 118
Table 10-1 Run and media combinations 162
Table 10-2 Sample collection information 163
Table 10-3 pH, specific conductivity, and temperature results. 167
Table 10-4 Dissolved metals sample results for Arsenic, beryllium, and calcium. All results in ug L^{-1-}.....170
Table 10-5 Dissolved metals sample results for cobalt, copper, iron, and potassium. All results in ug L^{-1-}.....174
Table 10-6 Dissolved metals sample results for magnesium, manganese, sodium, and nickel. All results in ug L^{-1} 178
Table 10-7 Dissolved metals sample results for lead, selenium, silica, and zinc. All results in ug L^{-1} 182
Table 10-8 Phosphorus sample results. All results in mg L^{-1} 186
Table 10-9 Neonicotinoid sample results. All results given in ug L^{-1}.....189

Table 10-10 Coefficient of variation (%) for metals samples. A mild variation exceedance is >10% and a substantial exceedance is >20%. 193
Table 10-11 Coefficient of variation (%) for phosphorus and all three neonicotinoids. A mild variation exceedance is >10% and a substantial exceedance is >20%. 195
Table 10-12 Contaminant front experiment results. Column initially saturated with DI water then an 11,000 μS cm^{-1} NaCl solution poured with 6 in. of ponding at the top of the bioretention simulation sand and effluent SC values measured. One pore volume was ~300 mL..... 196

Table of Equations

Equation 2-1 Phosphorus removal reactions in calcium rich materials (Scott & Penn, 2021).....28

Equation 3-1 Equation used for pore volume determination.....48

Equation 3-2 Influent - effluent ratio calculation 53

Equation 3-3 Simplified Gompertz function as defined by (Chu, 2020). 54

Equation 3-4 Rearranged Gompertz equation to determine volume at which media exhaustion occurs.....56

Equation 3-5 Mass removal rate calculation 58

Equation 5-1 Generalized dissolution reactions which contribute to solution pH increase. 115

Abstract

Around the world, stormwater is a frequent and growing source of contamination for waterbodies. Common sources of pollution include heavy metals such as, but not limited to aluminum (Al), arsenic (As), cadmium (Cd), cobalt (Co), copper (Cu), lead (Pb), manganese (Mn), nickel (Ni), selenium (Se), and zinc (Zn). Nutrients such as phosphorus (P) also pose a large risk to waterbodies. Neonicotinoid pesticides are the most commonly used pesticide in the United States and are of growing concern to waterbodies, aquatic life, and non-aquatic life. Low impact development (LID) structures such as bioretention have been effective in the management of stormwater pollutants for decades. More recently, areas for improvement in bioretention have been identified and a need for additional water quality improvements has been recognized. Industrial byproducts have been suggested as an augmentation to bioretention design as a way to provide low-cost water quality improvement while giving an otherwise disposed byproduct a second and sustainable use.

This study focused on using fly ash (a coal burning byproduct), steel slag (a steel smelting byproduct), and biochar (wood waste heated with little to no oxygen) in treating a complex synthetic stormwater. This proof of concept benchtop study looked at influent and effluent concentrations in flowthrough column studies for a suite of metals, phosphorus, and three selected neonicotinoids to identify which media yielded the best removal potential for the various contaminants. Columns were set up in two orientations, one vertical with constant flow and full saturation and another horizontal which included a bioretention simulation with head-driven flow which flowed into a treatment column filled with the experimental media.

Results showed that aggregated fly ash and steel slag yielded a noticeably higher pH, likely from the dissolution of different -oxide species into solution. This dissolution also contributed to

a noticeable increase in specific conductivity. These trends were observed for biochar as well but at noticeably lower magnitudes. In vertical columns, the small-sized fraction of steel slag proved to be the best to remove most contaminants from solution. Some exceptions existed where either the large-sized fraction of aggregated fly ash was more effective, or results were mixed. Removal is generally understood to be via sorption, however further studies would be required to confirm the mode of removal. Major cations such as Ca^{+2}, Na^{+}, Mg^{+2}, and K^{+} were generally leached from the media with aggregated fly ash and steel slag as the most common culprits due to their high composition of these elements. Because biochar posed a lesser leaching risk and showed comparable contaminant removal to aggregated fly ash, vertical column experiments suggest biochar as the next best treatment media behind small steel slag. Horizontal column experiments had the additional condition of results being compared to the removal rates of a bioretention simulation control column. Where the control failed to treat all three neonicotinoids, P, As^{+5}, and Na^{+}, the experimental columns containing the media of study proved to be effective treatments. Small steel slag again showed to be the best medium to remove As^{+5}, and P where biochar proved to yet again prevent meaningful major cation leaching and was a sink for Na and all three neonicotinoids. Depending on the contaminant of concern being treated, either biochar or small steel slag would be the standout options for bioretention effluent treatment.

Further studies are recommended to confirm the mechanism by which contaminants are removed, the stability of the removed contaminants to stay out of solution, and the environmental safety of deploying these media into the real world. Modeling is also recommended to help guide future studies by predicting the state and species of contaminants in solution and their likelihood to sorb to the experimental media or precipitate as a result of treatment.

1 Introduction

Stormwater is a common and increasing source of pollution to waterbodies worldwide. Increases in urbanization leads to reductions in permeable surfaces which leads to large quantities of water running off into receiving waterbodies. Additionally, the quality of stormwater is negatively impacted by urbanization. Amongst many others, roofs, cars, and roadway construction are prominent sources of heavy metal pollution to stormwater (Gunawardana et al., 2015; Kayhanian et al., 2012). The increased use of neonicotinoid pesticides over the last three decades has impacted invertebrate and increasingly so, vertebrate populations from the impacts of agricultural and urban runoff (Borsuah et al., 2020; Jeschke et al., 2011; Jeschke & Nauen, 2008; Morrissey et al., 2015). Additionally, both urban and agricultural uses of phosphorus-based fertilizers has created increasing concern for decades for its role in oversaturating waterbodies with nutrients, therefore leading to eutrophication and loss of aquatic life and beneficial uses (Davis et al., 2006; Lyngsie et al., 2014; Qin et al., 2018; Ulén et al., 2007). In terms of water quality, a "beneficial use" is often defined as "public and private water supply, fish and wildlife propogation, agriculture, primary body contact recreation (such as swimming), secondary body contact recreation (such as boating or fishing), navigation, and/or aesthetics" (*Water Quality Standards | Oklahoma Water Resources Board*, n.d.). This thesis will not go into depth on the many types and sources of stormwater pollutants, but rather rely on the evidence that stormwater pollution is widespread, highly dynamic, highly variable, and of increasing concern.

Despite the challenges, much work has been done in the field of low impact development (LID) to implement various best management practice (BMP) techniques such as, but not limited to, bioretention swales, pervious pavement, detention/retention ponds, infiltration basins, and green roofs. Bioretention swales (hereafter referred to as simply "bioretention" or "swales") have

been shown to improve water quality outcomes by capturing, retaining, treating, and slowly discharging stormwater back to the environment or stormwater infrastructure (Davis et al., 2006; Kandel et al., 2017; Paus et al., 2014; J. Vogel, personal communication, February 2022). Swales fundamentally consists of a soil containing 85-92% sand, 8-12% fines, and 0-5% organic material (J. Vogel, personal communication, February 2022). Also key to the success of bioretention is the addition of plants to assist in water and contaminant uptake and storage. This BMP is designed to receive stormwater from a designated impervious area and allow it to slowly dissipate either via seepage or to discharge more slowly to receiving streams or stormwater infrastructure. Meanwhile, natural processes such as settling, physical filtration, cation exchange, sorption, biological uptake, and pH buffering helps to improve water quality prior to flowing into a downstream waterbody (Davis et al., 2001, 2006). However, bioretention is not always comprehensive in its ability to remove all pollutants or effective enough to improve water quality to meet ambient water quality standards (*BMP Statistical Analysis Tool*, n.d.; Paus et al., 2014). Soil amendment studies have shown promising results for a variety of media such as fly ash (Cheung et al., 1994; Kandel et al., 2017; W. Zhang et al., 2008), wood chips (Ashoori et al., 2019; Trenouth & Gharabaghi, 2015), biochar (Ashoori et al., 2019; Cairns et al., 2022), various types of slag (Trenouth & Gharabaghi, 2015), and other metal-containing/metal-coated media (Trenouth & Gharabaghi, 2015) to assist in filling gaps in the performance of bioretention to meet water quality standards. While these amendments are encouraging, there are limitations to their application. All media have a limited lifespan in their ability to remove pollutants from stormwater due to the exhaustion of sorption/exchange sites or from the media itself dissolving to create complexes and precipitates or a combination of the two with precipitates coating the treatment media (Qin et al., 2018; W. Zhang et al., 2008). A solution suggested in this thesis is developing a permeable “sock” containing

treatment media which can be inserted in the underdrain of a bioretention swale and easily removed and replaced when exhausted. The objective of this study is to investigate the suitability of three different industrial byproducts to augment bioretention design and act as a water quality finisher. Results from this study will help to inform a scaled-up version including an underdrain sock design and to-scale bioretention design. Furthermore, this method has additional potential to serve as a retrofit to existing stormwater infrastructure where bioretention or other LID tools are cost prohibitive or infeasible.

The primary objective of this study was to investigate three media (aggregated fly ash, electric arc furnace steel slag, and biochar) and their ability to remove phosphorus, a series of trace metals, and neonicotinoid pesticides from a synthetic storm water (SSW). This was achieved by conducting a series of flow through column studies as suggested by Brown (2017) and by an original design. Brown (2017) developed an upward-flowing vertical column that is packed with a treatment medium. A contaminant-spiked solution is then created and flowed through the column to measure the medium's ability to remove the contaminant. This design is ideal because it minimizes variables by controlling velocity (6 mL min^{-1}), temperature (25˚C), and saturation (100%). The second design consists of a vertical constant head column filled with fine to medium sand as a proxy for bioretention media then an attached horizontal column packed with the media of interest and a 1/16 in. (0.16 cm) orifice. The second design was meant to serve as a laboratory proxy for the processes observed in a field-deployed bioretention swale. Samples were taken at the influent and effluent of each column to ensure a complete mass balance across the treatment media. Initial analysis was conducted by comparing the ratio of an individual contaminant at the influent and the effluent points such that a value of 1.0 represents no contaminant removal, 0.0 represents complete contaminant removal, and >1.0 represents contaminant leaching. Henceforth this will be

referred to as the IE ratio (influent-effluent ratio). Results from this study will help to better structure bioretention to achieve better and more thorough water quality outcomes.

1.1 Pollutants

The three pollutant groups were selected due to their growing or persistent concern to water and environmental managers (Dr. E. Rebek, personal communication, September 13, 2021). Each contaminant poses a threat to waterbody beneficial uses and the aquatic life therewithin across a variety of scales. As is discussed below, dangers include eutrophication of surface waters and acute and chronic impacts on aquatic or aquatic-dependent organisms, including humans The behavior of all contaminants are extremely variable and dynamic and will be highly dependent on environmental conditions.

1.1.1 Neonicotinoid Pesticides

Neonicotinoid pesticides are a class of nitroguanidine systematic insecticides that include six common sub-species: acetamiprid, clothianidin, dinotefuran, imidacloprid, thiacloprid, and thiamethoxam. The use of neonicotinoids grew in popularity in the 1990s as a soil and seed treatment due to their effectiveness against insecticide-intolerant pests and their ability to target invertebrate species with little to no effect to mammal and vertebrate species (Yamamoto et al., 1995). Acetamiprid, dinotefuran, and imidacloprid are all registered to treat sucking and chewing insects with applications including topical (for pets), on structures, on crops, or as seed treatments (*Imidacloprid Technical Fact Sheet*, n.d.; *Pesticide Fact Sheet: Acetamiprid*, 2002; *Pesticide Fact Sheet: Dinotefuran*, 2004). These pesticides are used on industrial and household scales to treat a variety of pests including (but not limited to) aphids, beetles, cockroaches, and fleas (*Imidacloprid*

Technical Fact Sheet, n.d.; *Pesticide Fact Sheet: Acetamiprid*, 2002; *Pesticide Fact Sheet: Dinotefuran*, 2004). One or more species of neonicotinoids are registered in over 120 countries and presently are the largest selling class of insecticide globally (Jeschke et al., 2011; Jeschke & Nauen, 2008). Despite their popularity, neonicotinoids possess properties that make them particularly susceptible to runoff as a result of rainfall or irrigation (Armbrust & Peeler, 2002). Water solubility and partitioning properties are particularly high (log K_{ow} ranging from -0.66 to 1.26) and soil adsorption is low (log K_{oc} ranging from 1.41 to 3.67) which not only promotes the aqueous transport of neonicotinoids away from applied sites to waterbodies, but it also promotes long term leaching and subsurface transport (Morrissey et al., 2015). The log K_{oc} values for three subspecies of neonicotinoids that are the focus of this study are shown in Table 1-1 below.

Table 1-1 Soil sorptive coefficients (log Koc) values for three subspecies of neonicotinoids which are the focus of this study.

Neonicotinoid	*Log K_{oc}*	*FOA Soil Mobility Classification*
Acetamiprid	2.3	Moderately Mobile
Dinotefuran	1.41	Mobile
Imidacloprid	2.19-2.90	Moderately Mobile

Soil persistence half-lives can range widely depending on a variety of environmental conditions but are generally on the scale of days to weeks. Degradation of the neonicotinoid molecule by water (water hydrolysis) largely does not occur in acidic to neutral waters, however, above pH 9, some species can hydrolyze with half-lives ranging from 2.9 days to greater than a year. Degradation of the neonicotinoid molecule by sunlight while in an aqueous solution (water photolysis) half-lives are especially shorter ranging from less than a day up to 63 days. Notably, acetamiprid has a water photolysis half-life of 34 days, dinotefuran of <2 days and imidacloprid of <1 day (Morrissey et al., 2015). Borsuah et al. (2020) and Morrissey et al. (2015) have published extensive reviews of the prevalence of neonicotinoids in surface waters around the world. Morrissey et al. (2015) conducted a review including 29 studies across 9 countries. Neonicotinoids were detected in "most" surface water samples including puddled water, irrigation channels, streams, rivers, and wetlands. The geometric mean of average surface water contamination was 0.13 µg L^{-1} (n = 19 studies) where geometric mean peak concentrations were 0.63 µg L^{-1} (n = 27 studies). Half of all available water monitoring studies showed detectable imidacloprid concentrations ranging from 0.001 to 320 µg L^{-1}. Other species of neonicotinoids were detected at similar rates with concentrations ranging from 0.008 to 44.1 µg L^{-1} for acetamiprid, 0.003 to 3.1

μg L^{-1} for clothianidin, and 0.001 to 225 μg L^{-1} for thiamethoxam. A study in Eastern Canada conducted in the mid-1990s showed water draining potato fields was found to contain imidacloprid concentrations up to 11.9 μg L^{-1} (Canadian Council of Ministers of the Environment, 2007). A study from Sydney, Australia looked at rivers draining horticultural areas. Upwards of 93% of samples had detectable concentrations of neonicotinoids with concentrations reaching levels of 4.6 μg L^{-1} (imidacloprid) and 1.3 μg L^{-1} (thiacloprid) after rainfall events (Sánchez-Bayo & Hyne, 2014). A study from California (U.S.) showed 89% of surface water samples in agricultural regions with detectable concentrations of neonicotinoids with imidacloprid concentrations upwards of 3.29 μg L^{-1} (Starner & Goh, 2012). Main et al. (2014) showed Canadian prairies sampled quarterly for one year had a maximum 3.1 μg L^{-1} clothianidin and 1.5 μg L^{-1} thiamethoxam with detection frequencies of 36.91%. Although not formally recognized waterbodies, scientists from Quebec (Canada) sampled puddles in corn fields to find maximum concentrations of 55.7 μg L^{-1} clothianidin and 63.4 μg L^{-1} thiamethoxam (Samson-Robert et al., 2014). Morrissey et al. (2015) found no regional patterns to neonicotinoid detection in surface waterbodies, but wetlands and rivers that drain agricultural areas are considered most at risk. However, the authors demonstrate that neonicotinoids have also been frequently detected in waterbodies draining urban areas at similar concentrations to those that drain agricultural areas. Furthermore, results showed multiple neonicotinoids can be found in single water samples outside of growing season(s), proving their persistence in the environment even after their initial application. In a second review, Borsuah et al. (2020) cites a review of 55 studies in rivers across 8 countries in which "most" samples taken detected the presence of neonicotinoid pesticides. In a study between 2012 and 2014, neonicotinoids were detected in half of the 15 sites sampled with the highest imidacloprid concentration reaching 11.9 μg L^{-1} (Struger et al., 2017). Studies from the U.S., Netherlands, and

Sweden showed the presence of imidacloprid, thiamethoxam, and acetamiprid in surface water with detection rates of 89-100% for imidacloprid, 31% for thiamethoxam, and 17% for acetamiprid at concentrations ranging between 0.22 to 200 μg L^{-1} (Starner & Goh, 2012; Van Dijk et al., 2013). A study conducted by the United States Geological Survey (USGS) showed concentrations as high as 142.8 μg L^{-1} (imidacloprid), 190.3 μg L^{-1} (thiamethoxam), and 38.2 μg L^{-1} (clothianidin) in streams across the U.S., including not only agricultural-draining, but also urban streams (Hladik & Kolpin, 2016). In a study of 79 samples across 7 streams in a heavily cultivated region of Iowa (U.S.), neonicotinoids were detected in upwards of 75% of stream samples (Hladik et al., 2014).

Further studies show that even after removal from the market, neonicotinoids are still detected for years in ecosystems downstream from where they are applied. Furthermore, neonicotinoids pose a threat to aquatic life despite their relatively short half-life for water photolysis. Neonicotinoids bind to the post-synaptic nicotinerginic acetylcholine receptors (nAChR) in insect nervous systems leaving the channel open and effectively overwhelming the nervous system to the point of death (Morrissey et al., 2015; Sánchez-Bayo et al., 2016). It was previously understood that mammal and other vertebrate nervous systems express less affinity to bond to neonicotinoids based on differing nAChR configurations (Yamamoto et al., 1995). However, more recent studies by Bal et al., (2012), Han et al. (2018), and Kimura-Kuroda et al. (2012) suggest that neonicotinoids can have adverse effects on vertebrates (including humans) which include reproductive toxicology, neurotoxicity, hepatotoxicity/hepatocarcinogenicity, immunotoxicity, genetic toxicity (Han et al., 2018) as well as adverse effects on human reproductive health and brain development (Bal et al., 2012; Han et al., 2018; Kimura-Kuroda et al., 2012). In invertebrates specifically, it is documented that once neonicotinoids are bonded to the nACh receptors, it is irreversible, which leads to bioaccumulation of these compounds

therefore posing not only acute but also chronic threats (Sánchez-Bayo et al., 2016; Yamamoto et al., 1995). Sánchez-Bayo et al. (2016) cites several studies which indicate well documented cases of lethal and sublethal affects to aquatic organisms, including feeding inhibition, impaired movement, reduced fecundity, and reduced body size (in mayflies and fish). The authors go into detail of the negative impacts that neonicotinoids have on the broader aquatic ecosystem including loss of biodiversity and lethal and sublethal impacts on the species that rely on these waterbodies as a source of food and water (Sánchez-Bayo et al., 2016). A variety of chronic and acute neonicotinoid concentration aquatic standards have been suggested and are summarized in Table 1-2 (amended from (Morrissey et al., 2015; US EPA, 2015b).

Table 1-2 Summary of acute and/or chronic values suggested for aquatic neonicotinoids (amended from Morrissey et al., 2015 and US EPA (2015a)).

Source	*Reference Value (µg L^{-1})*
(US EPA, 2015a)	[1]Acetamiprid 2.1 (chronic), 10.5 (acute) [1]Dinotefuran 6360 (chronic), >49550 (acute) [1]Imidacloprid 0.01 (chronic), 0.385 (acute)
(Canadian Council of Ministers of the Environment, 2007)	0.23
(European Food Safety Authority (EFSA), 2008)	0.2 (acute)
(Posthuma-Doodeman, 2008)	0.067 (chronic)
(Smit, 2014)	0.0083 (chronic)
(Mineau & Palmer, 2013)	0.0086 or 0.029 (chronic)
(Morrissey et al., 2015)	0.035 (chronic), 0.2 (acute)

[1] *Values represent the most stringent criteria for either fish or invertebrates*

In a study conducted by Klarich et al. (2017), batch studies were completed to test the effectiveness of granular activated carbon (GAC) and chlorination on the removal of neonicotinoids from drinking water. Kinetic GAC tests showed initial sorption of 75%-80%. Authors suggest this is likely due to the binding interactions between the GAC and specific moiety

structures found in neonicotinoids. Chlorination had mixed results in the removal of neonicotinoids, however, where successful. Chlorination reduced the half-life of clothianidin and imidacloprid from stable to ~2.5 days and ~70 days, respectively. In a study by Voorhees et al. (2017), columns of GAC were used to treat Nanopure™ water spiked with varying levels of imidacloprid flowing at rates of 25 mL min^{-1} and 50 mL min^{-1}. The experiments were run for either 4, 8, 50, or 100 minutes with only one experiment showing effluent above the detection limit (detection limit 0.007 µg L^{-1}, single effluent of 0.757 µg L^{-1}). Other studies summarized by Negro et al. (2021) demonstrated the efficient removal (71%-100%) potential of five isoreticular metal−organic frameworks (MOFs). These are engineered synthetic materials that are both environmentally non-toxic and water-stable and boast very effective removal rates (for a variety of contaminants) based on their high microporosity and stability. Although GAC is the most widely studied material for neonicotinoid removal via sorption, many other materials have been studied to a lesser extent. These studies have been predominately promising with some studies showing more promise than others. Materials studied for sorption have included kerolites (magnesium silicate) (Socías-Viciana et al., 2003), sepiolite (hydrated magnesium silicate clay) (González-Pradas et al., 1999), zerovalent iron (Roccamante et al., 2022), bentonite (Jain et al., 2017), and smectite (Cox et al., 2000).

Only one study investigated the removal of neonicotinoids from an aqueous solution using bioretention (Ahmad Zubairi et al., 2022). Results showed that in treatment train setups without plants, only 65% of imidacloprid was retained within the bioretention system regardless of any soil amendment. However, adding plants to the system greatly improves the outcome with only 4 out of 12 planted treatment train setups resulting in any imidacloprid leaving the system. Of which, the imidacloprid reported leaving the system ranged from 0.53% to 2.58% of the original influent

concentration. This study showed that bioretention can be an effective tool in removing neonicotinoids, especially with the addition of carefully selected plants.

1.1.2 Metals

Metals and metalloids are a common water quality contaminant and are of concern due to their toxicity to both humans and aquatic life. Some metals are essential micronutrients for supporting life, however all metals are toxic at some level. The USEPA lists metals of concern for human health and consumption to include aluminum (Al), arsenic (As), antimony (Sb), barium (Ba), beryllium (Be), cadmium (Cd), chromium (Cr), cobalt (Co), copper (Cu), lead (Pb), manganese (Mn), mercury (Hg), molybdenum (Mo), nickel (Ni), selenium (Se), silver (Ag), strontium (Sr), thallium (Tl), vanadium (V), and zinc (Zn) (Langmuir et al., 2004). Amongst these, Sb, As, Mo, Se, and V are commonly considered metalloids, however henceforth both metals and metalloids will be referred to under the umbrella term "metals". Metals can exist in many different forms in aquatic environments however they become an impairment when they are biologically available or exist at high concentrations. This impairment can affect the ability of aquatic life to reproduce and behave naturally and survive (Baby et al., 2011; US EPA, 2015c). Furthermore, metals have also been shown to negatively affect human health either through direct exposure or through bioaccumulation in food sources (Baby et al., 2011; OSHA, 2004).

Evidence of metals contamination in stormwater is widely documented (Gunawardana et al., 2015; Huber et al., 2016; Kayhanian et al., 2012; Rommel et al., 2021; US EPA, 2015c). In a comprehensive review, Huber et al. (2016) compiled 294 studies across all continents (excluding Antarctica) investigating traffic related metals pollution in stormwater. Measurable levels of Co, Mn, palladium (Pd), platinum (Pt), rhodium (Rh), titanium (Ti), and tungsten (W) were found in

stormwaters worldwide and are reported to be associated with anthropogenic sources. Of higher frequency, Cu, Pb, and Zn were also found worldwide and were identified to be the more prolific and concerning due to anthropogenic contamination. Rocks and soils are a natural source of metals to aquatic environments however human activities can either introduce or magnify the flux of metals into, within, and out of aquatic environments (Schlesinger & Bernhardt, 2013). Atmospheric deposition is also a common source of metals in aqueous environments, however it constitutes a smaller percentage of overall metals flux into fresh waterbodies than soils, rocks, and anthropogenic activities (Schlesinger & Bernhardt, 2013). Common anthropogenic sources of metals are mines, smelters, firing ranges, municipal waste treatment outfalls, industrial point sources, junkyards, landfills, and non-point sources such as parking lots, roads, fertilizers, pesticides, legacy contamination, and land/land cover disturbances (US EPA, 2015c). Once introduced in an aquatic environment, metals are indefinitely persistent and conservative (Langmuir et al., 2004) and contamination is difficult to detect beyond conducting water quality analyses (US EPA, 2015c). Metals can exist within an aquatic environment as aqueous complexes, flocculates, , organometallic compounds, sorbed onto solid particles, and/or as free metal ions (Langmuir et al., 2004; Rommel et al., 2021; US EPA, 2015c). Factors that affect the form of metals in aquatic environments include pH, temperature, redox potential, ionic strength of the water, the presence of methylating microbes, and the availability of binding sites (Langmuir et al., 2004; US EPA, 2015c). Dissolved metals are more bioavailable and therefore more toxic as opposed to their complexed or particulate-bound form (Rommel et al., 2021; US EPA, 2015c). Operationally, the fraction that passes through a 0.45 μm filter is generally considered as metal ions in solution (i.e., dissolved metals) (US EPA, 2015c). Under low pH conditions, metals are typically found as free metal ions into solution (US EPA, 2015c). Free metal ions have the greater

bioavailability for fish due to metal ions competing with nutrient binding sites on the gill epithelia (US EPA, 2015c). This impairs the fish's respiratory function and ability to regulate blood pH and ionic concentrations ultimately leading to negatively impacted health and reproduction, and/or ultimately death (US EPA, 2015c). The toxicity and impairment ability of metals in aquatic environments are dynamic and are dependent on a range of factors such as metal to nutrient ratios, metal species (free ions, complexes, particulate bound, precipitants, or organometallic compounds), metal-specific concentrations, organism-level sensitivities as well as a broad range of other chemical and kinetic variables (US EPA, 2015c). Much like a metal's speciation in solution, a metal's ability to come out of solution is driven solution chemistry as well as the chemistry and properties of potential adsorptive materials (Langmuir et al., 2004).

Changes in the concentrations of metals in water is commonly the result of two main processes: precipitation and sorption (Langmuir et al., 2004). Unlike organics where the adsorption of metals is often modeled using isotherm approaches, metals are a more complex sorption process (Langmuir et al., 2004). In the case of metal ions in solution, these ions interact with a sorptive medium with a charge opposite of that of the metal ion (electrostatic sorption). However, obfuscating this interaction is the complexity of what speciation each metal ion will take as well as the variability of surface charge on a specific solid (Attard & Barnes, 1998). Surface complexation reactions involving metals are influenced by environmental conditions such as pH, temperature, redox potential, ionic strength, the presence of organic matter, and the availability of binding sites (Genç-Fuhrman et al., 2007; Gunawardana et al., 2015; Langmuir et al., 2004; Rommel et al., 2021; US EPA, 2015c).

The point at which the surface charge of a media switches is referred to as the zero point charge (Genç-Fuhrman et al., 2007; Langmuir et al., 2004). An example by (Dzombak & Morel,

1990) demonstrates that under low pH conditions the surface charge of ferrihydrite was more positive which lent surfaces to bind with dissolved anionic metal species where at higher pH conditions the surface charge became more negative which allowed for the binding with metallic cation species in solution. Although this phenomenon can occur, for many absorptive media the zero point charge is outside the environmental conditions one would realistically expect, therefore in many cases an absorptive media can be considered constant as either a positive or negative surface charge (Langmuir et al., 2004). Langmuir et al. (2004) lists a series of clays as well as organics/humic materials, Mn-oxyhydroxides, and ferrihydrite as excellent metal-adsorbent materials based on their surface area and sorption site densities. There are many ways to model metal adsorption, however Langmuir et al. (2004) and the USEPA agree that the best methods include surface complexation, electrical double layer theory, and diffuse layer models. In short, these models consider the arrangement of charged particles around individual sorptive grains and how they interact with environmental conditions as well as dissolved metal ions in solution (Langmuir et al., 2004). Many studies have been conducted to investigate the feasibility of using a sorptive media to remove dissolved metals from solution (Genç-Fuhrman et al., 2007; Gunawardana et al., 2015). Results found that sorptive media that poses a large surface area (or high porosity in the case of low surface area media), a large amount of sorption sites, and surfaces that tend to be highly charged at common natural water pH (6-8) are best suited to remove metals from solution (Genç-Fuhrman et al., 2007; Gunawardana et al., 2015; Langmuir et al., 2004). In a dynamic system many factors (such as solution pH, ionic strength, organic matter content, etc.) can change which will ultimately impact the effectiveness and mode of metals removal. For instance, Langmuir et al. (2004) state that "[a]s metal concentrations further increase and fill available sorption sites, most metals tend to be incorporated in the structures of major mineral

precipitates as coprecipitates in which they substitute for major metal cations, forming so-called solid solutions." Genç-Fuhrman et al. (2007) alluded to this phenomenon when showing that for many, if not most cases the removal of metals from solution eventually was driven by oversaturation and precipitation in the form of the aforementioned "coprecipitates." As they relate to metals, bioretention swales are effective in retaining particulate bound metals by means of physical filtration and settling out of particulate matter (Rommel et al., 2021). However Rommel et al. (2021) and data from the *BMP Statistical Analysis Tool* (n.d.) summarized in Table 1-3 show that this best management practice (BMP) technique is not always the most effective or comprehensive at removing the dissolved fractionation of metals in an aqueous solution.

*Table 1-3 Median influent and effluent values for metals in various BMP devices (grass swale, infiltration basin, percolation trench, bioretention, high rate biofiltration, and multi-chambered treatment train) for available studies nationwide. (*BMP Statistical Analysis Tool*, n.d.)*

	Dissolved Metals In (µg L^{-1})	*Dissolved Metals Out (µg L^{-1})*	*% Difference*
Al	62.92	50	21
As	3.64	3.51	4
Be	0.25	0.25	0
Cd	1.05	0.3	71
Cr	2.15	1.29	40
Co	NA	NA	NA
Cu	49.46	9.8	80
Fe	72.79	122.07	-68
Pb	3.53	1.97	44
Mn	26.67	68.6	-157
Ni	2.76	3.18	-15
Se	0.58	0.58	0
V	NA	NA	NA
Zn	65.79	30.96	53

Changes in environmental conditions (such as a decrease in pH) are likely to lead to desorption of bound metals from their sorbents (Langmuir et al., 2004; Rommel et al., 2021), so careful consideration needs to be taken when engineering a sorption filter for metals removal. The primary federal programs (United States) which pertain to the limiting of metals in aquatic environments are the Safe Drinking Water Act (maximum contaminant levels for human consumption), the Clean Water Act (ambient water quality criteria), CERCLA (site remediation targets), and RCRA (waste management) (Langmuir et al., 2004). Ambient water quality standards (Table 1-4) are recommended by the US EPA (2015b) for adoption by individual states under section 304a of the Clean Water Act.

Table 1-4 EPA National Recommended Aquatic Life Criteria for freshwater (US EPA, 2015b).

Metal	*Acute ($\mu g\ L^{-1}$)*	*Chronic ($\mu g\ L^{-1}$)*
As	340	150
Cd	1.8	0.72
Cr^{+3}	570	74
Cr^{+6}	16	11
Fe	--	1000
Pb	65	2.5
Ni	470	52
Zn	120	120

1.1.3 Phosphorus

Phosphorus (P) is another element that contributes to pollution of stormwater. Phosphorus can exist in many forms, however, the most common form discussed for P in the environment is in the form of the phosphate ion (PO_4^{3-}). Fundamentally, PO_4^{-3} is bioavailable in the environment, however this term is commonly used more broadly to refer to any compound containing the phosphate molecule therefore obscuring whether it is bioavailable or not. On the other hand, orthophosphate (ortho-P) refers to "free" phosphate that is fundamentally bioavailable. Phosphorus is a limiting nutrient which supports the growth of photosynthesizing organisms and commonly is used in agricultural and domestic applications as a fertilizer to assist in the growth of crops, grass, and other plants (Schlesinger & Bernhardt, 2013). Unlike other pollutants discussed in this thesis, P is not considered for its direct toxicity to aquatic life, and it does not have associated acute or chronic toxicity thresholds. Rather P, at high levels, is considered potentially environmentally hazardous for the role it plays in the eutrophication of waterbodies (Davis et al., 2006; Lyngsie et al., 2014; Schlesinger & Bernhardt, 2013; Ulén et al., 2007; US Department of Commerce, n.d.). Eutrophication is a phenomenon that occurs when excess nutrients collect in a waterbody allowing for an overwhelming growth of algae in the water. If dense enough, these algae can block out sunlight and kill other plants in the water which provide a vital source of oxygen to the aquatic life. In the meantime, it is not uncommon for these algae to release toxins which can be detrimental to humans and aquatic life. Once dead, the algae are consumed by microbes who's increased activity can further prolong the depleted or absent oxygen supply (US Department of Commerce, n.d.; US EPA, 2015d).

The US EPA (2015) cites many different sources for increased P flux in the environment both from point sources such as industrial discharges as well as semi-point and non-point sources

such as mining, resource extraction, agriculture, and urban development. A prominant flux of P in the environment is through soil erosion, although this source alone is not often likely to spark a eutrophication event in a downstream waterbody (Schlesinger & Bernhardt, 2013). However, the application of P-rich fertilizers used in urban development and/or agriculture is often thought of as the primary source for eutrophic events (Ulén et al., 2007; US EPA, 2015d). The acceptable limit for P in a waterbody is highly dependent on the ecology, chemistry, and geometry of the receiving waterbody and its associated watershed and is often regulated and monitored on a site-by-site basis (US EPA, 2013; *Water Quality Standards | Oklahoma Water Resources Board*, n.d.). There are many strategies for preventing the flux of P through aquatic systems such as fertilizer management and conservation tillage, however these methods often fall short of reaching the necessary P reductions for protecting waterbodies and may not always be an applicable method for P management (Qin et al., 2018).

Instead, a common strategy is to utilize bioretention swales to provide a low cost, aesthetic, and small footprint solution (Arias et al., 2001; Davis et al., 2001, 2006; Hsieh et al., 2007; Lyngsie et al., 2014; Paus et al., 2014; Qin et al., 2018). Previous studies have shown promising results with total P removals between 55% and 85% (Carleton et al., 2001; Davis et al., 2001, 2006) with one study reporting only 39% total P removal (Barrett, 2003). While the contents and chemistry of a bioretention swale are major contributing factors to a swale's success at removing or adding P, other factors such as media layering, plant type, and proper maintenance play a prominant role in P removal efficiency (Hsieh et al., 2007). A wide array of sorptive media have been explored for P sorption (Agyei et al., 2002; Arias et al., 2001; Davis et al., 2006; Hsieh et al., 2007; Kandel et al., 2017; S. Li et al., 2017; Lyngsie et al., 2014; Okochi & McMartin, 2012; Paus et al., 2014; Scott & Penn, 2021; Tang & Nairn, 2021; W. Zhang et al., 2008) with, the content of Al-, Ca-, Fe-

, and Mg-(hydr)oxides and carbonates proving the best chemical predictor for highly efficient P removal via sorption (Lyngsie et al., 2014).

Qin et al. (2018) discusses several of the various complexes that result in the removal of can form when P is removed from an aqueous solution. The authors show that sorption is common with Al- and Fe-hydroxides and in many cases, precipitates are formed with varying levels of crystallinity in the way of Al-phosphate species such as wavellite, Fe-phosphate species such as strengite, and Ca-phosphate species such as monetite. Once removed from solution, P is not always static in the form that it takes. A study conducted by Ippolito et al. (2003) suggested that P can form outer sphere Al-complexes which, given time, can transition to more stable inner-sphere complexes and eventually an even more stable mineral phase, variscite. In a dynamic system, many different reactions can both inhibit and promote the removal of P from solution. One example of this is dissolved organic matter (DOM) which is a great source of debate and is relevant to the applicability of P sorption in bioretention swales. The broadly accepted convention is that DOM inhibits the sorption of P in soils (von Wandruszka, 2006), however, some authors argue that decomposing organic matter releases P into the system which increases the overall total P in the system therefore making it appear as if DOM hinders P sorption (Guppy et al., 2005). While this specific point is hotly debated, Guppy et al. (2005) raises the excellent observation that organic matter can also be a source of P in a system designed to remove P. Furthermore, mismanagement of bioretention swales can also increase P leaching through poor soil management or from the wrongful addition of compost or organic mulch (von Wandruszka, 2006).

As mentioned, the chemistry of the media is not the only influence on the ability of a media to remove P from solution. The surface area of the sorptive media and geometry (such as media depth, development of macropores, and media conductivity) of a bioretention swale will impact

the P removal efficiency (Davis et al., 2006; Lyngsie et al., 2014; Qin et al., 2018). Once sorbed or precipitated, P is immobilized and allows for the more metered uptake by plants within the bioretention swale which will allow it to be stored in an organic form within the plants themselves. This process serves as a sink for P and increases the capacity for the media to remove more P from solution (Davis et al., 2006).

1.2 Treatment Media

Three different types of treatment media were selected for, among other reasons, their abundance, low cost, and lack of widespread secondary uses. The intent with the three media is to identify a beneficial secondary use while also providing a low-cost solution to stormwater management and bioretention deficiencies. Media preparation and sourcing will be discussed in the methods; however, this section highlights the most common characteristics of each media and provides a review of existing literature as it pertains to the various media uses for stormwater application.

1.2.1 Fly Ash

Fly ash is a portion of the product left after burning coal, typically for power generation. After combusting coal, 75-80% of the material remaining is fly ash which accounts for roughly 500 million tons worldwide every year (Ahmaruzzaman, 2010). This byproduct has several uses beyond power generation including its use in concrete, as a road base, and as a contaminant-sorbing medium (Ahmaruzzaman, 2010). However, estimates from 2009 show that only 16% of all fly ash produced worldwide is reused in any way (Ahmaruzzaman, 2010).

Generally, fly ash is primarily composed of SiO_2, Al_2O_3, Fe_2O_3, and CaO with other compounds such as MgO, SO_3, Na_2O, and K_2O found at much lower concentrations

(Ahmaruzzaman, 2010). Variations in the composition of any particular fly ash will be highly dependent on the source and quality of the coal that is combusted. Additionally, the American Society for Testing Materials (*ASTM C618-05*, 2005) delineates ash that has a wt% of combined SiO_2, Al_2O_3, Fe_2O_3 content greater than 70 as "class F" and ash with a combined wt% of the mentioned compounds between 50% and 70% as "class C." In addition, fly ash is known to contain elements such as P, K, Zn, Fe, Cu, Mn, B, and Mo (Ahmaruzzaman, 2010). Fly ash is typically grey to tan in color and measures 0.075mm or less in diameter (Ahmaruzzaman, 2010). It can be utilized in its powder form or it can be mixed with water (in the case of class C ash) or water and calcium hydroxide (in the case of class F ash) to form a hardened form (Ahmaruzzaman, 2010).

Ahmaruzzaman (2010) provides an excellent and comprehensive review of fly ash and its utilization in removing several aqueous contaminants. Other studies have shown adsorption capacities (in mg g^{-1}) for a variety of metals shown in Table 1-5 below.

Table 1-5 Selected literature of heavy metal removal capacities of fly ash.

Metal	*Adsorption capacity (m g^{-1})*	*Reference*
Cd^{+2}	0.08-0.29, 6.19; 198.2; 207.3	(Chandra Srivastava et al., 2006); (Apak et al., 1998)
Cr^{+6}	3.7-89.2; 7.7-27.8	(Chandra Srivastava et al., 2006)
Cu^{+2}	7.5; 207.3	(Ricou et al., 1999); (Apak et al., 1998)
Ni^{+2}	6.48	(Chandra Srivastava et al., 2006)
Pb^{+2}	18.8; 444.7	(Ricou et al., 1999); (Apak et al., 1998)
Zn^{+2}	7.03; 3.4	(Chandra Srivastava et al., 2006); (Ricou et al., 1999)

Overall, the body of literature on fly ash as a sorptive media supports its utilization for removing metals, phosphorus, and pesticides. Sorption of a variety of metal ions was studied with fly ash and the composition, thermodynamics, and kinetics were determined for the most efficient removal (Apak et al., 1998; Ayala et al., 1998; Bayat, 2002a, 2002b; Diamadopoulos et al., 1993; G. Gupta & Torres, 1998; V. K. Gupta et al., 1998, 2003; V. K. Gupta & Ali, 2000, 2004, 2004; V. K. Gupta & Sharma, 2003; Hsu et al., 2008; Lin & Chang, 2001; S.-C. Pan et al., 2003; Panday et al., 1985; Rao et al., 2003; Rio et al., 2002; S. Wang et al., 2008; Yadava et al., 1987). The content of CaO (Bayat, 2002a), C (Lin & Chang, 2001), and humic acid (S. Wang et al., 2008), as well as the designation as a silico-aluminous fly ash (Rio et al., 2002) had a positive correlation on the removal of Cr(VI) and Cd(II), Cu(II), Pb(II), and Ni(II), respectively. Removal efficiency can rely on a great number of variables, primarily environmental conditions. The control of removal efficiency is pH, temperature, and concentration of metals in solution (Bayat, 2002a; V. K. Gupta & Ali, 2004; Panday et al., 1985; Yadava et al., 1987) with removal typically increasing with increasing pH up to a certain point and at high solution metal concentrations (Ahmaruzzaman, 2010). Low solution temperatures favored removal for exothermic reactions, however, high temperatures were found to generally be more favorable indicating typically endothermic reactions

(Bayat, 2002a; G. Gupta & Torres, 1998). Surface area of the fly ash itself can also impact sorption with higher surface areas resulting in more efficient removal (Ahmaruzzaman, 2010). This surface area will impact kinetics which were found to largely be first order with mechanisms such as intraparticle transport (Yadava et al., 1987) or diffusion (Lin & Chang, 2001) the limiting factors. As shown in Table 1-5, fly ash has been studied to be effective in the removal of Cd(II) (Apak et al., 1998; Ayala et al., 1998; Bayat, 2002a, 2002b; V. K. Gupta et al., 2003), Cu(II) (Apak et al., 1998; Ayala et al., 1998; V. K. Gupta & Ali, 2000; V. K. Gupta & Sharma, 2003; Hsu et al., 2008; Lin & Chang, 2001; Rao et al., 2003; S. Wang et al., 2008), Pb(II) (Apak et al., 1998; G. Gupta & Torres, 1998; Rao et al., 2003; Rio et al., 2002; S. Wang et al., 2008), Zn(II) (Bayat, 2002a; V. K. Gupta & Ali, 2000; V. K. Gupta & Sharma, 2003; Rio et al., 2002), Cr(VI), and Cr(III) (Rio et al., 2002).

Fly ash has also been found to be a good source for P removal. Though not studied as thoroughly as metals, P seems to have an affinity to bind with Ca^{+2} ions forming calcium phosphates and precipitating out of solution or creating weak Ca-P bonds in the case of sorption (Chen et al., 2007; Cheung & Venkitachalam, 2000; S. Li et al., 2017; Qin et al., 2018; Tsitouridou & Georgiou, 1988; Ugurlu & Salam, 1998; Vordonis et al., 1988; W. Zhang et al., 2008). Chen et al. (2007) calculated a maximum sorption capacity of P onto fly ash to be between 5.51 to 42.55 mg g^{-1} and correlated very strongly and positively with Ca and Fe content ($r = 0.9836$ and 0.8049, respectively) and negatively with Al and Si content. Increasing pH also favors the removal of P via the Ca-P reactions (Chen et al., 2007). Phosphorous removal for low-Ca fly ash was more favorable at more neutral pH likely due to P preferring to bond with Al- and Fe-oxides (Qin et al., 2018; W. Zhang et al., 2008). Zhang et al. (2008) points out that at higher solution pH (which is the more likely resulting condition to find when water interacts with fly ash), the Al- and Fe-oxide

reactions are not likely to be the primary driver of P removal. However, the authors do mention that P removal via bonding with Al- and Fe-oxides is still likely at more neutral pH and Qin et al. (2018) goes into greater depth of this reaction as a primary sink for P out of solution.

No literature was found which studied the efficacy of fly ash in treating aqueous neonicotinoid pesticides. However, fly ash has been studied for the removal of DDD [2,2-bis(4chlorophenyl)-1,1-dichloroethane] and DDE [2,2-bis(4-chlorophenyl)-1,1-dichloroethene] (V. K. Gupta & Ali, 2001), lindane and malathion (V. Gupta et al., 2002), carbofuran (Kumari et al., 1988), and TCB and HeCB (Nollet et al., 2003). DDD and DDE were removed from an aqueous solution between 93-98% (V. K. Gupta & Ali, 2001), lindane and malathion was removed from solution between 97 and 98% (V. Gupta et al., 2002), and TCB and HeCB was removed from solution up to 97% (Nollet et al., 2003).

1.2.2 Steel Slag

Slag is a byproduct from the manufacturing of steel either by blast furnace (iron slag), basic oxygen furnace, or electric arc furnace steel generation (steel slag). For every ton of steel produced, between one half and one ton of slag is produced (Lobato et al., 2015). In 2021, nearly 1.95 billion tons of steel was produced globally, therefore by the estimations proposed by Lobato et al. (2015), slag production should be between 8.5 and 1.95 billion tons ("2021 Global Steel Production," n.d.). There are many identified uses for slag, however, the simplest and most common disposal is into landfill (X. Zhang et al., 2020). Other uses include bases for various construction applications (Biskri et al., 2017; Ferreira et al., 2016; Pasetto et al., 2017; Vijayaraghavan et al., 2017), fertilizers and soil conditioning (Ali & Shahram, 2007; Y. Li & Dai, 2018; X. Wang & Cai, 2006), removal of heavy metals and phosphorus from water (Kim et al., 2008; Piatak et al., 2019; Scott

& Penn, 2021; X. Wang & Cai, 2006; Wu et al., 2014; F.-S. Zhang & Itoh, 2006), as a neutralizing agent for acid mine drainage (Goetz & Riefler, 2014; Moodley et al., 2018), and for carbon dioxide fixation (S.-Y. Pan et al., 2016). Additionally, reclaiming elements from the slag itself to be re-used in the steel-making process is seen as a potential use or reuse of iron slag (Lan et al., 2017). Reclaiming elements from slag usually requires pre-treatment which can release not only the desired metals, but other toxic metals, creating an environmental concern (Baciocchi et al., 2015; Gomes & Pinto, 2006). Piatak et al. (2019) shows, however, that ferrous slag, compared to non-ferrous slag is more environmentally safe for different forms of reuse. Table 1-6 taken from X. Zhang et al. (2020) shows the compositional breakdown of the two major types of slag.

Table 1-6 General composition of iron and steel slags (X. Zhang et al., 2020).

Composition	*Iron slag (wt%)*	*Steel slag (wt%)*
Calcium (CaO)	30-50	30-60
Silica (SiO_2)	25-45	10-45
Aluminum (Al_2O_3)	0-10	0-15
Magnesium (MgO)	3.5-15	5-20
Iron (FeO and Fe_2O_3)	10-30	0.1-3.6
Others (P, S, other metals)	<5%	<5%

Kim et al. (2008) performed batch experiments looking at the removal of copper using three different slags at varying pH. Each slag varied in its proportion of CaO, SiO_2 Al_2O_3, MgO, MnO, and total Fe. Sorption was found to be likely in slags with high calcium oxide, magnesium oxide, and aluminum silicates. However, results showed that when pH was above 3.0, sorption only contributed to 12% of the total Cu removed from solution. As pH increased, the potential for the formation of metal hydroxides increased. This mechanism successfully precipitated copper out of solution. Though not the primary mechanism of removal, copper sorption onto the three slags were 17.4 mg g^{-1}, 7.2 mg g^{-1}, and 6.2 mg g^{-1}. Another study performed by Wu et al. (2014) looked at removing $^{Pb+2}$ from a preprepared aqueous solution by using dry desulfurization slag. This slag had a high proportion of CaO and SO_2 as opposed to other slags which are higher in Si-, Al-, Mn-, and Fe-oxides. Results showed great promise for this slag to remove wastewater Pb^{+2}. As was seen with Cu(II), removal was highly dependent on pH. Generally, higher removal efficiency was observed at higher pH, however the optimal efficiency observed at pH 6. The maximum sorption capacity was found to be 130.2 mg g^{-1}. In a study conducted with washed and unwashed steel slags, Liem-Nguyen et al. (2020) demonstrated both slags to be effective at removing arsenate (As^{+5}) from solution. Adsorption alone was reported to account for 4.0 mg g^{-1} of As^{+5} removal

from solution, however when adsorption and precipitation combined, the retention capacity jumps to 13.7 mg g^{-1}. An initial solution pH helps to optimize the removal of arsenate and washing the steel slag with a low pH solution prior to use helps to get a more uniform fit to the Langmuir equation, representing a more uniform removal behavior. The authors also note that adsorption kinetics are instant and adsorption is not noticeably affected by common ions also in solution such as sulfate, carbonate, chloride, iron(III) and organic matter. Scott & Penn (2021) explain the removal of P from solution as shown in equations (1) and (2):

Equation 1-1 Phosphorus removal reactions in calcium rich materials (Scott & Penn, 2021)

$$Ca_2SiO_4 + 4H^+ \rightarrow 2Ca^{2+} + 2H_2O + SiO_2$$

$$Ca^{2+} + H_xPO_4^{x-3} \rightarrow CaH_xPO_4^{x-1} \quad with\ 0 < x < 2$$

This equation is further backed by Piatak et al. (2019) where experiments showed a positive linear correlation ($R^2 = 0.5$, n = 12) between P removal capacity and Ca content. Silicate dissolution (Zuo et al., 2018), pH and initial P concentrations (Bowden et al., 2009), and residence time (Drizo et al., 2006; Scott & Penn, 2021) also are shown to have strong correlations with dissolved P removal. Qin et al. (2018) investigated phosphorus removal using, amongst other materials, four different slags. The authors reported slag composition in "total" Ca, Al, and Fe, although from other studies we can assume these are largely in the –(hydr)oxide form. One of the slags was a recovered slag that was rejuvenated by treating it with Al-sulfate. Phosphorus was shown to be removed via a mix of sorption and precipitation. Overall, the slags were all found to remove 98% of total P from solution. Hydroxyapatite ($Ca_{10}(PO_4)_6(OH)_2$) was found to precipitate out 37-87% of total P in solution with the remaining fraction (11-61%) accounted for by the formation of Al- and Fe-phosphates. Another study conducted by Scott & Penn (2021) tested the efficacy of eighteen

different steel slag samples at removing dissolved P from solution in flow through experiments. Several of the slag samples were treated with an Al coating and flow through velocities were varied. Results showed between 12% and 96% dissolved P removal with the variability explained by differences in residence time, slag source, and level of Al-coating. Additional variables affecting P removal were pH buffering capacity, electrical conductivity, total Mg content, particle density, and bulk density. Al coating was found to improve removal in rapid flow through conditions as this slag relies more on Al-phosphate reactions rather than the Ca mechanism of removal, which is highly dependent on residence time. The authors also state that their experiments showed no statistically significant connection between slag Ca content and P removal. This contradicts much of the literature but is in line with the objectives of the authors' study which was to show that P removal is dependent on a more complex combination of slag composition and environmental conditions rather than simply Ca content.

Unlike metals and phosphorous, pesticide removal using slag has largely gone unstudied. While not a perfect proxy for neonicotinoids, atrazine (a commonly used herbicide) removal from water was studied using several sorbent media, including steel slag (Gonzalez et al., 2016). Results from this study were not promising for steel slag, with atrazine removal at only 0.3% from solution. The authors point out that sorption by oxides is highly pH dependent with low pH favoring removal. This is shown in slags that are primarily composed of Ca-, Al-, and Fe-oxides. In their experiments, the resultant pH after being treated with steel slag was 9.6 which was deemed to be the primary reason steel slag was found to not be effective for this specific herbicide removal. In another study the removal of 2,4-D and carbofuran pesticides from water using a variety of sorbents was tested (V. K. Gupta et al., 2006). Blast furnace slag was used and was yet again found to be "negligible" in the removal of these pesticides. The authors did not expand further into the

role of blast furnace slag in removing these pesticides preferring instead to discuss other materials that performed better. However, the study did go on to show that sorption was highly dependent on pH with a noticeable drop off in sorption around pH 8 and greater. With Gonzalez et al. (2016) the resultant pH from water treated with slag is expected to be at or above pH 8, therefore low sorption can be assumed to be low largely due to pH impacts. Lastly, a review of pesticide removal from drinking water by Cosgrove et al., (2019) indicated steel slag as a potential source of pesticide removal, however the authors did designate it as "low removal" albeit "low cost."

1.2.3 Biochar

Biochar is a material similar to charcoal which is composed of hard woods that underwent decomposition at high temperatures between 350-1000°C with little to no oxygen available during heating (pyrolysis) (Cairns et al., 2022). This process develops "highly aromatic clusters" which make biochar chemically stable and highly porous (Yang et al., 2018). Different biochar sources and production methods (slow pyrolysis, fast pyrolysis, gasification, and hydrothermal carbonization) can have large impacts on the medium's ability to remove contaminants (Mohanty et al., 2018). The most common method is slow pyrolysis which heats the source at 5-7°C min^{-1} to a temperature between 300-800°C and results in less syngas (CO, CH_4, and H_2) production (Mohanty et al., 2018).

A useful property of biochar is a large surface area achieved by the media itself being highly porous, unlike fly ash and steel slag. One study by Tan et al. (2016) reported surface areas of 32.85, 53.58, and 59.23 m^2 g^{-1} for pristine, slow pyrolysis biochar and two modified, slow pyrolysis biochars, respectively. Source material and production type can have large impacts on surface area with soft woods having higher surface areas than hard woods (Mohanty et al., 2018).

Most importantly, however, is the aromatic ring structure that is provided by the high organic C content of the biochar (Table 2-6) (Shi et al., 2022; P. Zhang et al., 2018). Organic aromatic ring structures provides further electrostatic forces such as π-π bonding, cation-π bonding, and h-bonding (Shi et al., 2022; P. Zhang et al., 2018). Other properties such as pH, cation/anion exchange capacity, hydrophobicity, and ionic strength are also affected by source and production method (Mohanty et al., 2018). For instance, cation exchange capacity is thought to be higher in biochars produced through the low pyrolysis method because tvolatile organics remain on the biochar (Mukherjee et al., 2011; Suliman et al., 2017). Hydrophobicity is also a key property of biochar and measures the organic carbon content which can enhance pollutant sorption especially for hydrophobic organic compounds (such as neonicotinoids) and pathogens (Mohanty et al., 2018). Al-Wabel et al. (2013) broke down the elemental composition of biochar further to show the primary constituents to be C, O, and Ca and more minor compositional constituents to be H, N, S, Mg, K, and P. This same study looked at the compositional breakdown of the same biochar at different pyrolysis temperatures. Results showed that C, N, Ca, Mg, K, and P became more concentrated in the biochar likely due to increased loss of O, H, and S due to volatilization at higher pyrolysis temperatures.

A review by Gwenzi et al. (2017) identified the major paths of metals removal from solution as cation exchange, electrostatic interactions (between media and metal), sorption, and co-precipitation. Zhou et al. (2016) investigated the role that ash content of a biochar plays in the removal of metals (specifically copper). Results found that removal of ash increased Cu sorption for one biochar. However, biochars with ash still present had mixed results. Biochars with high anion content and ash present improved the removal of Cu, however, biochars with a high cation and ash present content showed the opposite effect. Furthermore, the presence of ash on the biochar

was found to increase resultant pH which is likely to lead to precipitation of metals from solution. Ding et al. (2016) found a low pyrolysis biochar to have a sorption capacity of 11.2 mg Pb g^{-1} in a solution spiked with only Pb. Competitive sorption isotherms between Pb, Cu, Zn, Cd, and Ni showed that in mixed-metal solutions, some Pb (and other metal) sorption occurred, however, each individual metal's sorption capacity was negatively impacted resulting in sorption capacities of ~2 mg g^{-1} for Pb and Cu, ~0.1 mg g^{-1} for Cd and Ni, and ~0.4 mg g^{-1} for Zn. Pretreating the biochar with an alkaline solution yielded enhanced metals removal but also increased the cost of the treatment media. In a flow-through column experiment, Reddy et al. (2014) found that a gasified biochar removed 47% of dissolved phosphate from a solution prepared with 0.57 mg L^{-1} phosphate. Notably, the authors show that when flushing the columns with deionized water prior to introducing the spiked solution, the biochar leached 0.12 mg L^{-1} phosphate. This is likely due to most source materials (in this case, waste wood pellets) containing some form of phosphorus that does not get entirely volatilized upon combustion. Furthermore, the same study reported that heavy metals were removed from solution at a rate of 18, 19, 65, 75, 17, and 24% for Cd, Cr, Cu, Pb, Ni, and Zn, respectively. Sarkhot et al. (2013) investigated a slow pyrolysis biochar's role in removing nutrients (NH_4^+ and PO_4^{3-}) from dairy manure runoff. Results showed that 0.24 mg g^{-1} (equivalent of 50% the spiked solution) phosphate was retained by the biochar in the batch experiment via cation exchange and coadsorption with organic matter. Desorption experiments were also run on the exhausted biochar that showed up to 60% of the sorbed phosphate was released proving potential for biochar as a source for recoverable phosphate. A study conducted by Yao et al. (2011) showed digested sugar beet tailings biochar as an effective sorbent of phosphate in batch experiments. Maximum capacity of phosphate removal was found to be 133 mg PO_4^{-3} g^{-1} with moderately to slightly acidic conditions favoring removal. Competing anion

concentrations had slight to substantial effects with Cl^- and NO_3^- showing less of an interference, but HCO_3^- reduced phosphate sorption by over 40%. The removal was found to be driven largely by sorption to nano sized particles on the biochar surface. Magnetically treated biochar was studied by Tokarčíková et al. (2021) in removing beryllium from an aqueous solution. Although the effect of the biochar alone was not investigated, the augmented biochar was demonstrated to remove Be^{+2} from solution with a capacity from 1.6 – 2.4 mg g^{-1}. Generally, increasing solution pH yielded better Be^{+2} removal with pH 6 deemed the optimal removal point. The authors argue this pH affect is due to the deprotonation of active sites (carboxyl and hydroxyl groups) on the biochar surface which make them available for cation bonding. Convention would suggest that increasing pH would continue the deprotonation of these active sites, however, above pH 4, the complexation and subsequent precipitation of Be^{+2} as $Be(OH)_2$ begins to reduce Be^{+2} in solution. Therefore the further sorption of Be^{+2} onto the biochar surface is limited due to the reduction of the overall Be^{+2} concentration in the solution.

Little literature exists that investigates the interaction between biochar and neonicotinoids, specifically. Despite this, P. Zhang et al. (2018) investigated the mechanisms of neonicotinoid sorption onto different biochars coming from two different sources (maize straw and pig manure) at two different pyrolysis temperatures (>500°C and ≤500°C). Results from a dual-mode partition model showed that the two biochars used have promise to remove neonicotinoids from solution. High temperature pyrolysis and biochar preconditioning tended to improve the sorption capacity of the biochars, however, these processes often are more expensive than un-conditioned, low temperature pyrolysis. Sorption mechanisms varied across different sub-species of neonicotinoids (here imidacloprid, clothianidin, and thiacloprid) and different biochars (sources, preparation, and conditioning). Overall, the dominant mechanisms were cation-π interactions, π- π interactions, H-

bond interactions, and hydrophobic effects. Imidacloprid and clothianidin sorption under cation-competitive conditions (Ca^{2+} in this case) were found to not be greatly affected showing that cation-π and π- π interactions are likely more important removal mechanisms than electrostatic effects. With thiacloprid, π- π and h-bond interactions were thought to be the primary removal mechanism. Another study by Shi et al. (2022) used a high temperature pyrolysis, pre-conditioned biochar made from *Tenebrio molitor* frass as a way to remove three different neonicotinoids. Sorption capacities were 155.08 mg g^{-1}, 195.86 mg g^{-1}, and 325.81 mg g^{-1} for thiacloprid, nitenpyram, and dinotefuran, respectively. Similar to the previously discussed study, the mechanisms of removal were found to be π-π interactions, h-bonding, hydrophobic interactions, and micropore filling. The authors also found that neonicotinoid sorption was highly selective (thiacloprid > nitenpyram > dinotefuran) regardless of pH or inorganic ionic strength. Furthermore, variable pH did not appear to noticeably impact the sorption of neonicotinoids onto the biochar. One final study looked at a low temperature pyrolysis, wood derived biochar as a soil amendment to increase neonicotinoid removal in pot experiments (You et al., 2020). By adding biochar as a soil amendment, thiamethoxam and clothianidin retention was increased by 22.8% and 37.6%, respectively. Furthermore, this biochar was found to increase the half-life of thiamethoxam from 89.4 to 120 days likely due to the biochar-sorbed pollutant no longer being bioavailable to thiamethoxam-degrading microbes.

One final distinction to make is the difference between biochars and activated carbon. Fundamentally, they are produced in the same way both undergoing pyrolysis at high temperatures. However, the variation is in the activation process where activated carbon will be treated with either zinc chloride, phosphoric acid, potassium hydroxide, carbon dioxide, or steam (Marsh & Reinoso, 2006). Despite this difference, both biochar and activated carbon have similar properties

and remove contaminants through similar processes. Generally, activated carbon is commonly more effective in contaminant removal, however, in some cases, biochar can be more effective (Mohanty et al., 2018). Table 1-7 amended from Mohanty et al. (2018) demonstrates the properties and performance of biochar vs. activated carbon. As is evident, the cost to produce activated carbon is almost always greater than biochar making the cost per unit of contaminant removed less feasible and supports the widespread use of biochar for pollution control.

Table 1-7 Comparison of biochar and activated carbon properties and performance (Mohanty et al., 2018).

Parameter	*Biochar*	*Activated Carbon*
Cost (USD per metric ton)	350-1200	1100-1700
Energy demand (MJ kg^{-1})	6.1	97
Greenhouse gas emission (kg CO_2 e kg^{-1})	6.6	-0.9
Surface area	-[a]	+[b]
Biomass yield in amended soil	+	-
Cd uptake in amended soil	+	-
Bioaccumulation of PAHs[c] in plants	+	-
Chromium and zinc removal	+	-
Polychlorinated dibenzo-p-dioxin/dibenzofurans removal	-	+
Polychlorinated biphenyl adsorption	-	+
DDT accumulation[d]	-	+
Pyrene removal	+	-
Lowered toxicity	+	-
Chemical oxygen demand removal	+	-
Inhibition of seed germination	+	-
Soil toxicity towards Vibrio fischeri and Folsomia candida	+	-
Dissolved organic carbon removal	No effect	+
Mineralization of C-14-catechol	+	-
Hg(II) adsorption[e]	+	-
Trace organic contaminants removal	+	-
Atrazine adsorption	-	+

[a] *Lower parameter performance*
[b] *Higher parameter performance*
[c] *polycyclic aromatic hydrocarbons*
[d] *Dichloro-diphenyltrichloro-ethane*
[e] *Contradiction between results of both studies*

2 Methods and Materials

2.1 Methods

The purpose of this study was to determine the suitability of several industrial byproducts to treat a solution spiked with common stormwater contaminants. This was achieved by passing a synthetic stormwater (SSW) through different flow-through columns and measuring contaminant concentrations at the influent and effluent points over many pore volumes. Column setups were used to determine the removal capabilities of the media under ideal laboratory conditions (vertical columns) and under laboratory-simulated bioretention conditions (horizontal columns). Samples were taken from the effluent of each column and at the influent of the system on a semi-logarithmic schedule either based on pore volumes passed through the column (vertical columns) or simply total volume passed through (horizontal columns). These samples were analyzed for P, dissolved metals, and neonicotinoids. Influent concentration to effluent concentration ratios (IE ratios) were calculated and visualized on a volume passed vs. IE ratio graph. The Gompertz equation (an asymmetric, logistic function) was used to fit the data and to determine the exhaustion point of the media.

2.1.1 Synthetic Stormwater

Synthetic stormwater (SSW) was prepared in a 100 gal (378.5 L) tank using deionized (DI) water as the base for the solution. Synthetic stormwater was preferred over collecting actual stormwater to maintain a level of reproducibility between each tank filling and to ensure concentrations of contaminants of concern were above the measurable concentrations needed for the study. Water was measured into the tank by filling and emptying 5 gal (18.9 L) glass carboys and further approximated by using the 50 L graduation markings of the tank.

2.1.1.1 Nutrients and General Rainwater Chemistry

Basic rainwater chemistry was achieved by spiking the tank with the contaminants and concentrations outlined by Ricci et al. (2010) and displayed in Table 2-1 below. Concentrated aqueous stock solutions were made of each chemical and each stock solution was added in concordance to the volume of the SSW being created. Tank mixing was achieved by using an aquarium fan which was washed and prepared for use for metals, nutrients, and neonicotinoid sampling.

Table 2-1 List of basic rainwater chemistry and chemicals used to create a synthetic rainwater (Ricci et al., 2010).

Contaminant	*Spiking Chemical(s) Used*	*Target Concentration (mg L^{-1})*
Ammonium	NH_4Cl $NH_4H_2PO_4$	0.91
Chloride	NH_4Cl	1.96
Fluoride	NaF	1.94
Magnesium	$Mg(NO_3)_2 \bullet 4H_2O$	1.45
Nitrate	$NaNO_3$ $Ca(NO_3)_2 \bullet 4H_2O$ $Mg(NO_3)_2 \bullet 4H_2O$	2.01
Ortho-phosphate	K_2HPO_4 $NH_4H_2PO_4$	1.00
Sulfate	Na_2SO_4	1.46
Calcium	$Ca(NO_3)_2 \bullet 4H_2O$	0.30
Potassium	K_2HPO_4	0.15
Sodium	$NaNO_3$ NaCl NaF Na_2SO_4	1.36

2.1.1.2 Metals

Metals were added using an Inductively Coupled Plasma (ICP) Trace Metals Standard from Inorganic Ventures™ (*ICP Metals Standard*, n.d.). Each metal and their concentration in the standard is shown in Table 2-2. Because the application of this study is for bioretention effluent, the targeted metals concentrations were determined by collecting BMP metals effluent data from the *BMP Statistical Analysis Tool* (n.d.). Metals were added as a dissolved fraction, therefore the dissolved fraction of bioretention effluent values were used as the target as shown in Table 2-2. Double the target concentration of each metal was used to increase the likelihood that values stayed above detection limits as to effectively characterize both influent and effluent contaminant levels. In most cases, the ICP Trace Metals Standard was more than sufficient to spike the SSW to or above the desired concentrations. However, Fe and Zn concentration requirements were not met with this ICP Trace Metals Standard. Aqueous concentrated stock solutions of Fe^{+3} and Zn^{+2} were created and added to achieve the desired concentrations.

Table 2-2 Target metals concentrations in the synthetic stormwater.

Metal	*Literature Concentration ($\mu g\ L^{-1}$)*	*Target Concentration ($\mu g\ L^{-1}$)*	*Standard Concentration ($\mu g\ mL^{-1}$)*
Al	50	100	500
As	0.73	1.46	100
Be	0.25	0.5	100
Cd	0.14	0.28	25
Cr	1.4	2.8	100
Co	0.44	0.88	100
Cu	5.9	11.8	100
Fe	60	120	100
Pb	1	2	100
Mn	17.4	34.8	100
Ni	2	4	100
Se	0.5	1	25
V	2.34	4.68	250
Zn	24.1	48.2	100

2.1.1.3 Neonicotinoids

Acetamiprid, dinotefuran, and imidacloprid have been characterized as "the big three [neonicotinoids]" in Oklahoma by Dr. Eric Rebek, former Extension Entomology Specialist at Oklahoma State University (Dr. E. Rebek, personal communication, September 13, 2021). Concentrated stock solutions were created by using granulated, store-bought chemicals mixed with DI water. Assail 30 SG Insecticide was used for acetamiprid (30% active ingredient), Safari 20 SG Insecticide was used for dinotefuran (20% active ingredient), and Bonide Annual Tree & Shrub Insect Control was used for imidacloprid (1.47% active ingredient). Due to the volatile nature of neonicotinoids in solution, stock solutions were stored in a dark cabinet and were not used if they had been created more than one month prior. Initially, the target concentration for each neonicotinoid was set to 1 mg L^{-1}. Vertical column experiments were run at this level. Further literature research and communications with the analyzing lab revealed that this concentration was

above their existing upper standard limit. A decision to reduce neonicotinoid concentrations in the SSW was made and the new target was chosen to 1 µg L^{-1} based on the maximum reported regulatory standard compiled by Morrissey et al. (2015). A comparison study was done with the horizontal columns where the same sample setup and medium was used. Influent SSW with 1 mg L^{-1} neonicotinoids and another with 1 µg L^{-1} neonicotinoids were run to compare the effect of exceptionally high neonicotinoid concentrations on removal and other contaminant removal.

Upon completion of each experiment, media samples were collected in 15 mL test tubes at the effluent, influent, and mid-column points and frozen (-20˚C) for potential future studies.

2.1.1.4 pH

Once the spiking of the tank was complete, the pH of the SSW was measured. Because the buffering capacity was extremely low, the acidity of the ICP Trace Metals Standard caused the tank to be below the desired pH. A sodium hydroxide (NaOH) stock solution was added to the SSW until the measured pH was 7.00 ±0.20. This naturally will increase the concentration of Na in solution above the target as outlined in Table 2-1.

2.2 Materials: Industrial Byproducts

General properties and compositions of each medium used was characterized in the Introduction of this thesis. The sections below are to provide further insight, where available, as to the source and characteristics of each medium used. All media was sieved to yield two sizes of media: large – 0.25” – 0.5” (0.635 cm – 1.27 cm) and small – 0.0787” – 0.25” (0.200 cm – 0.635 cm). The latter of which is the size of a standard #10 sieve. After sieving, media were stored in plastic bags in a dry, dark location. Table 2-3 below shows the composition of each specific media

used in this study. Fly ash was reported as % composition as the metal-oxide species (W. Zhang et al., 2008), steel slag was reported as is (Bowen, 2021), and the biochar was reported as mass component per mass biochar (J. Gaspard, personal communication, October 10, 2022). All were converted for the table below to represent % composition of each element shown.

Table 2-3 Composition of media used in this study. Fly ash is converted from % metal-oxide to % metal composition. Biochar is converted from mass/mass to % composition. BDL refers to a value being reported below the detection limit.

Component	*Fly Ash (%)*	*Steel Slag (%)*	*Biochar (%)*
Al	9.7	1	-
As	-	<0.0001	<0.0001
Cd	-	BDL	<0.0001
Co	-	-	<0.0001
Cr	0.007	0.18	<0.0001
Cu	-	0.01	0.00303
Fe	4.1	10	0.0210
Mn	0.02	2.4	-
Mo	-	-	<0.0001
Ni	-	0.0014	<0.0001
Pb	-	0.00014	0.00020
Se	-	<0.001	<0.0001
Si	17.8	-	-
Zn	-	0.0018	0.0181
B	-	-	BDL
Cl	-	-	0.00923
Ca	16.3	7.5	-
Na	1.4	0.016	0.0582
Mg	3.27	2.9	0.0164
K	0.5	0.0084	0.1422
P	0.6	0.053	0.0324
Organic N	-	-	0.5280
Organic C	-	-	87.4

2.2.1.1 Aggregated Fly Ash

The fly ash and its properties used in this study were the same as was used in W. Zhang et al. (2008). W. Zhang et al. (2008) characterized this fly ash as sourced from "sub-bituminous coal from the Powder River Basin, Wyoming, [USA]" and obtained from the Sooner Power Plant in Red Rock, Oklahoma. Table 2-4 below is a summary of the fly ash's composition as reported by W. Zhang et al. (2008). Notably, reported composition for Si-, Al-, Fe-, Mn-, and Ca-oxides were 38.1%, 18.4%, 5.93%, 0.02%, and 22.9%, respectively. The powder fly ash was aggregated by mixing it with DI water at a ratio of 2:1 (fly ash (g):water (g)) and allowed to cure for a minimum of 30 days. This hardened mixture was then crushed and prepared to sieve.

Table 2-4 - Composition of the fly ash used in this study as reported by W. Zhang et al. (2008).

Composition	*Content (%)*
SiO_2	38.1
Al_2O_3	18.4
Fe_2O_3	5.93
MnO	0.02
MgO	5.43
CaO	22.9
Na_2O	1.82
K_2O	0.56
Ti_2O	1.39
P_2O_5	1.37
BaO	0.69
Cr_2O_3	0.01
SrO	0.30
Loss on ignition	0.69
Total	97.6

2.2.1.2 Steel Slag

Steel slag was procured from Commercial Metals Corporation, a rebar manufacturing plant in Sayreville, New Jersey, United States by way of TMS International Corporation©. The toxicity characteristic leaching procedure (TCLP) report was provided which outlined the primary composition of the specific steel slag used (Bowen, 2021). The full elemental composition is provided in Table 2-5 below and the normalized % elemental composition is provided in Table 2-3 above.

Table 2-5 Elemental composition of the steel slag used in this study (Bowen, 2021). Elements measured at levels below the detection limits of the instrument are reported as BDL.

Element	*Composition (mg kg^{-1})*
Al	10000
Ar	0.71
Ba	320
Be	0.50
B	58
Cd	BDL
Cu	100
Fe	100000
Ag	0.036
K	84
Magnesium	29000
Mn	24000
Mo	17
Na	160
Ni	14
Pb	1.1
Sb	0.18
Se	0.41
Th	BDL
Ti	1100
V	320
Zn	18

2.2.1.3 Biochar

Biochar was sourced from Biochar Now (www.biocharnow.com). The "chip" size was selected because it was rated to be between 1" (2.54 cm) and 0.118" (0.3 cm) and therefore fit within the range of media sizes targeted. Biochar was sourced from pine trees that had been killed by invasive beetles. This wood was shredded then underwent pyrolysis at around 550˚C. Testing results are shown in Table 2-6 below (J. Gaspard, personal communication, October 10, 2022).

Table 2-6 Reported compositions of the biochar used in this study (J. Gaspard, personal communication, October 10, 2022)

Composition	*Content (mg kg^{-1})*
As	<0.44
Cd	<0.18
Cr	0.59
Co	<0.44
Cu	30.3
Pb	2.0
Mo	<0.44
Hg	<0.001
Ni	0.57
Se	<0.89
Zn	181
B	<4.43
Cl	92.3
Na	582
Fe	210
Mg	164
K	1422
P	324
Organic N	5280
Organic C	874000*

**Organic C is given as 87.4% of total dry mass of biochar*

2.2.2 Vertical Columns

Columns were made of acrylic and had an inside diameter of 1.5 in. (4 cm) and a length of 5.9 in (15 cm). Column caps included a rubber gasket to ensure a water-tight seal. Inlet and outlet ports were threaded to allow for a 1/16" (0.159 cm) barb to be screwed into place for hose attachment. Clean columns were filled with DI water then filled with one of the media. Throughout the filling process, the sides of the column were gently tapped to encourage media to pack without tamping the media and therefore risk crushing. The media in the column was soaked in DI water for 24 hours prior to introducing any SSW. The columns weights were noted and recorded when the columns were empty. After filling the columns with DI water and media, they were left to soak

for 24 hours then the weight was taken and recorded again. The media used to fill the column was weighed and recorded before being placed in the column. Using the assumption that 1 g of water equates to 1 mL of water, Equation 2-1 below was used to determine the pore volume of a column.

Equation 2-1 Equation used for pore volume determination.

$$Water\ Wt.or\ Pore\ Vol.(g\ or\ mL) = Soaked\ Wt.(g) - Empty\ Wt.(g) - Media\ Wt.(g)$$

At the influent, tubing (Masterflex® L/S®16 Precision Pump Tubing) was attached, and SSW was introduced into the columns via a Cole-Palmer Masterflex® L/S® Peristaltic Pump pumping at a volumetrically calibrated rate of 6 mL min^{-1}. SSW flowed from the bottom of the column to the top to ensure a full saturation. Effluent tubing was placed in a graduated carboy to help ensure the flow rate was consistent across all columns. Sampling points were determined to be at the 10, 40, 90, 160, 270, 430, and 670 pore volumes to achieve a semi-logarithmic sampling schedule where the most change in contaminant removal is expected to be early in the experiment with contaminant removal declining with time. Samples were collected in 1 L amber glass containers and where possible, were prepared for analysis immediately. However, in some cases, samples were unable to be immediately prepared and instead were promptly refrigerated (4˚C) after collection to be prepared for analysis as soon as possible. An image outlining the vertical experimental setup is provided below (Figure 2-1).

Figure 2-1 Photograph of vertical column setup. Pictured from left to right is the sample bottles (collection point), vertical columns containing the media of interest, the peristaltic pumps, and the synthetic stormwater influent tank.

2.2.3 Horizontal Columns

Horizontal columns were composed of translucent, schedule 40, 1.5” (3.81 cm) PVC. Because this sampling orientation was to simulate bioretention, the sample setup was broken into two main components. First was the vertical tube which was comprised of 1 ft (30.48 cm) of concrete sand and 6 in. (15.24 cm) of SSW ponding. An overflow port which flowed back to the influent tank was placed at the 18 in. (45.72 cm) mark to ensure a constant head of 6 in. (15.24 cm) above the 1 ft (30.48 cm) of sand was achieved throughout. The vertical tube then connected to a 90˚ elbow joint where the horizontal tube was also connected. The horizontal tube was completely filled with one of the small-grained fractions of the media of study. A cap was placed on the end with a 1/16” (0.159 cm) barb to assist in sample collection. Differing from the vertical column setup, columns were filled dry due to the difficulties of filling and assembling the columns

while wet. Each component (vertical and horizontal) was wetted separately (to prevent fines from getting trapped in the horizontal portion) but were assembled to ultimately be saturated for the 24 hours prior to sampling. The sample setup was weighed while empty, while filled with media, and while filled with media and saturated with DI water to determine the pore volume of each column in concordance with Equation 2-1 above. Ultimately, the decision was made to sample each column based on a total volume passed convention rather than one based on pore volumes as was with the vertical columns. The sample points were also semi-logarithmic sampling at 0, 1, 2, 4, 6, 10, 17, and 27 L passed through. The "0" sampling point was determined to be 1 pore volume (as previously determined) based on a simple contaminant-front experiment performed on a replica of the sample setup as described above (Table 10-12). Samples were also collected into 1 L amber glass and, where possible, prepared for analysis immediately. Some samples were required to be refrigerated (4˚C) and prepared for analysis within 8 hours. An image of the horizontal sample setup is provided below.

Figure 2-2 Photograph of the horizontal column setup. Pictured from left to right are the experimental columns, peristaltic pumps, and the synthetic stormwater influent tank. Experimental columns each demonstrate 6 inches of ponding in the upper portion of the vertical tube followed by 12 inches of bioretention simulation sand, a 90 degree elbow, 12 inches of a media packed tube, and lastly a cap with a 1/16 inch orifice outlet.

2.2.4 Sample Preparation and Analysis

2.2.4.1 General Chemistry

The pH, specific conductivity (µS cm^{-1}), and temperature (˚C) were measured in the lab during sample preparation. Initially a bluelab® Combo Meter measured pH, conductivity, and temperature. Irregularities were found in SC results which led to eventually purchasing and deploying an Apera Instruments AI311 Premium Series PH60 multiprobe which calibrated and performed well throughout the remaining experiments. Specific conductivity results measured from the bluelab™ meter were thrown out and not considered for analysis.

2.2.4.2 Metals

Dissolved metals were syringed through an Allpure 0.45-micron nylon syringe filter tip into a 15 mL conical centrifuge tube. Each tube was preserved with a single drop of concentrated HPLC grade nitric acid (HNO_3) and refrigerated at 4˚C. Both metals fractions were measured via ThermoFisher Scientific iCap Pro XP Duo Inductively Coupled Plasma-Optical Emission Spectrometry (ICP-OES) instrument utilizing the Teledyne AXS-560 Autosampler. EPA method 200.7 (Martin et al., 1996) was used to analyze metals results. Results from this method are reported in µg L^{-1} elemental concentrations.

2.2.4.3 Phosphorus

Phosphorus samples were prepared and analyzed in accordance to the Soil, Water, and Forage Analytical Laboratory (SWFAL) at Oklahoma State University (*OSU SWFAL Procedures*, 2018). The SWFAL used ICP-OES (Spectro Ametek®) analysis on phosphorus samples and reported results as phosphorus (mg L^{-1}). Adherence to "Method 3120 B" (2005) was used for analyzing phosphorus samples.

2.2.4.4 Neonicotinoids

Neonicotinoid samples were prepared in accordance to Magalhaes et al. (2009). 50 mL of sample was passed through a Waters™ Oasis HLB 30 µm cartridge which was preconditioned with 6 mL of acetonitrile, 6 mL methanol, and 6 mL DI water, respectively. Cartridges were immediately frozen at -20˚C until being packaged and expressed shipped to the Water Sciences Laboratory at the University of Nebraska – Lincoln. Samples were then eluted and "analyzed by reverse-phase high performance liquid chromatography (HPLC)/tandem mass spectrometry

(MS/MS) by using a Waters 2695 HPLC autosampler/pump coupled to a Finnegan LCQ (Thermo Fisher Scientific) ion-trap mass spectrometer" (Magalhaes et al., 2009). Concentrations were reported in μg L^{-1} as individual species of neonicotinoid (acetamiprid, dinotefuran, and imidacloprid).

2.3 Data Analysis

Data were compiled in Microsoft Excel and matched with its parent sample ID. For vertical column experiments, influent samples were taken at the beginning and end points of the experiments with samples taken at the 160 pore volume sampling point. This was initially employed as a cost-savings measure, however initial results from vertical column experiments led to preferring direct measurement of influent concentrations for all contaminants at every sampling point for the horizontal column experiments.

2.3.1 Influent-Effluent Ratio Analysis

For the vertical column experiments, influent values that corresponded to each sampling point were interpolated using simple linear regression since influent concentrations differed slightly throughout the duration of the experiment. These measured or interpolated values were paired with their equivalent effluent concentrations to determine the influent-effluent (IE) ratio (Equation 2-2). As mentioned, for horizontal column experiments, influent values were directly measured and paired with their effluent value to determine the IE ratio (Equation 2-2).

Equation 2-2 Influent - effluent ratio calculation

$$Influent\ Effluent\ (IE)\ Ratio = \frac{Effluent\ Concentration}{Influent\ Concentration}$$

The IE ratio was then plotted using the statistical software R (R Core Team, 2022) with pore volumes or total volume passed as the predictor variable and the IE ratio as the response variable. This visualization shows whether the media was measured to be removing a specific contaminant (IE ratio <1), leaching it (IE ratio > 1) or was ineffective at removing the contaminant yet did not leach it (IE ratio = 1). An "error zone" was determined to be ±0.1 unit on either side of EI ratio of 1, meaning, any EI ratio value between 0.9 and 1.1 was interpreted to be neither removing nor leaching the contaminant.

2.3.2 Modeling Results

Logistic regression analysis was used to best fit the data's behavior over time. The power law Gompertz equation was used to fit an asymmetric breakthrough curve to the IE ratio data. This method is supported for its use in column sorption experiments as well as dosing-response and population studies due to its ability to fit asymmetric growth/breakthrough data, especially in column studies where sorption sites are near or at saturation (Chu, 2020).

Equation 2-3 Simplified Gompertz function as defined by (Chu, 2020).

$$f(x) = Y_{max} \exp[-\exp \beta(x - \alpha)]$$

Y_{max} = upper asymptote
a = fitting parameter
b = fitting parameter
x = pore/total volume passed

Statistical package "Dose Response Curve" (DRC) (Ritz et al., 2015) was used to fit Gompertz curves to the data. We used other statistical packages such as "DPLYR" (Wickham et al., 2022) and "SciViews" (Grosjean, 2022) to filter and plot data. Gompertz curves were fit to the data using two primary methods. First, the two fitting parameters and the upper asymptote were all optimized

which yielded the best fit curve for the data. This is the intended use for this function; however, it does not always yield an upper asymptote near or equal to one (media exhaustion). The second method was to hold the upper asymptote equal to 1. This forces the equation to be fit using only the two fitting parameters and will approach 1 on the IE ratio vs. volume graph despite what upper limit the data suggests is being measured. However, it is worth noting that for data that finish with IE Ratios >1, this asymptote-fixing could underestimate various precipitation/dissolution or sorption/desorption reactions. Furthermore, with data that never approached an IE ratio equal to 1 during our experiment, the curve will model the exponential growth of the Gompertz curve while leaving the optimization to interpolate the breakthrough (inflection) point and exponential decay without any data. This renders the Gompertz equation statistically inaccurate, however it does allow us to make an approximation as to when media exhaustion may occur. These approximations of media exhaustion could be used in developing further studies of contaminant-medium combination interactions in sorption experiments.

By finding the optimized fitting parameters for each Gompertz curve then rearranging the Gompertz function and setting the upper asymptote to 0.95 (Equation 2-4), we can estimate where each media reached exhaustion (i.e. the media could no longer remove the contaminant). When an upper IE asymptote above 0.95 is reached within the domain of the collected data, the exhaustion point is accurately characterized by the Gompertz model. When the upper IE asymptote reaches above 0.95 outside the domain of the collected data, the exhaustion point is not appropriately characterized by the Gompertz model, but rather this point serves as a best estimate of exhaustion. Likewise, if the model never reaches an upper IE ratio asymptote above 0.95 and the upper IE ratio asymptote is fixed to 1.00, this exhaustion point is also merely an estimate and does not accurately reflect the true exhaustion point of the media to remove the contaminant. Media exhaustion was

selected to be at IE ratio equal to 0.95 since in a theoretical perfect flow through sorption column experiment, the upper asymptote would be IE ratio equal to 1, meaning the model would never reach 1. Setting the upper asymptote to > 0.95 is likely to well overestimate the effective exhaustion point where anything < 0.95 would likely define exhaustion too early.

Equation 2-4 Rearranged Gompertz equation to determine volume at which media exhaustion occurs

$$x = \frac{\ln[-\ln\left(\frac{Y}{0.95}\right)] + \alpha}{\beta}$$

2.3.3 Statistical Analysis

Two different statistical analyses were conducted to test the significance of the Gompertz model fit to each individual data set. First, analysis of variance (ANOVA) was conducted which compared the uniqueness of each size and media combination's Gompertz model to a Gompertz model fit to the whole of the data for each column orientation. This will test the null hypothesis of "no significant uniqueness between a specific media's Gompertz model." Accepting the null hypothesis tells us that relative to the whole of Gompertz model results, one individual media's results are not unique. Conversely, rejecting the null hypothesis indicates that relative to the whole of the data, one individual media's results are unique.

The second statistical analysis was a pairwise ANOVA was conducted for each parameter in each media's fitted Gompertz model. The null hypothesis is "no significant variation between two models' individual parameter." Accepting the null hypothesis would indicate that a parameter is not statistically unique compared to the same parameter on another Gompertz curve. Rejecting the null hypothesis indicates that the analyzed parameter varies significantly between the two compared Gompertz curves. Because each Gompertz curve has three fitted parameters, a pairwise

ANOVA analysis was conducted for each parameter. For each pair of compared models, the total of parameters that successfully rejected the null hypothesis were totaled. Rejecting the null hypothesis for all three parameters indicated entire uniqueness between each Gompertz model. When two parameters rejected the null hypothesis, the curves were still considered unique, but are shown to share at least one parameter that is not. Finally, pairs that had one or zero parameters that rejected the null hypothesis were considered similar, or better yet, not unique.

2.3.4 Mass Removal Rate Analysis

Mass removal rate per underdrain unit volume is important in understanding the longevity of a medium's ability to remove a particular contaminant over time. For vertical column effluent results, calculating this was achieved by Equation 2-5 below.

Equation 2-5 Mass removal rate calculation

$$Mass\ Removal\ Rate\ (MRR) = (C_i - C_e) \times Q$$

MRR = Mass removal rate
C_i = Influent concentration
C_e = Effluent concentration
Q = Flow rate

MRR was then divided by the area of the column, referred to as "media volume" (MV), to produce the mass removal rate per unit volume (MMR MV^{-1}) value. This value was plotted against the cumulative contaminant mass input to yield the analysis referred to "mass removal rate analysis." For horizontal column experiments, there was one notable exception. C_i from Equation 2-5 above, was replaced with $C_{e,\ control}$ which is the measured effluent concentration of the control column. This was used as a proxy for the solution concentration entering into the media section of the horizontal column experiments. Therefore, this allowed for the direct comparison between column orientations of the MRR of the media, specifically, rather than comparing the systems as a whole.

2.4 Quality Assurance/Quality Control (QA/QC)

All equipment used was washed according to Norton (2004). Sampling equipment that was used to only process metals or phosphorus samples were washed with and soaked in a 5% Liquinox solution and rinsed with tap water. These same parts were then soaked in a 2% hydrochloric acid (HCl). Parts containing metal or rubber were dipped, swished, and immediately rinsed with DI water and left to air dry. Plastic or glass pieces were left to soak for 30 minutes then rinsed with DI water and left to air dry. Sampling equipment used in sample setup and/or neonicotinoid collection/processing underwent an additional triple rinse with methanol followed by a triple rinse with DI water and left to air dry.

Quality assurance (QA) samples were taken at randomized points throughout the sampling process. Two duplicate samples were taken for every run-column combination. The coefficient of variation was calculated for each duplicate pair to help identify error in the sampling process. Each duplicate pair was separated into a standard sample (QA code 1) and a duplicate sample (QA code 2). For the sake of analysis, only QA code 1s were used as to not bias any results by averaging duplicate pairs. Aliquots with duplicates with variability coefficients beyond 10 and 20% were flagged and considered before writing the Discussion and Conclusions sections.

For each run, the same sampling procedure as a standard sample was used to collect a blank sample of DI water at the end of the sampling period. This was used as an outside check on each labs' analysis procedures as well as a check on the purity of DI water and cleanliness of the environment in the lab where the experiment was being conducted. All

In performing ICP-OES analysis, several QC measures were used to ensure the quality of results. Primarily was the use of continuing calibration verification (CCV) standard samples. The instrumentation returned to the CCV standard after every 10^{th} unknown sample analyzed. This helped to identify calibration drift as well as catch any individual or systematic errors in the analysis. USGS reference standards were also used (*USGS Spring 2022 Reference Standards*, n.d.). These standards are environmental waters with solute of certified concentrations, which provide a more varied matrix for QC references. These reference standards were run at the start of each analytical run of the ICP-OES and after every 30 samples and/or at the end of each analytical run. Furthermore, an internal scandium (Sc) standard was used to determine the consistency of the delivery system into the instrument.

2.5 General Contaminant Removal Mechanisms

Generally, there are two main modes of contaminant removal: sorption and precipitation (Attard & Barnes, 1998). Contaminant removal from mixed waters is a highly complex process, especially when constant flow is involved like the design that was used for these experiments. Largely, there are two types of sorption, chemical and physical. Chemical sorption is monolayered while physical sorption is multilayered (Attard & Barnes, 1998). Physical sorption is highly complex and involves high levels of complexation and ion exchange over a multitude of layers. This can lead to changes in solution chemistry over both short and long periods of time not necessarily due to of a medium's *ability* to remove one contaminant or the other, but rather due to the complexity of the solution being treated and the physical complexities of multilayered sorption.

Precipitation commonly refers to the oversaturation of a solution with an element or molecule which leads to that element or molecule complexing or crystallizing to form a solid phase and "drop out" of solution. Precipitants are generally thought of as the difference between a dissolved sample (in this case, sample passed through a 0.45 μm filter) and a total sample (unfiltered). Precipitation itself can also complicate understanding sorption in flow through column experiments as complexes or minerals can precipitate out of solution and become additional surfaces for sorption.

Because of these complex reactions this discussion will largely focus on identifying the broadest category of removal, either sorption or precipitation. It is also worth noting that these removal mechanisms are highly complicated and are not binary or static. Meaning, once something is sorbed or precipitated, it does not mean that reaction is over, but rather that elements in solution can replace one another at sorption/exchange sites and solid phases can precipitate, dissolve, and reprecipitate.

3 Results

Results were analyzed based on column orientation, medium, and contaminant. Within these combinations, all media were compared against one another in order to (1) see individual patterns of contaminant-media interaction and (2) to compare each medium against the others. Each combination generally fell into 4 categories:

(1) >50% results were below the detection limit (BDL), or results were variable and did not resemble an apparent breakthrough curve.
(2) Experimental columns had no noticeable departure from the control column (in the case of the horizontal orientation), or columns did not remove or leach the contaminant (in both orientations). This indicates that the industrial byproduct did not impact column solution chemistry for the given contaminant.
(3) Columns leached the contaminant.
(4) Columns showed some type of behavior consistent with contaminant removal. In the case of horizontal columns, these combinations also had a noticeable departure from the control column.

While categories 1, 2, and 3 are important and worthwhile of further analysis and discussion, ample data exist within category 4 such that analysis and discussion will focus only on this category. Column combinations will be clearly categorized and, where appropriate, data tables and figures will be referenced to in the appendices. Column combination categorization are shown in Table 3-1 below.

Table 3-1 Categories of results. 1: results below detection limits or did not resemble a breakthrough curve, or were too scattered; 2: media had no effect either generally or compared to the control column; 3: the media leached the contaminant; 4: media/contaminant combination of interest

Contaminant	*Vertical Columns*	*Horizontal Columns*
Al	4	3
As	4	4
Be	4	1
Ca	3	3
Cd	1	1
Co	1	1
Cu	1	1
Fe	*	1
K	3	3
Mg	3	3
Mn	4	2
Na	*	4
Ni	*	1
Pb	*	1
Se	1	1
Si	3	3
Zn	*	1
Acetamiprid	4	4
Dinotefuran	4	4
Imidacloprid	4	4
P	4	4

** Results showed systemic errors which rendered the data uninterpretable*
*** ICP-OES QA/QC indicated poor results; some results were dropped resulting in poor graphical analysis*

3.1 Influent

Influent water chemistry varied slightly throughout the duration of each experiment. Contaminants spiked to lower concentrations will tend to show higher % variability than those with higher concentrations. Each IE ratio is calculated from the corresponding influent and effluent samples (whether measured or interpolated). Therefore, there should be no bias in results due to influent variability, rather this analysis is provided to demonstrate the necessity to sample influent values throughout the duration of the experiment rather than relying on an assumption of consistent influent concentrations.

pH was variable through the duration of the experiments. Generally, pH decreased over time with pH from both vertical column runs starting at or near 7.5 and ending at or near 6.5. An example of this for runs 1 and 2 is shown in Figure 3-1. Horizontal column influent pH initially was in the 7.7 to 8.0 range but generally followed a decreasing trend reaching 7.0 by the end of the experiment (Figure 3-2).

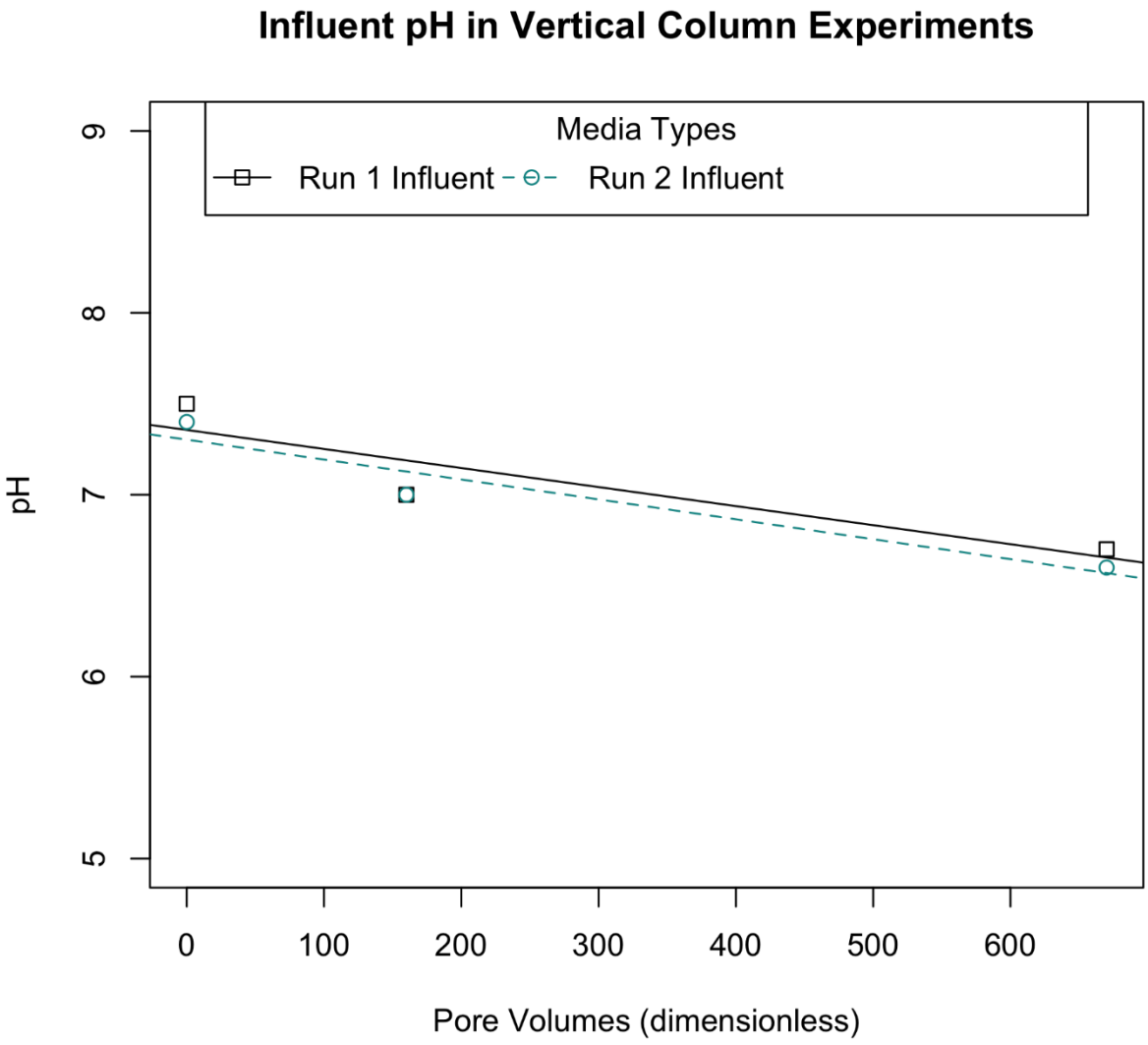

Figure 3-1 Influent pH in vertical column experiments

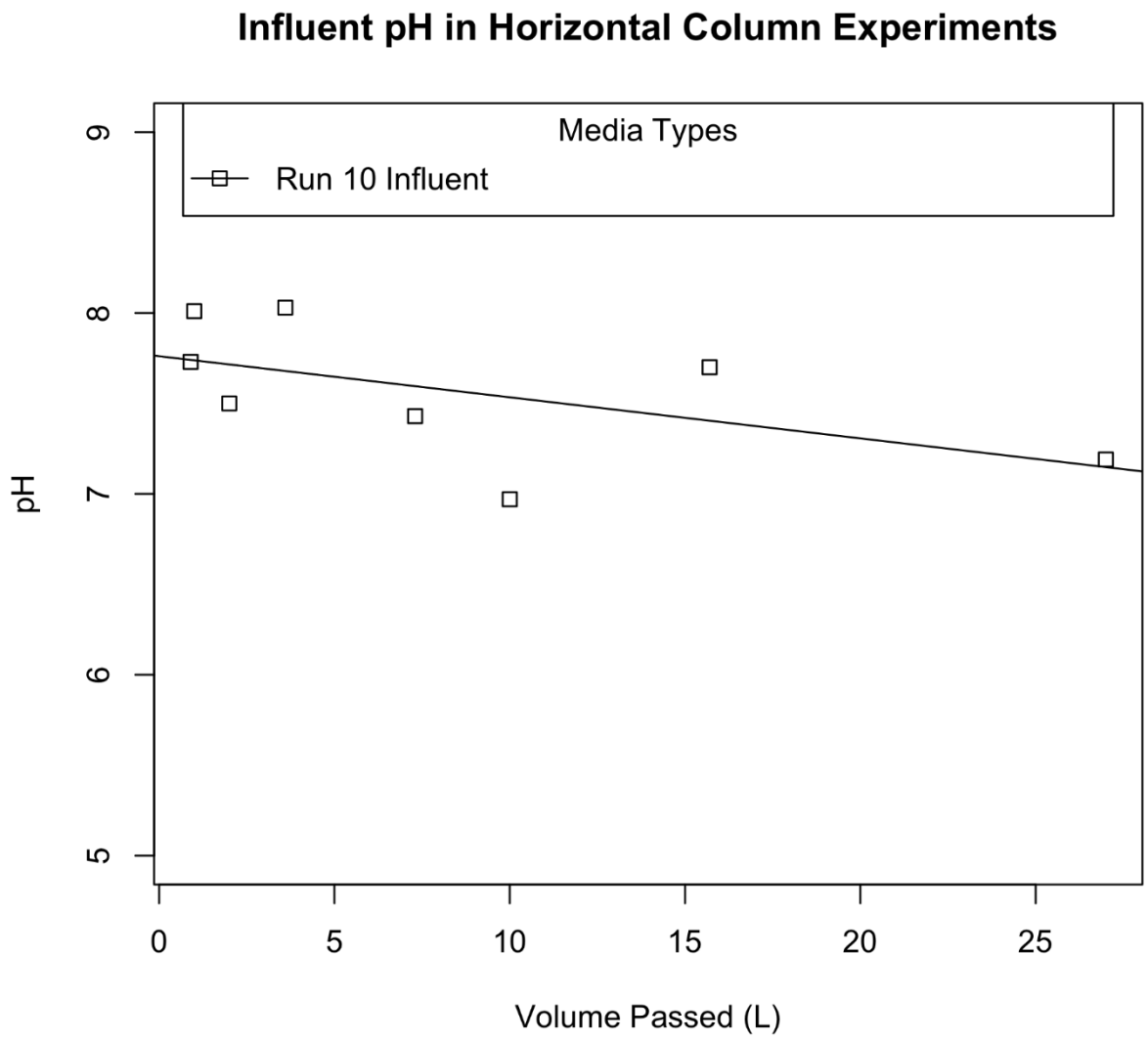

Figure 3-2 Influent pH in horizontal column experiments

Because of calibration issues with the conductivity probe during run 1, only half the data from the vertical column runs (Run 2) is available for analysis. Specific conductivity (SpC) in the available vertical column experiment initially was just below 80 µS cm^{-1} and showed a decreasing trend over time. The second measured influent point was 58.4 µS cm^{-1} with the final measured point at 50.0 µS cm^{-1} (Figure 3-3). The horizontal column experiment SpC was initially lower and showed a reverse trend of increasing over time. The first two influent SpC measurements were 50.8 µS cm^{-1} and 47.3 µS cm^{-1} after 0 L and 1 L passed, respectively. Generally, SpC showed an increasing trend over time with the final point of the experiment measuring 80.6 µS cm^{-1} (Figure 3-4).

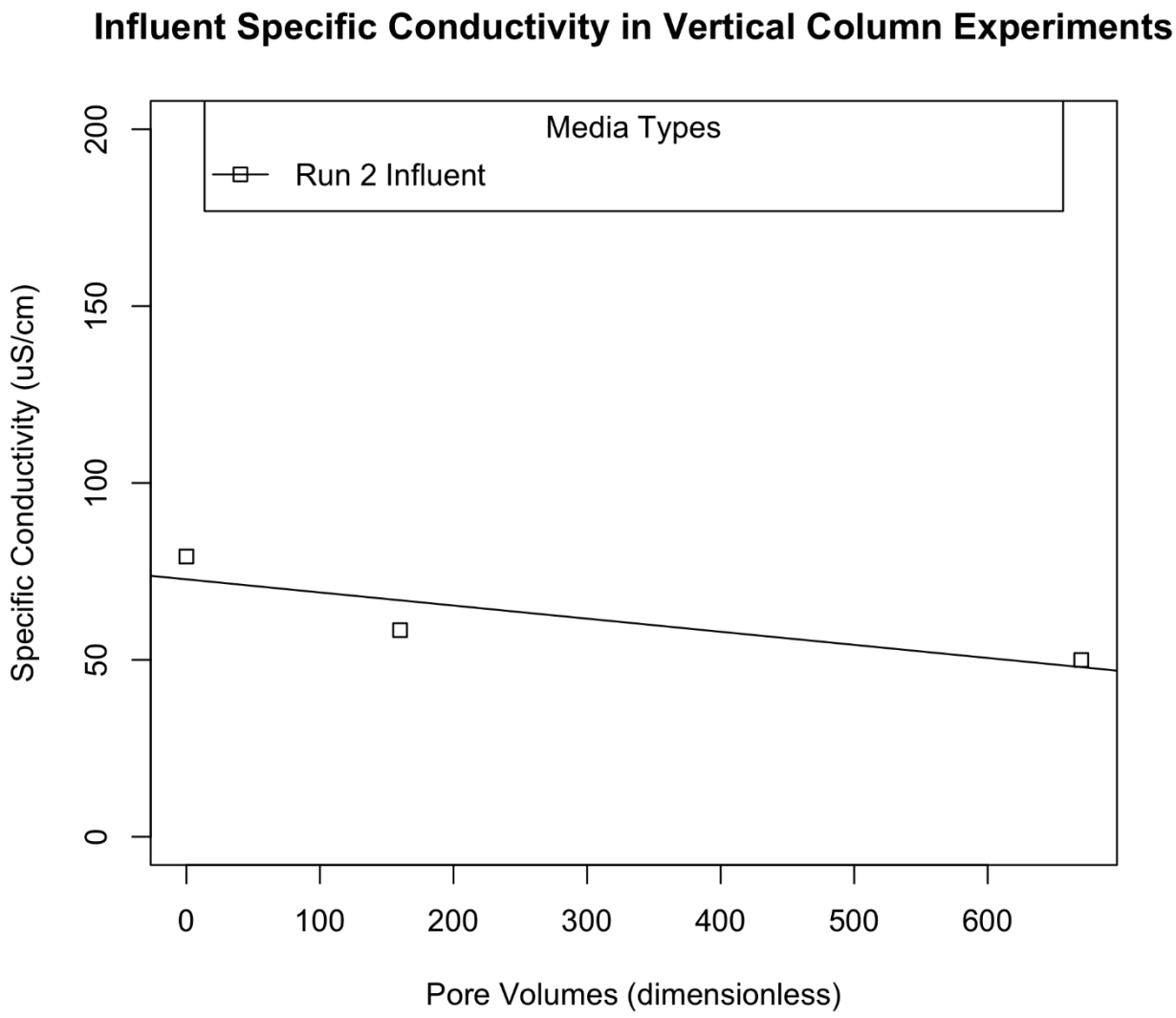

Figure 3-3 Influent specific conductivity in vertical column experiments (run 2 only due to calibration issues during run 1)

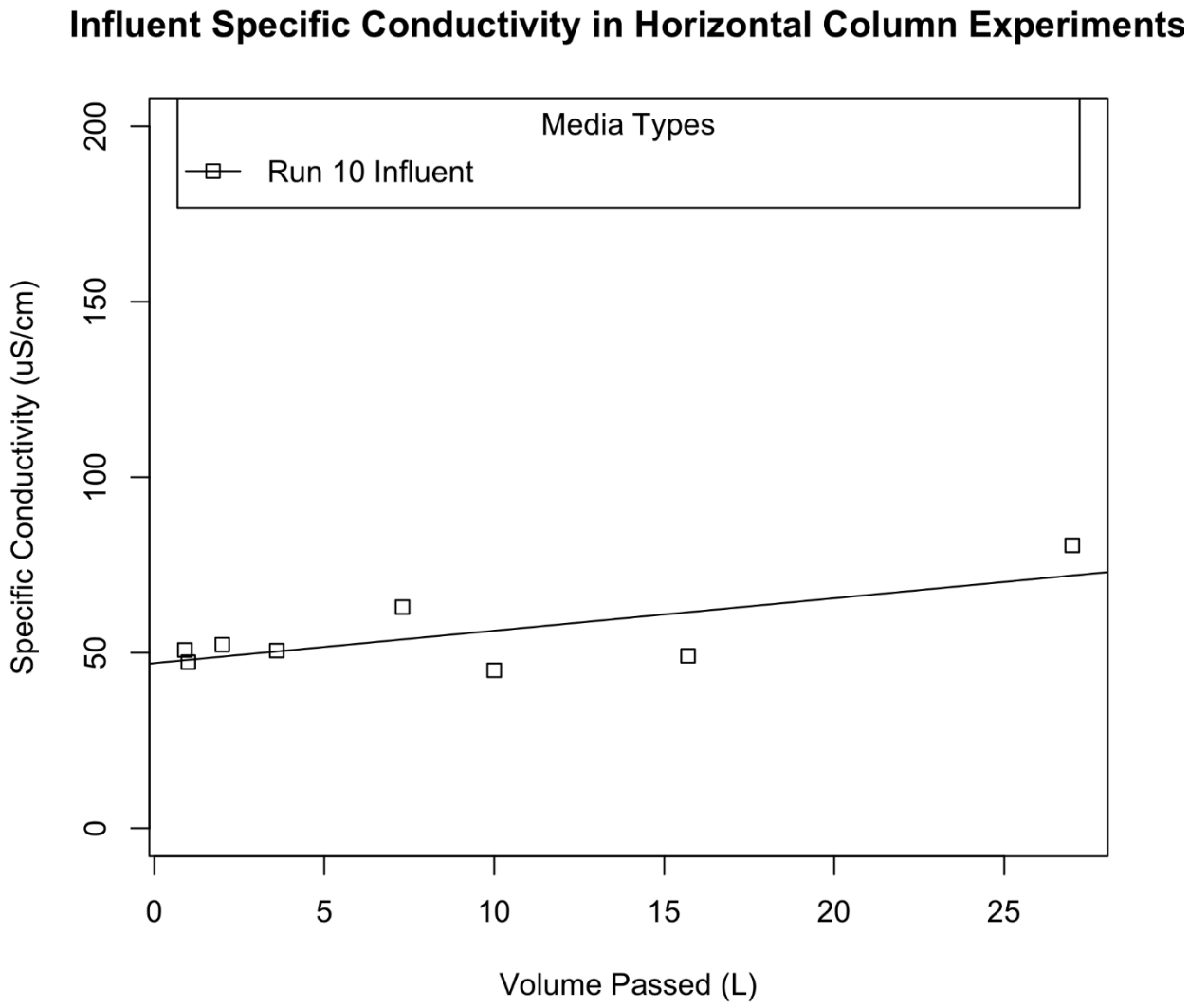

Figure 3-4 Influent specific conductivity in horizontal column experiments

3.2 QA/QC

Replicate samples were taken throughout all column experiments. Each analysis type (metals, phosphorus, and neonicotinoids) had two replicate pairs collected for each media type-column orientation combination. Full coefficient of variation (CV) results are included in Table 10-10 and Table 10-11. Al and As both had a single considerable exceedance for small steel slag in the vertical column (85% and 27%, respectively). Be and Mn had more exceedances with 4 and 6 considerable exceedances, respectively and 1 moderate exceedance each. Phosphorus replicates results showed all replicate values for small steel slag in the vertical column with considerable exceedances (25%, 90%, and 25%) and the majority of horizontal column replicates with exceedances (2 moderate and 3 considerable). Lastly, 4 samples (total of 10 moderate exceedances) showed CV exceedances in neonicotinoid samples. Neonicotinoid samples are known to have been highly diluted prior to analysis which is a likely source of variation in replicate samples.

Blank samples were collected once during each run to test the cleanliness of the sampling environment and as a QA check on the analytical method. All blank samples were returned with values below detection limits for all contaminants.

3.3 Vertical Columns

Vertical columns were run with the SSW as described with a constant flow rate of 6 mL min^{-1} with full saturation. Effluent samples were compared with the influent concentrations at the corresponding sample point to determine the influent-effluent ratio. In the case of vertical columns, influent concentrations were not measured at each sampling point, so influent concentrations were

interpolated from the 3 influent samples that were empirically measured throughout the duration of the experiment.

3.3.1 General Chemistry

Columns treated with biochar had no noticeable departure from the influent pH values with a pH ~7.5 and gradually decreasing to just below 7.0. Conversely, pH noticeably changed in columns containing aggregated fly ash and steel slag. Small steel slag impacted pH most noticeably with initial pH measured at 10.8 and moderate decline of pH over time to 10.5 by the end of the experiment. This slight decline in pH over time is consistent with the influent pH also declining throughout the experiment. Large and small aggregated fly ash showed an initial pH measured at 10.4 and decreasing slightly over time to an eventual pH of 9.8. Large steel slag also raised pH noticeably with an initial value measured at 10.2, declining over time to pH 9.8. Vertical column pH results can be seen in Figure 3-5.

Specific conductivity (SpC), where available, showed two different results. First, large steel slag had an initial SpC measured at 155.8 $\mu S\ cm^{-1}$ and decreased over time. Despite the linear regression used to visualize SpC (Figure 3-6), the data has a clear decaying trend with a lower asymptote appearing to be reached near 90 $\mu S\ cm^{-1}$. This indicates that large steel slag is a constant contributor of ions to solution and therefore to an increase in solution SpC. Both biochars, similar to pH, showed no noticeable change in SpC over time with the initial values measured at 58 $\mu S\ cm^{-1}$ and 52 $\mu S\ cm^{-1}$ for the large and small fractions, respectively. For small biochar, SpC immediately decreased to 51.7 $\mu S\ cm^{-1}$ after 1 L and both fractions stayed within 50 $\mu S\ cm^{-1}$ to 52.5 $\mu S\ cm^{-1}$ for the duration of the experiment.

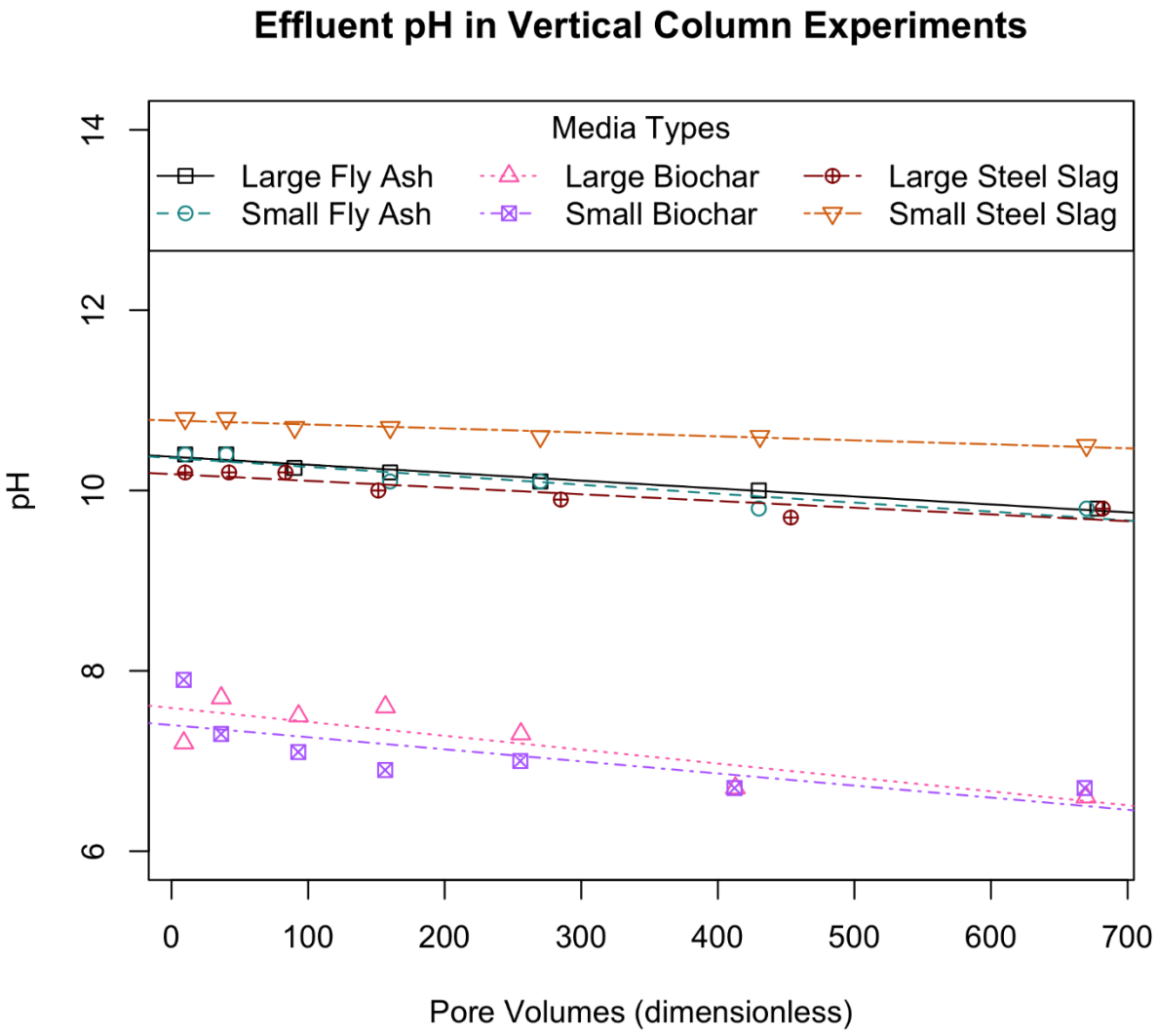

Figure 3-5 Effluent pH results from vertical column experiments

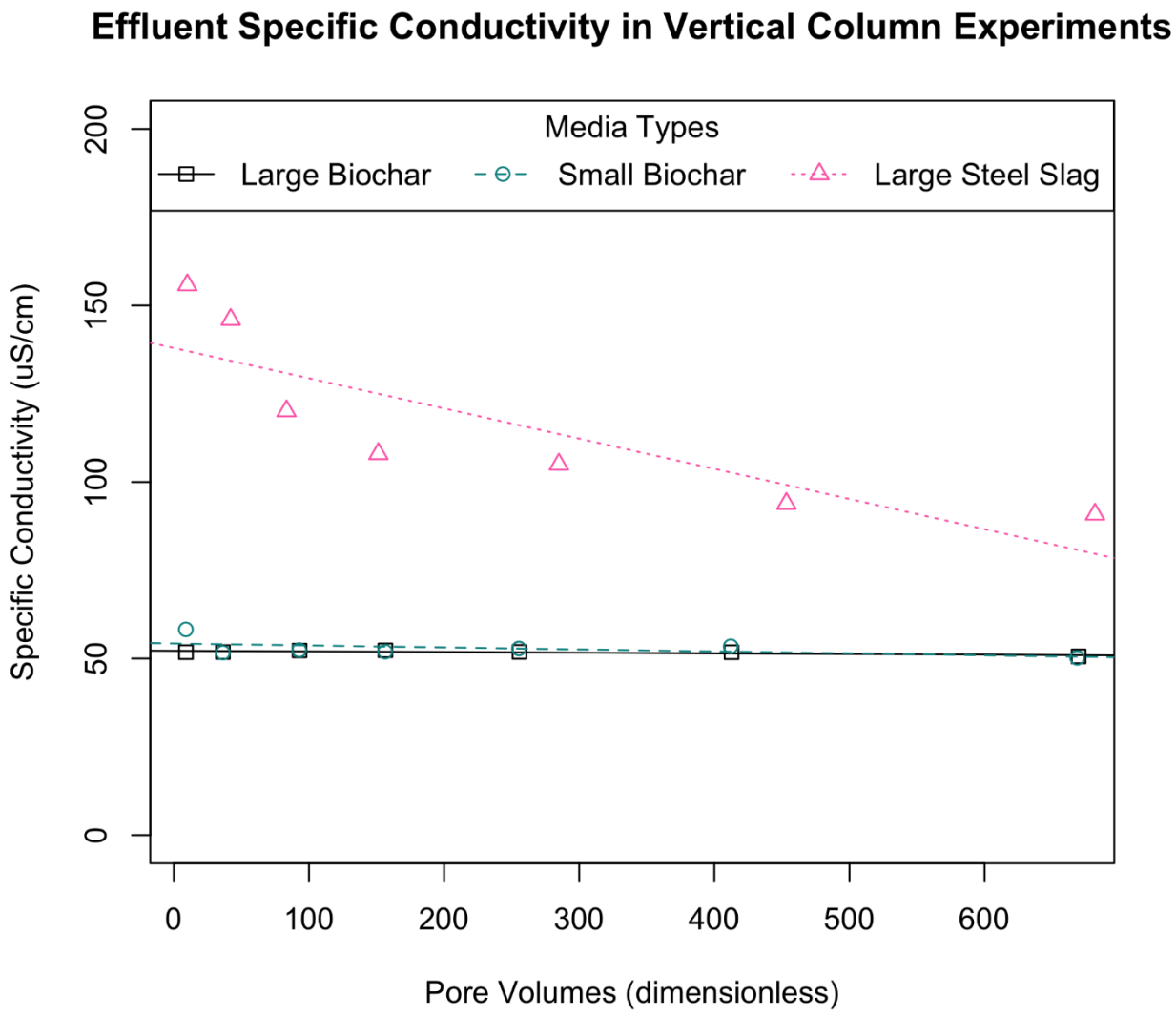

Figure 3-6 Effluent specific conductivity results from vertical column experiments (run 2 only due to calibration issues in run 1)

3.3.2 Metals

3.3.2.1 Aluminum (Al)

Despite aluminum's (Al) designation as category 4 in Table 3-1, only large and small biochar produced results of interest. The fitted model results indicated that biochar was effective in removing Al^{+3} from solution for the first 1 to 2 samples and quickly broke through with the model at or near an IE ratio of 1.0. Figure 3-7 below only plots results for small and large biochar. This is due to small and large sizes of both steel slag and aggregated fly ash leaching Al^{+3} into solution (category 3) and leaching ratios/quantities can be seen in Table 10-4 in the appendix. This media composition effect will be investigated in the Al discussion section.

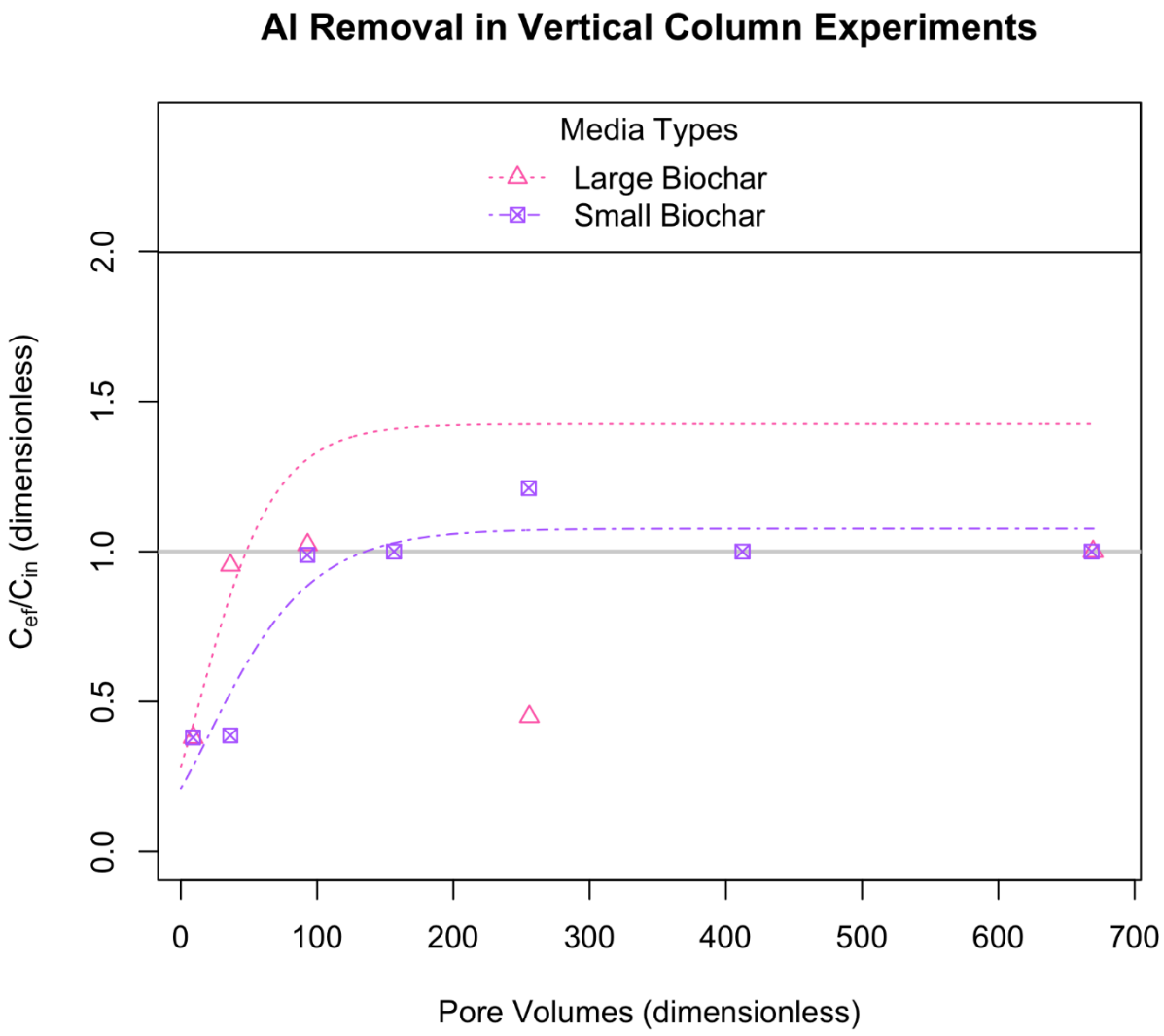

Figure 3-7 Dissolved Al^{+3} removal in vertical column experiments as demonstrated by the influent-effluent ratio as defined by effluent concentration (C_{eff}) divided by influent concentration (C_{in}) and plotted against pore volumes passed. Aggregated fly ash and steel slag is not shown due to Al^{+3} leaching which places IE ratio values outside the range of 0.0 – 2.0.

3.3.2.2 Arsenic (As)

As^{+5} removal (Figure 3-8) for all 6 media followed a very similar trend with no one medium standing out as outperforming the group ($p = 0.12 – 0.99$ and only small biochar and small aggregated fly ash significantly different from one another with two model parameters with $p < 0.05$). Initial removal ranged from around 20% removal (large and small biochar) to around 50% (large and small steel slag). Large aggregated fly ash and small steel slag reached an asymptote of ~0.85 indicating 15% As^{+5} removal after approximately 270 pore volumes. Fixing the asymptote to 1 for these two media predicts exhaustion at 840 pore volumes for small steel slag and 1575 pore volumes for large aggregated fly ash. All other media tapered off and achieved an upper asymptote that was within 0.05 of an IE ratio of 1.0.

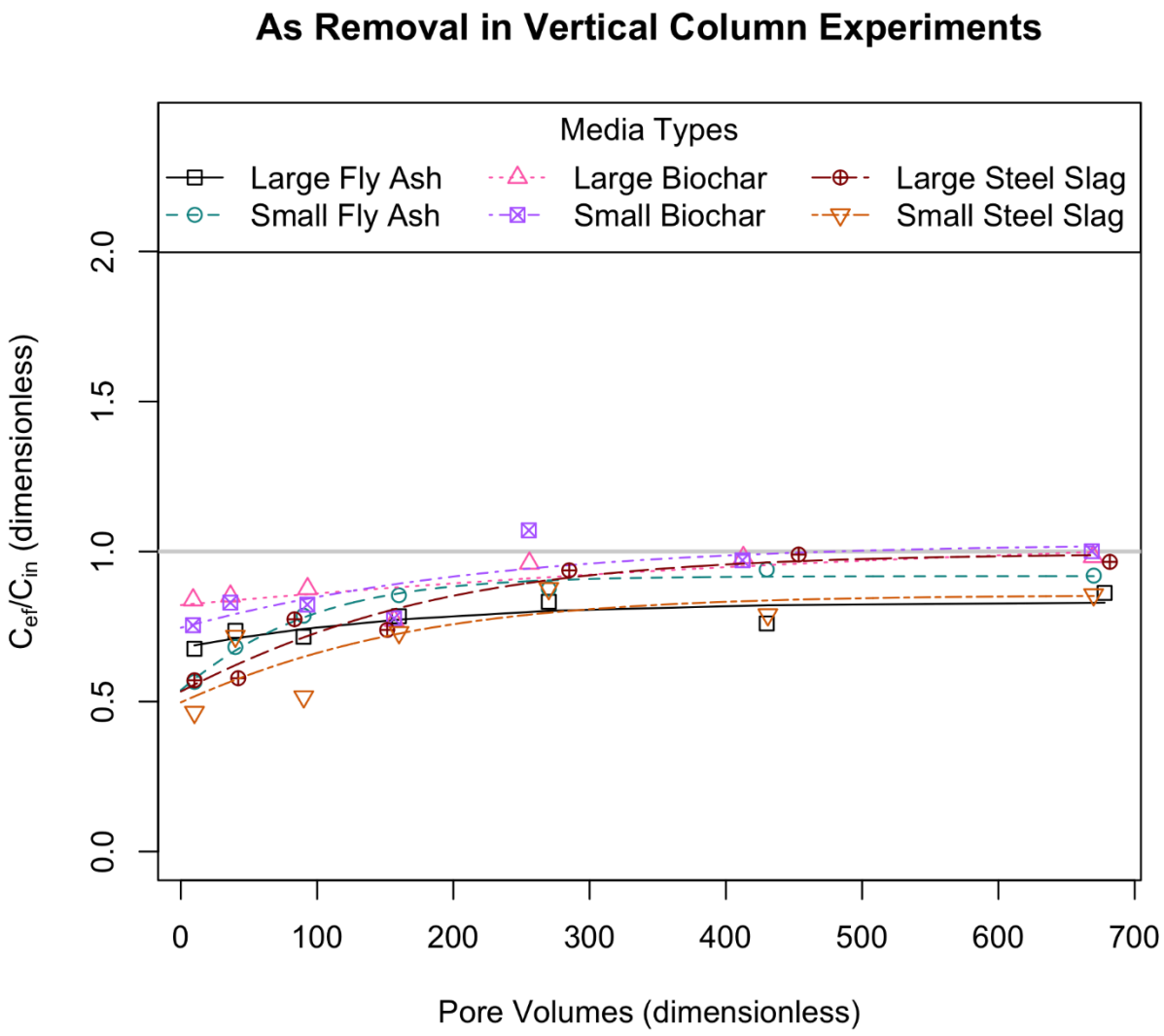

Figure 3-8 Dissolved As^{+5} removal in vertical column experiments as demonstrated by the influent-effluent ratio as defined by effluent concentration (C_{eff}) divided by influent concentration (C_{in}) and plotted against pore volumes passed.

3.3.2.3 Beryllium (Be)

Beryllium (Be) showed more a wider range of results than Al, with a variety of trends and removal efficiencies observed (Figure 3-9). Large steel slag was the only model which was significantly unique compared to all the vertical column results ($p = 0.03$). Initial Be^{+2} removal by large steel slag was around 55% and resulted in an upper IE ratio asymptote of 0.85. When the upper IE ratio asymptote is fixed to 1, the new model predicts an exhaustion at 810 pore volumes. Although not significantly so, large aggregated fly ash appeared to initially remove Be^{+2} well (75% after 40 pore volumes passed), with a relatively rapid tapering off to exhaustion at around 390 pore volumes. The model predicts that large aggregated fly ash will go above an IE ratio of 1.0 around 430 pore volumes indicating the later stages are leaching Be^{+2}. Initially small steel slag removed around 80% of Be^{+2} in solution however, by the end of the experiment, removal was around 25%. The Gompertz fit predicts an upper asymptote for small steel slag just above an IE ratio of 1 with exhaustion at approximately 1330 pore volumes. The results from the other materials reached an asymptote within the duration of the experiment. Initial removal was observed to be around 45% (small aggregated fly ash and small biochar), and around 25% (large biochar). Large biochar and small biochar achieved upper asymptotes below an IE ratio of 0.95, where small aggregated fly ash was deemed to be exhausted after approximately 300 pore volumes. When the asymptote is fixed to 1, small biochar reaches exhaustion at approximately 5320 pore volumes and large steel slag is precited to reach exhaustion at approximately 810 pore volumes. Large biochar did not result a predicted exhaustion value due to the negative slope of the curve at the termination of the experimental data.

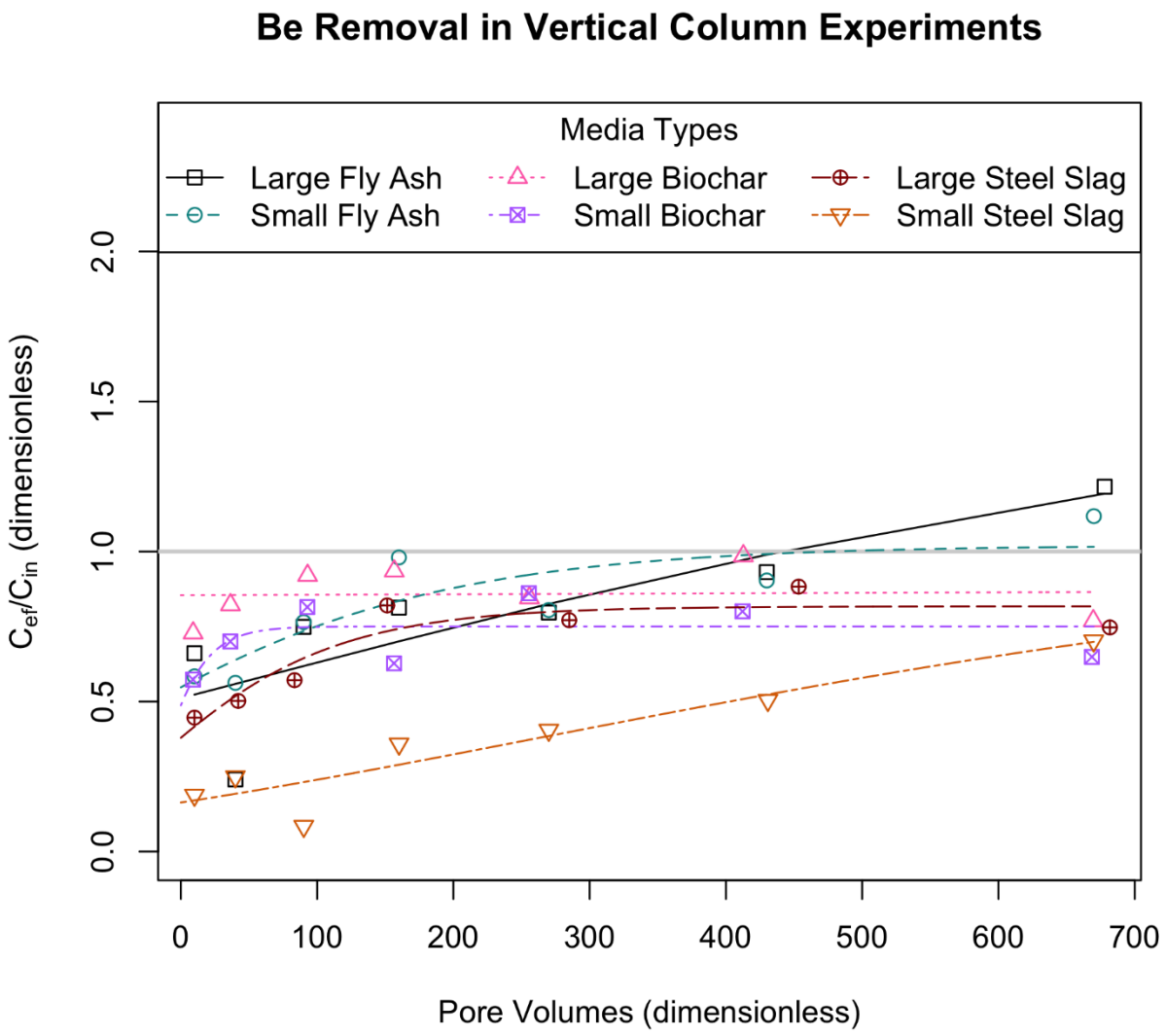

Figure 3-9 Be^{+2} removal in vertical column experiments as demonstrated by the influent-effluent ratio as defined by effluent concentration (C_{eff}) divided by influent concentration (C_{in}) and plotted against pore volumes passed.

3.3.2.4 Manganese (Mn)

Dissolved Mn^{+2} removal (Figure 3-10) results generally fall with two categories into two categories and all models were highly significant ($p \leq 0.001$). First, both large and small biochar appear to be a source of Mn^{+2} early in the experiment, eventually tapering to an IE ratio at or near 1.00. The second group includes both large and small aggregated fly ash and steel slag media types. All four media removed Mn^{+2} from solution with initial IE ratios ranging from 0.25 to 0.02 (75% removal to 98% removal). Both steel slags remained relatively constant throughout the experiment ending at an IE ratio of 0.30 (70% removal) and 0.06 (94% removal) for the large and small fractions, respectively. Both aggregated fly ash sizes visually appeared to have the same rate and magnitude with initial IE ratios of 0.10 (90% removal) and finishing at 0.25 (75% removal). Visually, small steel slag was the best performer followed by both sizes of aggregated fly ash. Aside from biochars, visually, large steel slag was the least effective, albeit with removal rates at or below 75% for the duration of the experiment. Both steel slags finished the experiment with a negative slope, so no exhaustion estimates, or upper IE ratio asymptote could be determined. Aggregated fly ash however yielded an upper IE ratio asymptote of 0.90 for the large fraction and 0.56 for the small. Because these did not reach the designated exhaustion IE ratio of 0.95, to determine exhaustion, the upper IE ratio asymptote was fixed to 1.00 which yielded exhaustion points at approximately 3970 pore volumes for large aggregated fly ash and 6400 pore volumes for small aggregated fly ash.

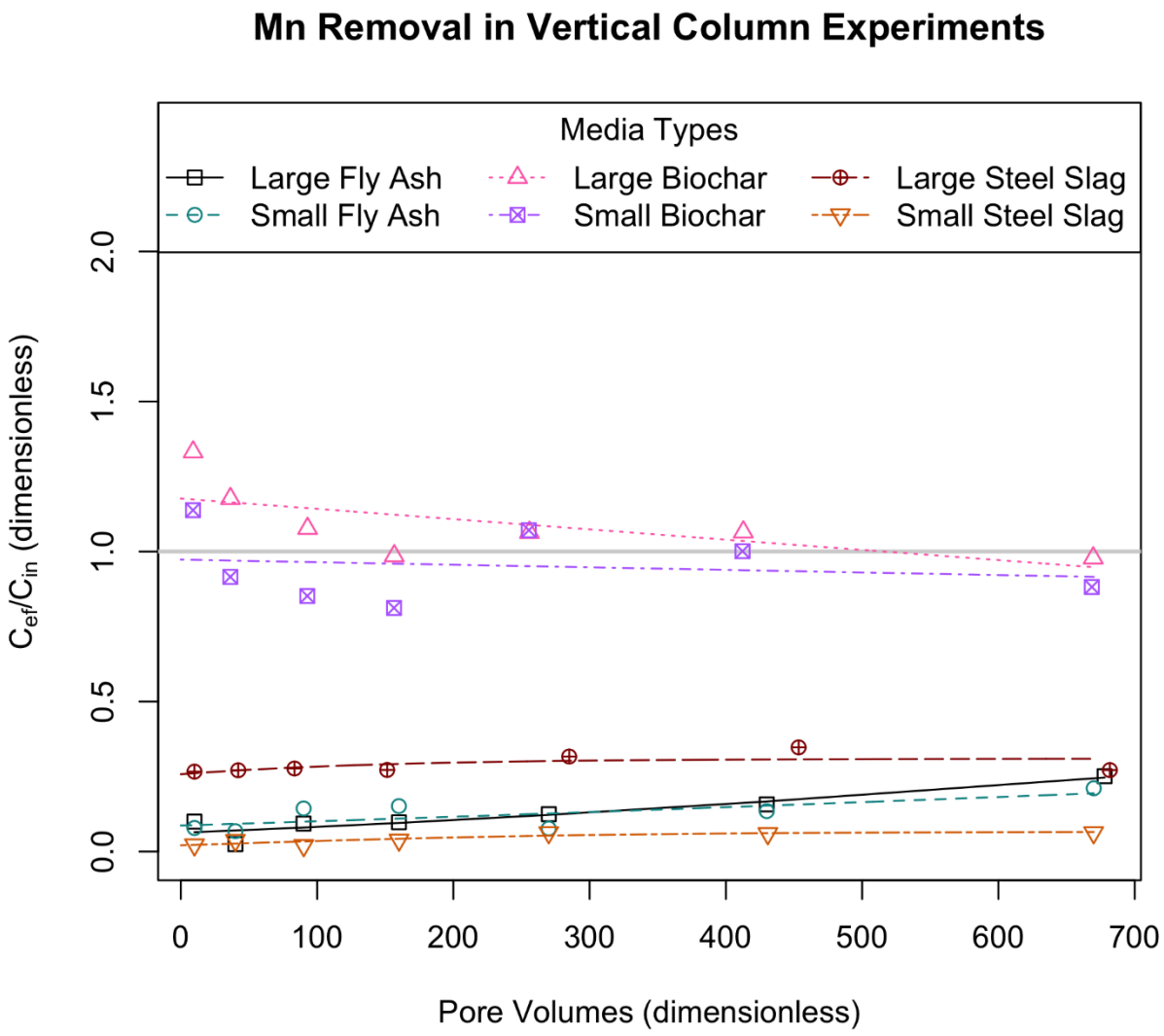

Figure 3-10 Mn^{+2} removal in vertical column experiments as demonstrated by the influent-effluent ratio as defined by effluent concentration (C_{eff}) divided by influent concentration (C_{in}) and plotted against pore volumes passed.

3.3.3 Neonicotinoids

Neonicotinoid results were analyzed as has been described. Each sub-species was analyzed separately to determine differences between different properties of each. Overall, results were consistent with variation in the overall magnitude of removal between the sub species.

3.3.3.1 Acetamiprid

Acetamiprid removal largely followed two patterns, one with a near-linear behavior over the duration of the experiment and one which follows a decaying asymptotic curve (Figure 3-11). Modeled results were significant ($p < 0.05$) for large biochar ($p = 0.04$), small biochar ($p = 0.04$), and small steel slag ($p = 0.01$) with large steel slag being highly significant ($p = 0.001$). Modeled curves for large and small aggregated fly ash were not statistically significant when compared to the collective results. Near-linear behavior was observed in large steel slag, small steel slag, and large aggregated fly ash at different removal levels. Large steel slag initially was not removing nor leaching acetamiprid into solution, however by 430 pore volumes, the IE ratio became >1.0. Large aggregated fly ash initially removed just under 50% of acetamiprid from solution with a near-linear decline in removal efficiency finishing at around 10% removal. Small steel slag removed nearly 80% of acetamiprid from solution initially and removal declined over time to about 40% removal (highest ending removal rate). Small steel slag did show a slight decay starting at around 270 pore volumes but generally appeared to decrease in removal efficiency in a near-linear fashion through the duration of the experiment. Asymptotic decay curves best describe small aggregated fly ash and both biochar removal of acetamiprid. Large biochar had an initial removal of about 45% with a steady decay finishing the experiment within 0.05 of an IE ratio of 1.00. Small biochar started with the second-best removal at around 75% and tapered off to about 15% by the end of

the experiment. Small aggregated fly ash had an initial removal of about 60% and by 270 pore volumes, the curve indicates an asymptote was reached at about 20% removal (upper IE ratio asymptote 0.79). Upper IE asymptotes were 1.99, 0.79, 0.96, 0.86, 4.38, and 0.81 for large and small aggregated fly ash, large and small biochar, and large and small steel slag, respectively. Exhaustion was reached at approximately 870, 660, and 63 pore volumes for large aggregated fly ash, large biochar, and large steel slag, respectively without having to fix the upper IE ratio asymptote. For all small media, the upper IE ratio asymptote was fixed to 1.00, which yielded an exhaustion estimate of approximately 830, 650, and 1520 pore volumes for small aggregated fly ash, small biochar, and small steel slag, respectively.

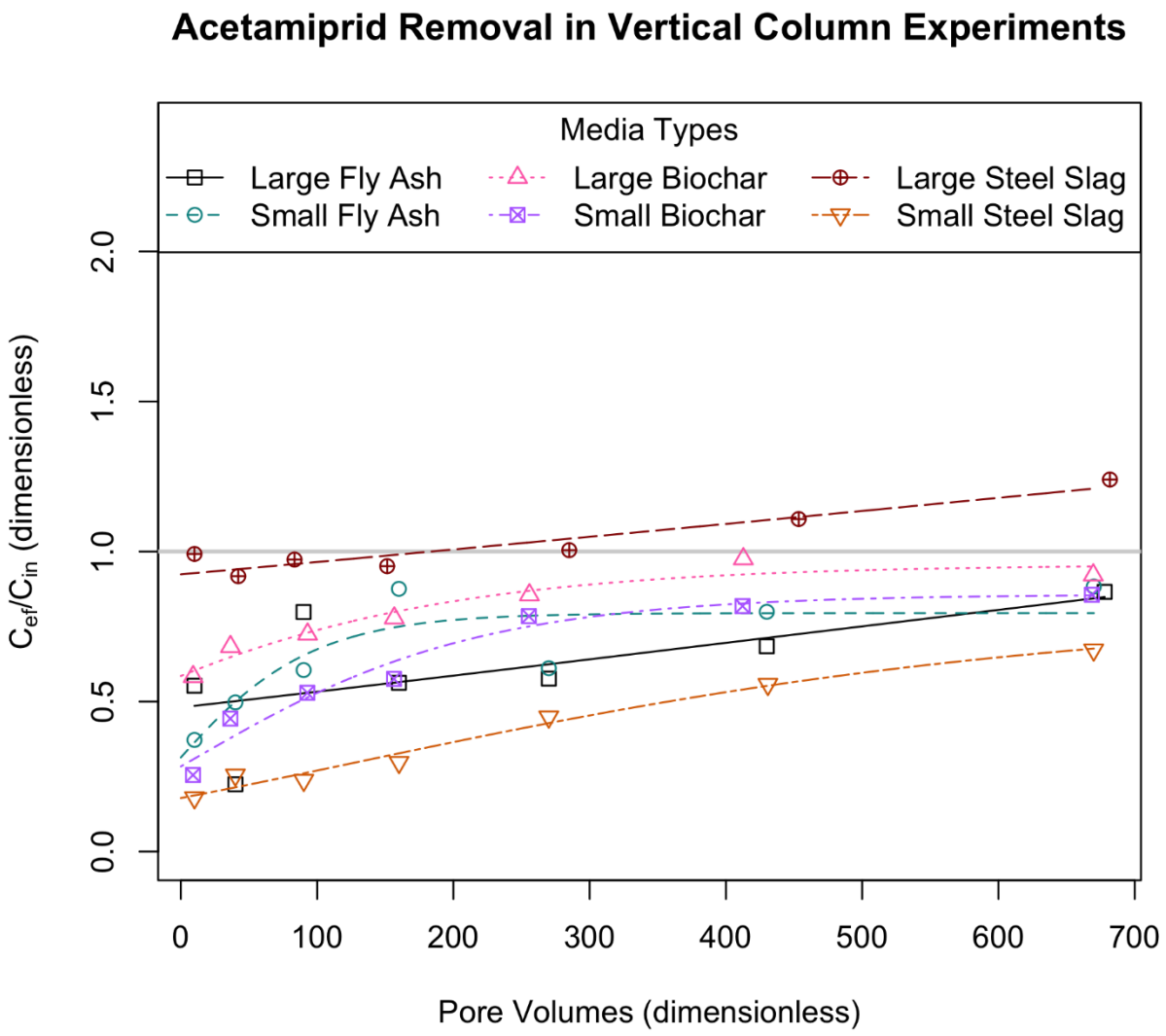

Figure 3-11 Acetamiprid removal in vertical column experiments as demonstrated by the influent-effluent ratio as defined by effluent concentration (C_{eff}) divided by influent concentration (C_{in}) and plotted against pore volumes passed.

3.3.3.2 Dinotefuran

Dinotefuran results (Figure 3-12) yielded only one statistically unique modeled fit with small biochar ($p = 0.09$). Small biochar initially had the best dinotefuran removal of 50% and the modeled removal rate tapered off to 0% removal by the end of the experiment. Although not significant, large biochar showed a similar pattern albeit with a lower initial removal of around 25%. Large biochar's exhaustion was predicted at 200 pore volumes while the small fraction was predicted at 280 pore volumes. Visually, large aggregated fly ash and small steel slag had similar magnitudes and trends both initially measured to remove between 20 and 25% of dinotefuran with removal modeled at the same rate for the duration of the experiment. Large steel slag was measured to initially remove little to no dinotefuran, and the modeled trend showed small steel slag with an IE ratio above 1.0 by approximately 160 pore volumes with a final measured IE ratio of approximately 1.55.

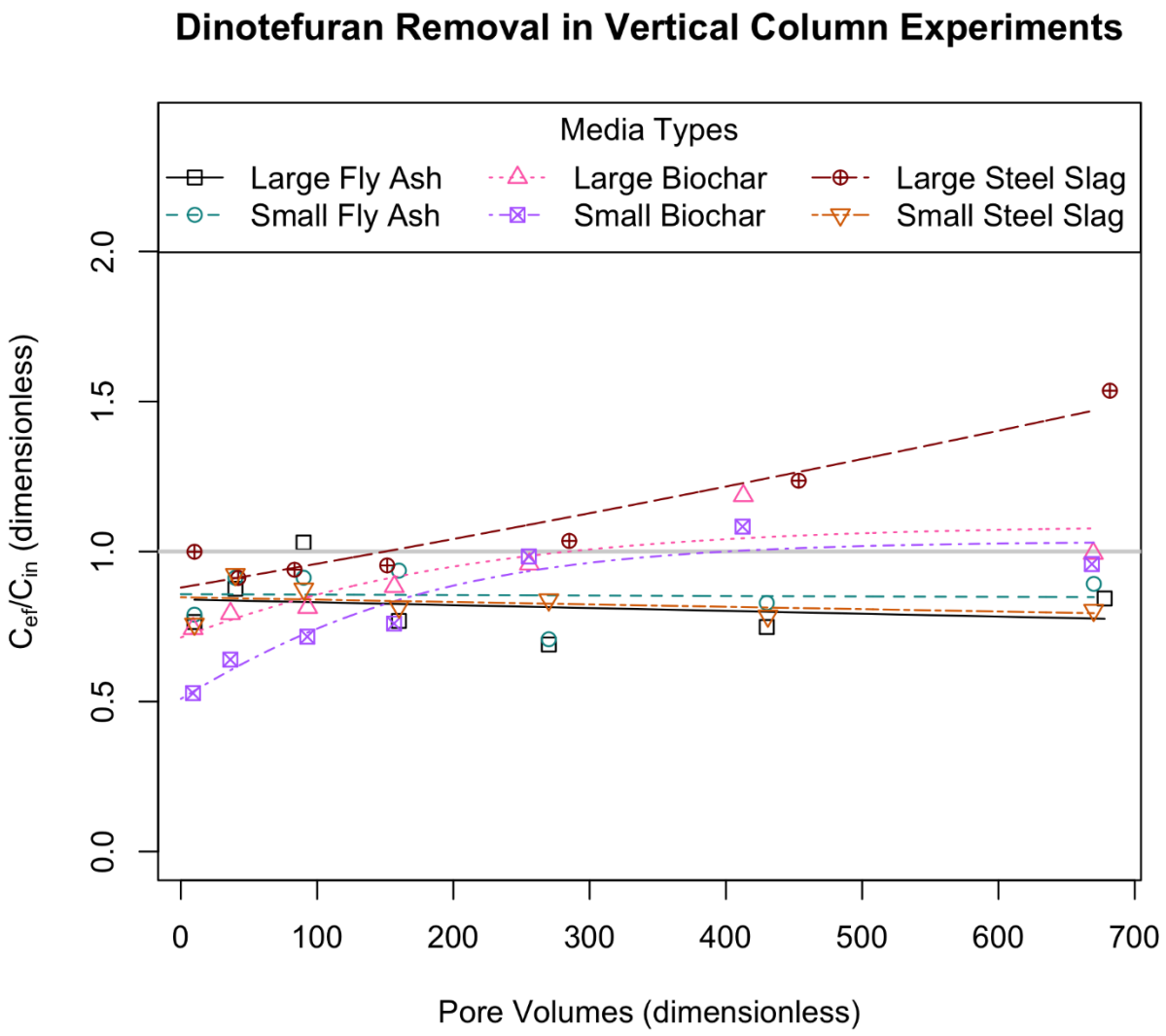

Figure 3-12 Dinotefuran removal in vertical column experiments as demonstrated by the influent-effluent ratio as defined by effluent concentration (C_{eff}) divided by influent concentration (C_{in}) and plotted against pore volumes passed.

3.3.3.3 Imidacloprid

Data from imidacloprid (Figure 3-13) resulted in two media with significantly unique model fits: large biochar ($p = 0.06$) and small biochar ($p = 0.02$). Visually, both model fits are very similar, and in fact, all parameters for both biochar sizes were not unique (parameter pairwise p values all >0.05). Large biochar had an initial removal rate of approximately 50% and the model tapered off asymptotically to an IE ratio just below 1.0 and exhaustion modeled at 520 pore volumes. The same trend was observed with small biochar however at a magnitude of removal higher than the large fraction. Initial removal was 75% and tapered to a removal rate of 15% by approximately 430 pore volumes passed. When the upper IE ratio asymptote is fixed to 1.0 and the model re-run, the predicted exhaustion point is 630 pore volumes. Pairwise comparison of the model parameters for both aggregated fly ash sizes determined no significant difference between the modeled fit between each size (all parameter pairwise comparison > 0.05), nor are the results for either determined to be unique ($p = 0.99$; 0.70). Visually, both had an initial removal rate between 40 and 50% and tapered to a removal rate between 10 and 20%. The fitted model predicts an eventual upper asymptote for large aggregated fly ash at 1.58 after 1200 pore volumes. Small aggregated fly ash, on the other hand, has an upper IE ratio asymptote fitted at 0.81, therefore the model was re-run with the asymptote set at 1.0 which yielded a predicted exhaustion after 950 pore volumes. Lastly, the two steel slag sizes were quite different despite only one model parameter being statistically unique ($p << 0.001$). Small steel slag had an initial removal of 70% and had a mild taper resulting in a removal rate of 25% by the end of the experiment. The upper IE ratio asymptote was modeled at 0.79, therefore that parameter was fixed to 1.0 and the model re-run. This resulted in a predicted exhaustion at 1660. Large steel slag had initial removal rates at or near 0% then eventually increasing to a final upper IE ratio asymptote of 4.60.

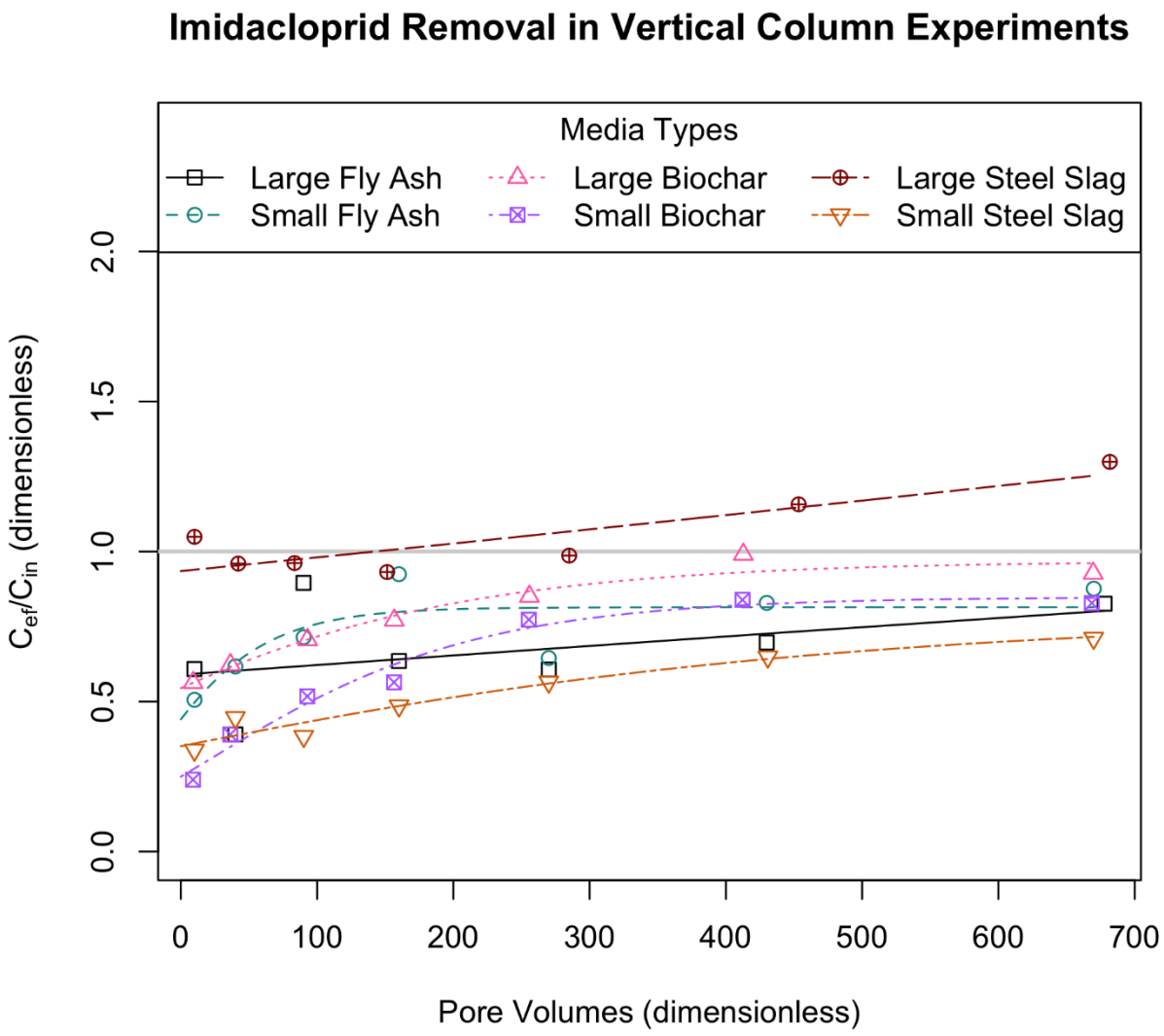

Figure 3-13 Imidacloprid removal in vertical column experiments as demonstrated by the influent-effluent ratio as defined by effluent concentration (C_{eff}) divided by influent concentration (C_{in}) and plotted against pore volumes passed.

3.3.4 Phosphorus

Phosphorus removal from solution (Figure 3-14) is generally be broken into three categories: no removal or leaching, removal then exhausted/leaching, and constant removal. Large biochar yielded a statistically unique result ($p = 0.03$) as well as large steel slag ($p = 0.003$). Both biochar fractions neither removed nor leached P into solution. A pairwise comparison of the model parameters was not able to be run, however, visually, their results are highly similar. Second, both sizes of aggregated fly ash and large steel slag initially removed some P but all finished the experiment neither removing or leaching large amounts of P into solution. Parameter pairwise comparisons between these three media demonstrates that the small aggregated fly ash and large steel slag are unique from one another (two parameters with $p < 0.1$) and large aggregated fly ash and large steel slag are similar, but not entirely so with one parameter statistically unique between them ($p = 0.001$). Despite these curves being somewhat unique from one another, the category of removal and exhaustion/leaching still holds true. Initially large aggregated fly ash removed nearly 85%, small aggregated fly ash removed around 70%, and large steel slag removed just under 50%. Upper IE ratio asymptotes were measured at 0.96 for large steel slag and 1.09 for both large and small aggregated fly ash. Exhaustion was reached at 402, 395, and 367 pore volumes for large aggregated fly ash, small aggregated fly ash, and large steel slag, respectively. The last category was small steel slag alone which yielded an initial removal near 85% and a steady decay was observed with a final removal measure at 50%. The upper asymptote was measured at 0.45 (55% removal) and when the upper IE ratio asymptote was fixed to 1.00, the exhaustion was estimated to be at 2280 pore volumes.

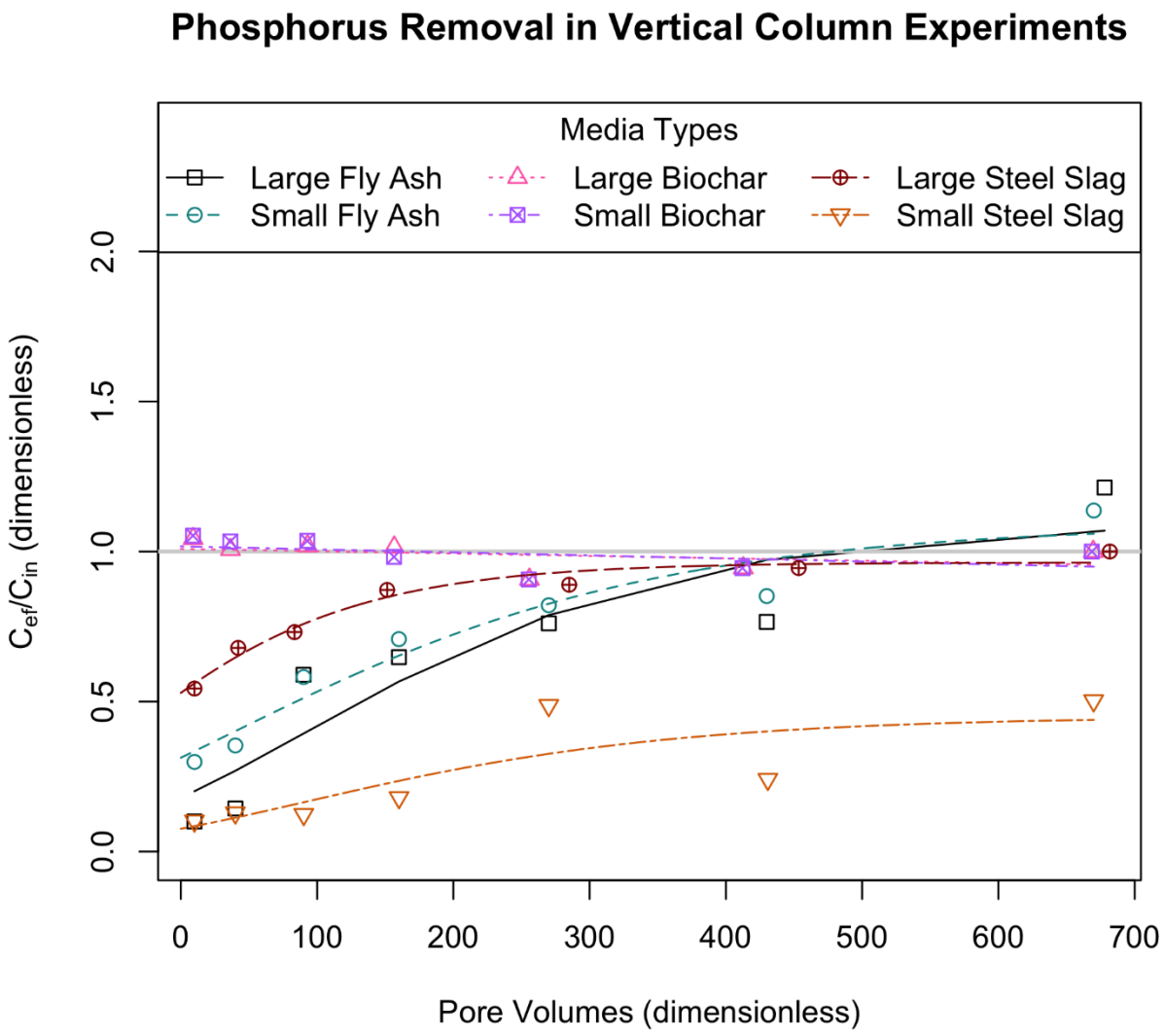

Figure 3-14 Phosphorus removal in vertical column experiments as demonstrated by the influent-effluent ratio as defined by effluent concentration (C_{eff}) divided by influent concentration (C_{in}) and plotted against pore volumes passed.

3.4 Horizontal Columns

This horizontal column orientation included the implementation of a "bioretention simulation" where a vertical column filled with concrete sand fed into a horizontal tube filled with the media of study. Although the exact composition of the concrete sand is not known, the control column results provide an understanding of the impact of the sand on the solution chemistry. Results for this orientation primarily focus on the separation of experimental columns (i.e. columns containing the media of study) from the control column (only a vertical tube with concrete sand).

3.4.1 General Chemistry

The pH in the control column (Figure 3-15) showed that sand alone facilitated a reaction that increased solution pH with initial pH values measuring 10.2 and 10.3 for the 0 L and 1.0 L measuring points. Solution pH generally decreased over time with the final pH measured at 9.8. Biochar showed the same trend as was shown in the vertical columns (Figure 3-5) with effluent pH initially at 8.1. Biochar effluent pH was within a relatively tight window of 7.5 to 8.7 pH units. Treatment with steel slag yielded an increase solution pH with an initial effluent pH of 11.9 and a generally decreasing trend over time resulting in a final pH of 11.2. Lastly, aggregated fly ash also increased solution pH with an initial pH measured at 11.3. For the first 5 measured points (0 L to 10 L) pH generally was increasing with pH measured at 11.8 at 10 L. However, the latter half of the experiment saw decreasing pH with the final two points (17 L and 27 L) measuring 11.2 and 10.7, respectively, which lead to an overall decreasing trend in the data.

Effluent SpC in horizontal column experiments (Figure 3-16) showed two very distinct trends. First, both the control and the biochar showed a slight increase in SpC from the influent values measuring between 70 $\mu S\ cm^{-1}$ and 80 $\mu S\ cm^{-1}$ through the duration of the experiment. Two

notable exceptions to this were the 1 L and 6 L biochar sampling points. The 1 L point was measured at 731 µS cm^{-1} which severely skewed the linear regression and was likely a result of fines flushing through the sample setup. Furthermore, the 6 L measurement was slightly above the 70-80 µS cm^{-1} range, measuring at 93.5 µS cm^{-1}. Steel slag showed a near identical relationship to the vertical columns only with values spiking much higher than those observed in the vertical columns (approximately 150 µS cm^{-1}). The initial SpC measurement was 775 µS cm^{-1} and despite the linear regression, the data shows a decaying curve which appears to be reaching a lower asymptote between 250 µS cm^{-1} and 350 µS cm^{-1}. Aggregated fly ash showed a similar relationship to steel slag, only with initial SpC values of approximately 500 µS cm^{-1} but a tapering to a similar SpC around 200 µS cm^{-1}.

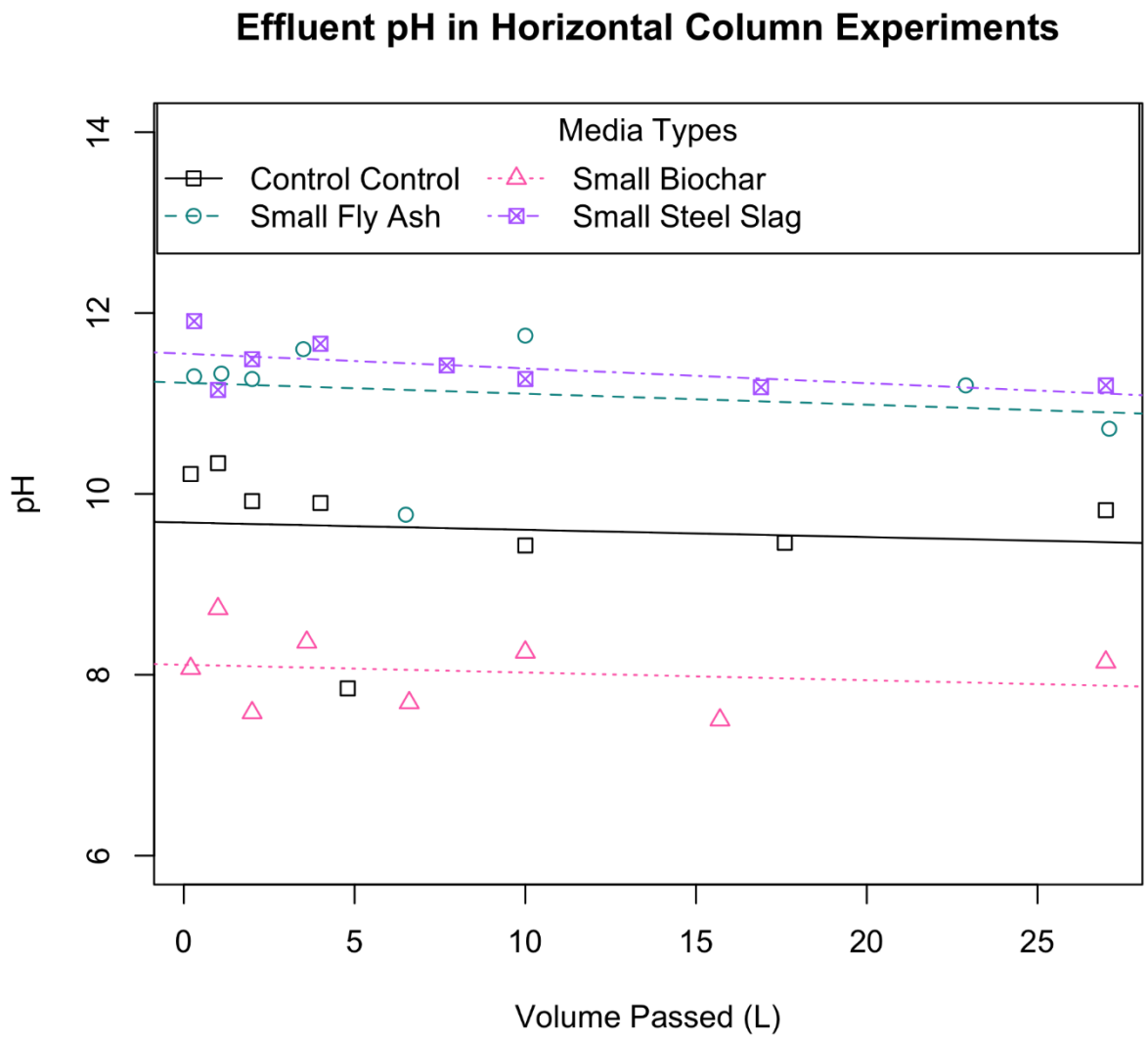

Figure 3-15 Effluent pH results from horizontal column experiments.

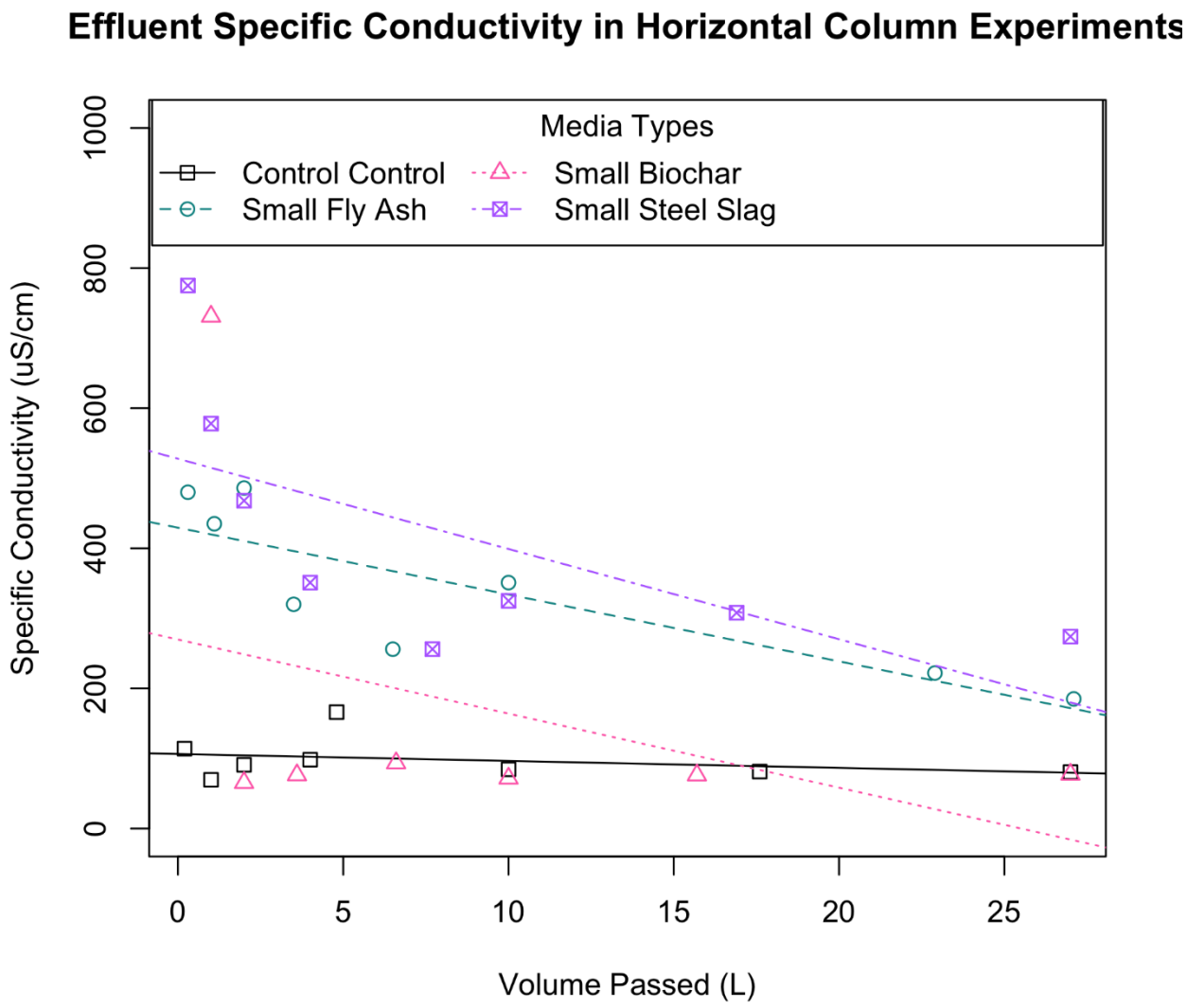

Figure 3-16 Effluent specific conductivity results in horizontal column experiments.

3.4.2 Metals

Horizontal metal results yielded many results below the detection limit, therefore hindering the discussion of the horizontal orientation's effect on metal concentrations in solution. Furthermore, other metals yielded data above detection limits, however, there was no noticeable departure from the control column indicating any contaminant removal/leaching is likely solely due to the impact of the bioretention simulation sand. These categories can be referenced in Table 3-1.

3.4.2.1 Arsenic (As)

Arsenic (As) results from the horizontal column experiment showed a noticeable separation from the control column (Figure 3-17) with the control column remaining at or around an IE ratio of 1.00 for the entirety of the experiment. Although for some points the biochar performed marginally better than the control, results was not a far enough departure from the control to constitute the biochar adding any additional removal of As^{+5} from solution. Pairwise comparisons of the fitted model parameters were unsuccessful due to a square root of a negative error in the pairwise calculations. Despite a visual separation between the control and aggregated fly ash columns, both were not determined to be uniquely different from the whole of results ($p > 0.05$). In spite of this, initial As^{+5} concentrations in the aggregated fly ash column was reduced by just below 50%. Removal decayed over time to an upper IE ratio asymptote of 0.81 (19% removal) at around 10 L passed through the columns. If the upper IE asymptote is fixed to 1.00, aggregated fly ash reaches exhaustion at 55 L passed. Steel slag was statistically unique ($p = 0.01$) and had a traditional s-curve relationship. Dissolved As^{+5} removal initially was at or just below 100% followed by a period of exponential decrease in removal. The curve reached an inflection point at

about 10 L passed where the removal was measured to be about 80%. The curve then entered exponential decay and the experiment ended with a removal of about 45%. The upper IE ratio asymptote for steel slag was fit at 0.63, and with the upper IE ratio asymptote fixed to 1.00, the estimated exhaustion is reached at 51 L.

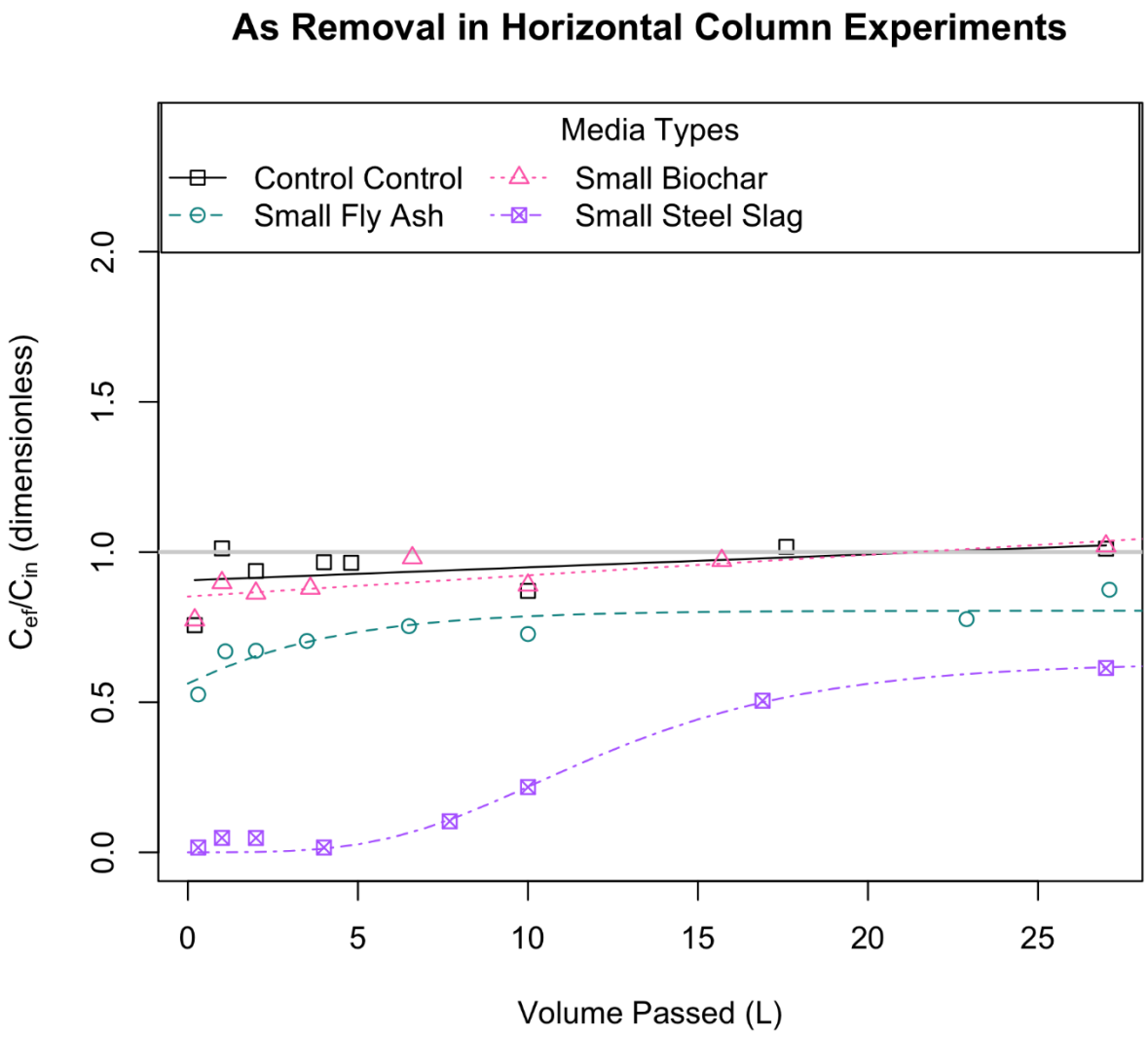

Figure 3-17 Dissolved As^{+5} removal in horizontal column experiments as demonstrated by the influent-effluent ratio as defined by effluent concentration (C_{eff}) divided by influent concentration (C_{in}) and plotted against volume passed.

3.4.3 Neonicotinoids

All three neonicotinoid results (acetamiprid, dinotefuran, and imidacloprid) yielded the same removal relationship between the three media and the control (Figure 3-18, Figure 3-19, and Figure 3-20). The control column showed little to no removal (IE ratio 0.85-1.00) of neonicotinoids through the duration of the experiments. For each neonicotinoid, no change in removal was shown from start to finish with approximately 15% of acetamiprid, 0% dinotefuran, and 5% imidacloprid removed by the control column. Across all three neonicotinoids, there was an initial departure from the control for aggregated fly ash and steel slag followed by a convergence to the same removal as the control column. Although, the control, biochar, and steel slag models are all not statistically unique and model parameter pairwise comparisons were not successfully run due to a mathematical error in the statistical calculations. Initial removal for acetamiprid was 50% and 40% for aggregated fly ash and steel slag respectively with these models converged with the control near 15 L passed. For dinotefuran very little of a departure was observed with both aggregated fly ash and steel slag accounting for <10% removal initially and converging to 0% removal around 13 L passed. Lastly, imidacloprid removal was initially approximately 20% for both aggregated fly ash and steel slag with curves converging with the control column by the end of the experiment.

Notably, however, biochar yielded significant results across all three neonicotinoids $p << 0.01$ for acetamiprid and imidacloprid and $p = 0.05$ for dinotefuran). For acetamiprid and imidacloprid, biochar maintained a removal between 90% and 100% for the entirety of the experiment with little to no fluctuation in results. Because no upward or downward trend was identified for these two media, no upper IE ratio asymptote was able to be calculated. For dinotefuran, biochar had removal rates similar to the other two neonicotinoids, however, around 7 L passed, there was a noticeable decrease in removal, albeit still removing between 70% and 80%

of dinotefuran from solution. The Gompertz curve fit the data with a near-linear fit and calculated an eventual upper IE ratio asymptote of 0.37 (63% removal). If the upper IE ratio asymptote is fixed to 1.00, then exhaustion would be estimated to be after 134 L passed.

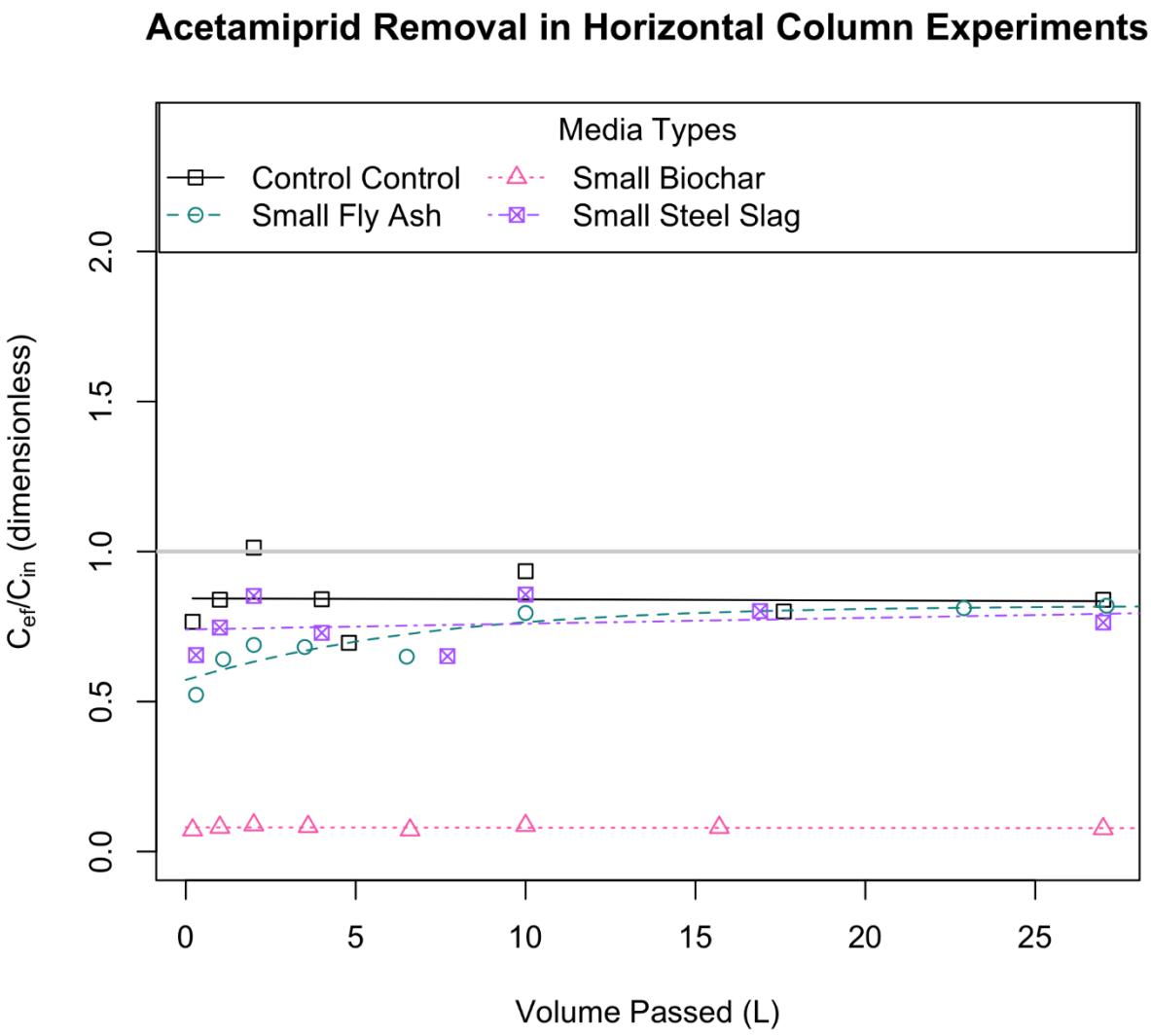

Figure 3-18 Acetamiprid removal in horizontal column experiments as demonstrated by the influent-effluent ratio as defined by effluent concentration (C_{eff}) divided by influent concentration (C_{in}) and plotted against volume passed.

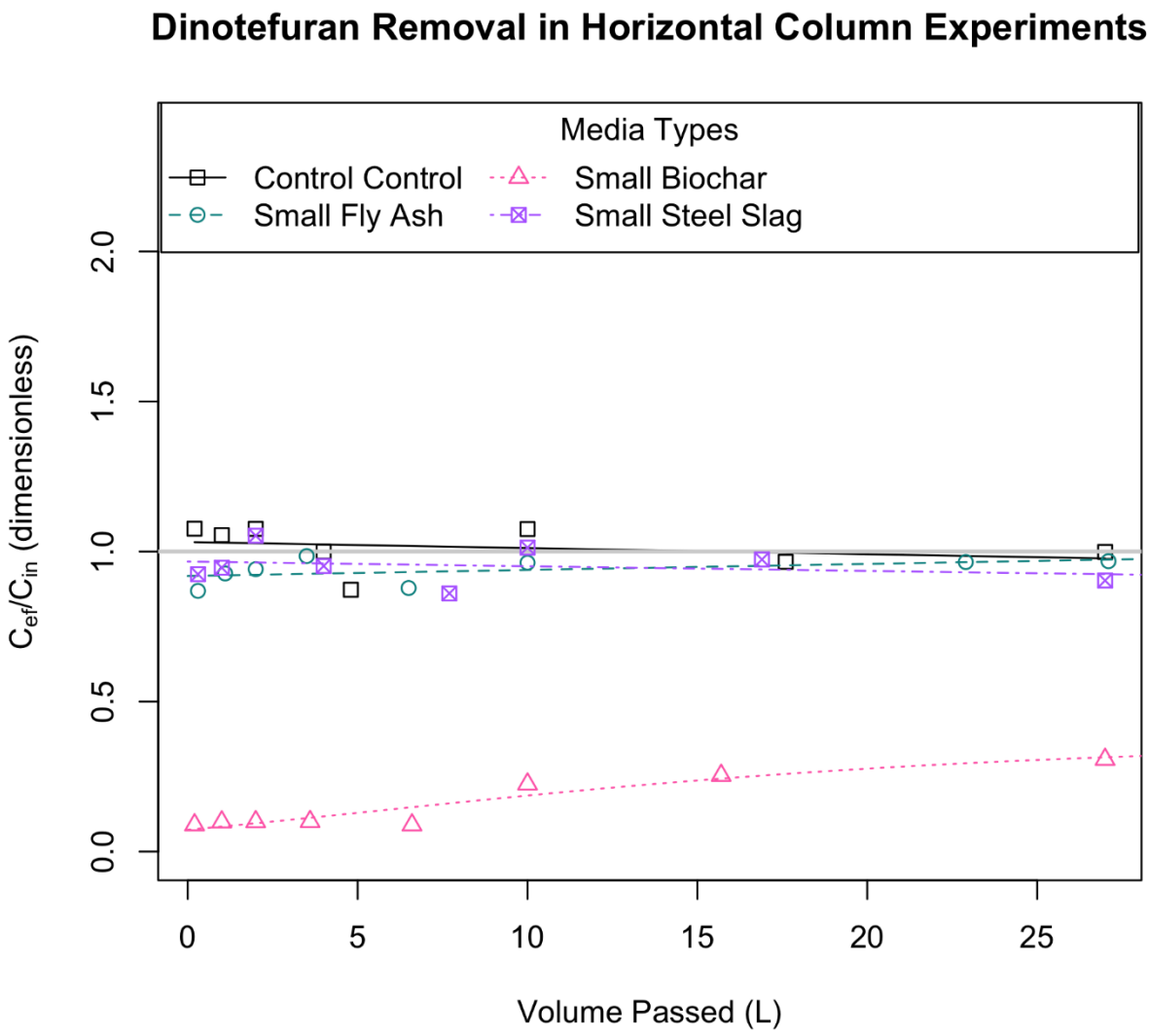

Figure 3-19 Dinotefuran removal in horizontal column experiments as demonstrated by the influent-effluent ratio as defined by effluent concentration (C_{eff}) divided by influent concentration (C_{in}) and plotted against volume passed.

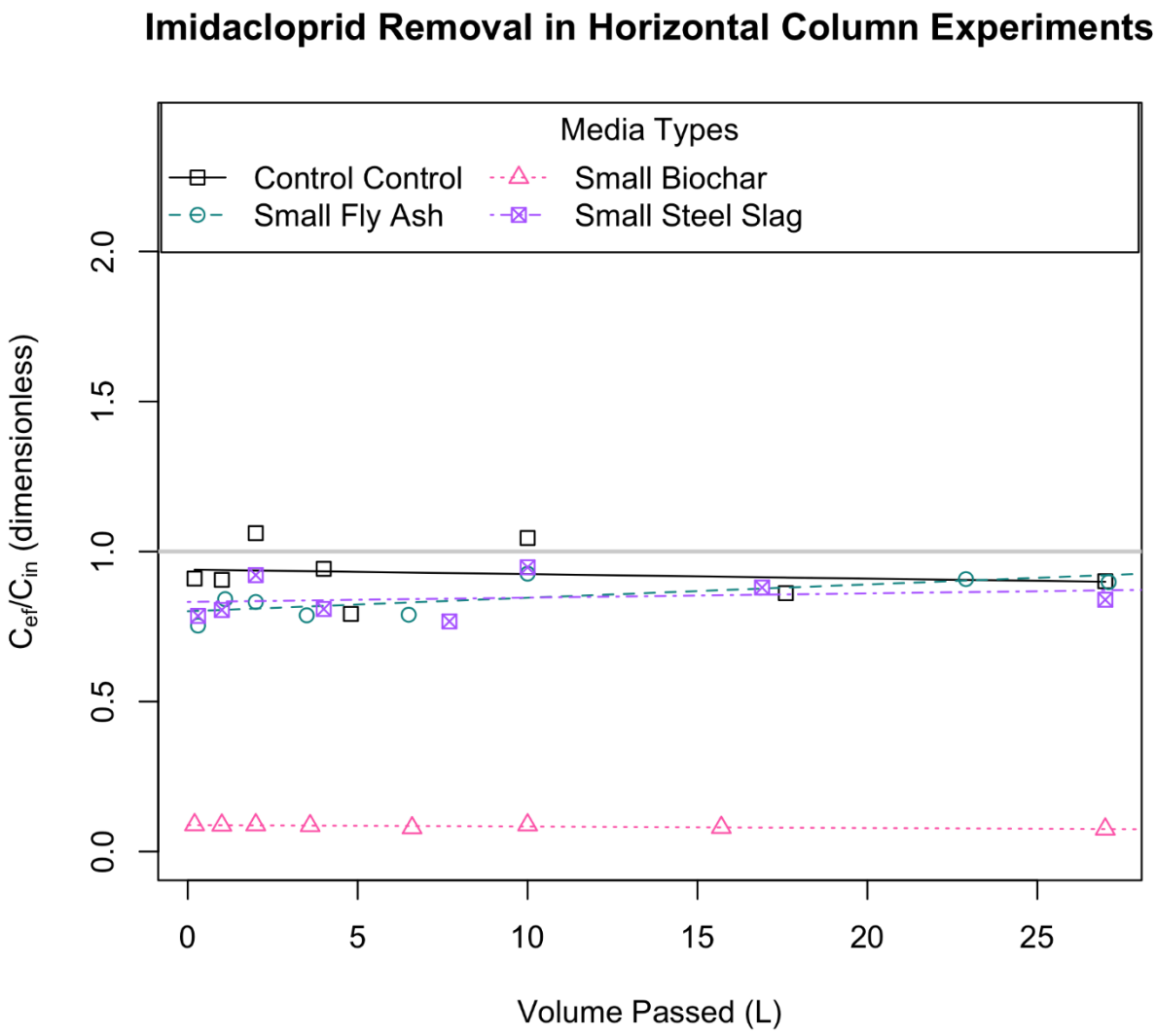

Figure 3-20 Imidacloprid removal in horizontal column experiments as demonstrated by the influent-effluent ratio as defined by effluent concentration (C_{eff}) divided by influent concentration (C_{in}) and plotted against volume passed.

3.4.4 Phosphorus (P)

Phosphorus removal in the horizontal column experiment showed varied results (Figure 3-21). First, the control column initially had P removal just below 100%, however removal efficiency decayed immediately and an upper IE ratio asymptote just below 0.95 was reached by the end of the experiment. When the control column's upper IE ratio asymptote is fixed to 1.00, the exhaustion is estimated to be at 16 L. Aggregated fly ash yielded a unique result ($p = 0.1$) with an initial removal of P from solution of 90%. However, as removal rates declined with solution passing, it declined in a near-linear trend with an upper IE ratio asymptote calculated to be 1.10 and exhaustion being reached at 37 L passed. Steel slag was also unique ($p = 0.001$) with an initial removal of approximately 85%, however, removal efficiency appeared to slightly improve over time with a final removal rate at approximately 90% to 95%. Because the curve for steel slag ended with a negative slope, no upper IE ratio asymptote fixing for media exhaustion determination was calculated. Lastly, biochar initially had a removal of about 40% (lower removal than the control), but in subsequent sampling points the data indicated between 70% and 75% removal. P removal followed a similar pattern to aggregated fly ash with a near-linear relationship fitted to the data. Biochar ended the experiment with a removal of approximately 10%, similar to that of the control and aggregated fly ash. Exhaustion for the biochar was calculated to be at 32 L passed.

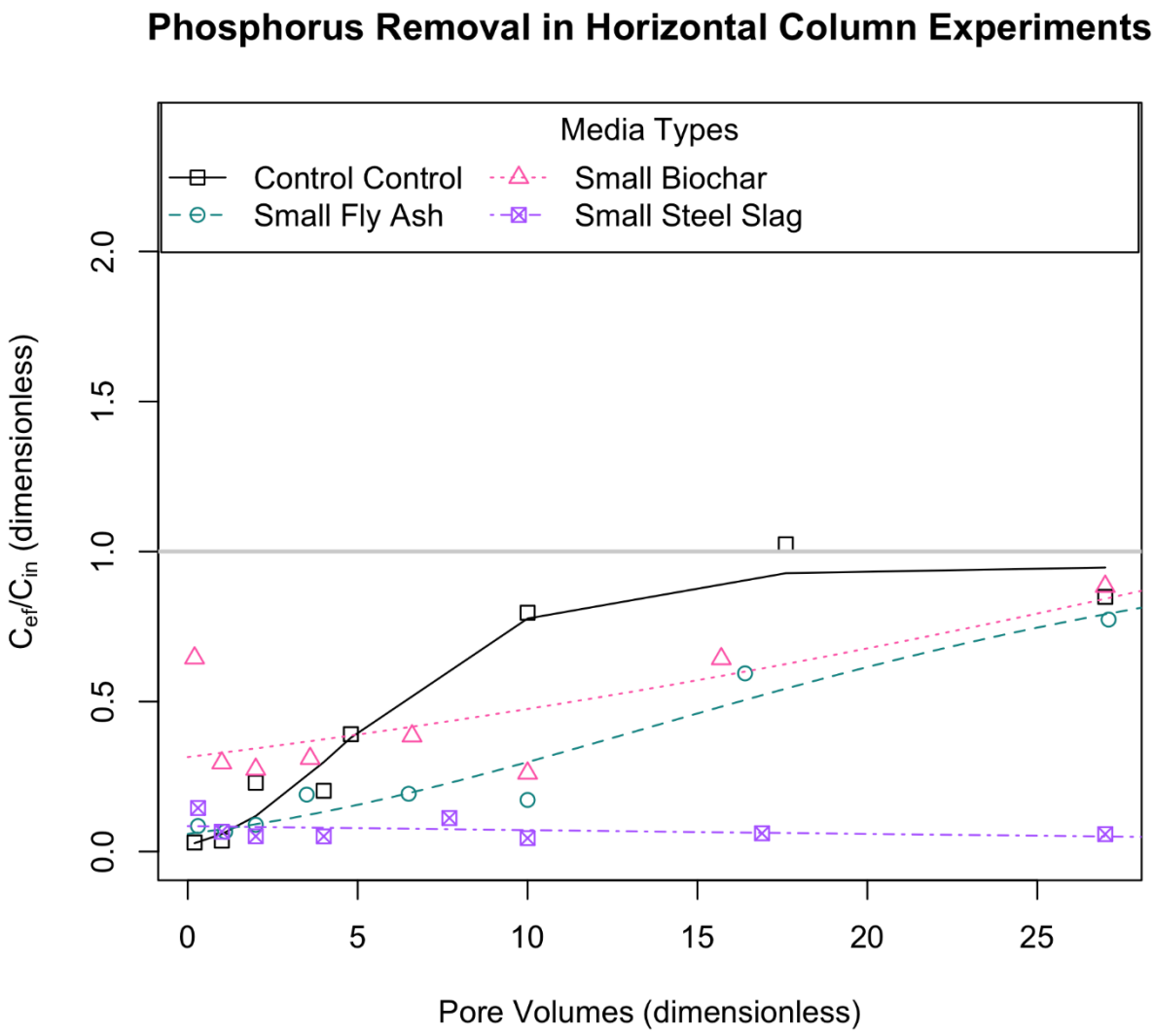

Figure 3-21 Phosphorus removal in horizontal column experiments as demonstrated by the influent-effluent ratio as defined by effluent concentration (C_{eff}) divided by influent concentration (C_{in}) and plotted against volume passed.

3.4.5 Mass Removal Rate

Plots comparing the mass removal rate as a function of cumulative contaminant passed into the column were produced to compare results from horizontal and vertical column experiments. Important to note is that results from this analysis do consider an element of time. Meaning, individual points on each plot do not represent a removal rate at a given solution concentration for an independent study, but rather it is representative of the removal rate once a given amount of contaminant has been passed into the column. Furthermore, this analysis was only able to be conducted for contaminants where both horizontal and vertical columns fell into category 4 (from Table 3-1). Additionally, the analysis contaminant needed to have a similar spike concentration between the two orientations due to results being dependent on solution concentrations and not concentration ratios.

Results demonstrated that less overall solution, and therefore less contaminant mass was passed through the sample setup in horizontal column experiments when compared to vertical experiments. Enough cumulative contaminant was passed through to ensure results were comparable, however, horizontal experiments did not measure long-term removal rates as compared to vertical experiments.

3.4.5.1 Arsenic

Mass removal rate (MRR) analysis on small steel slag (Figure 3-22) yielded horizontal and vertical results clustered together with a negative relationship between MRR MV^{-1} (mass volume) and the cumulative As mass input. As was demonstrated, the control column (bioretention simulation sand) yielded modest As^{+5} removal and therefore is not considered a reasonable source of As^{+5} removal.

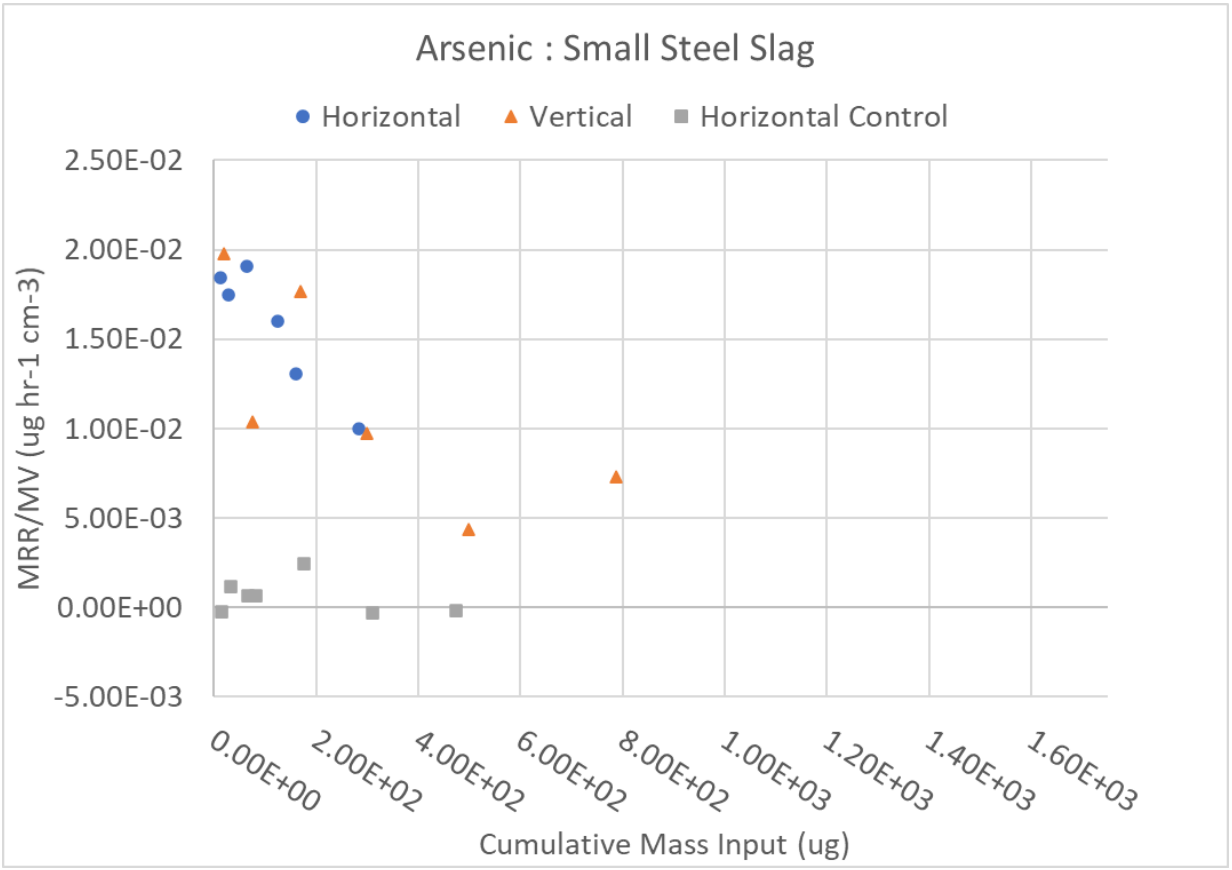

Figure 3-22 Comparison of column orientation on the mass removal rate (MRR) of As^{+5} per media volume (MV) of small steel slag against cumulative As^{+5} input.

Small aggregated fly ash yielded results (Figure 3-23) which demonstrated that in vertical column experiments, the MRR MV^{-1} was high (~0.015 μg hr^{-1} cm^{-3}) when little mass had been input, however in horizontal column experiments, the same mass input yielded much lower removal rates

(~0.005 μg hr^{-1} cm^{-3}). Despite this departure in magnitude, visually, the trend remained the same between the two experiments with a high initial removal that tapered off over time. Horizontal control column data demonstrated the bioretention simulation sand as an infeasible source of As^{+5} removal.

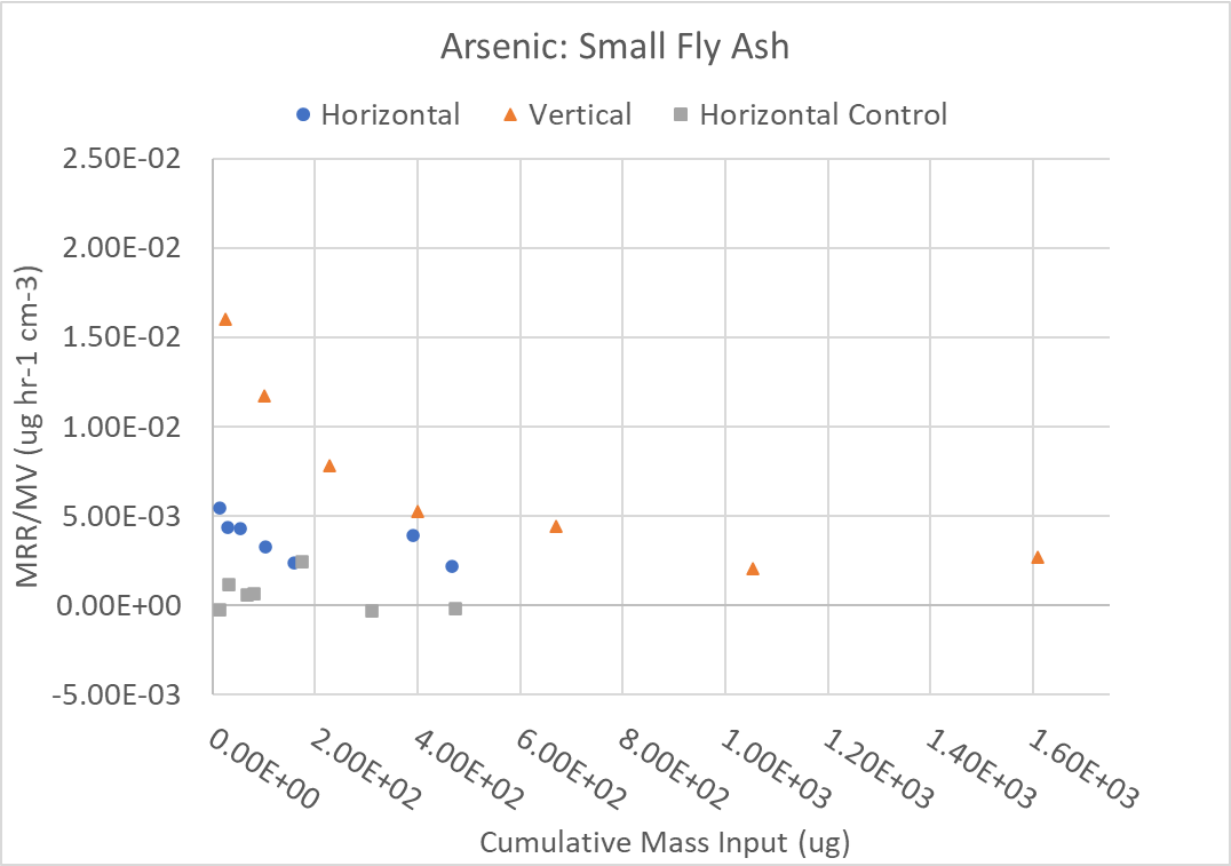

Figure 3-23 Comparison of column orientation on the mass removal rate (MRR) of As^{+5} per media volume (MV) of small aggregated fly ash against cumulative As^{+5} input.

Small biochar results yielded an MRR MV^{-1} of ~0.01 μg hr^{-1} cm^{-3} which was not as high as compared to the other media (0.015 – 0.02 μg hr^{-1} cm^{-3}). Similar to small aggregated fly ash, the small biochar resulted in a separation between the vertical and horizontal column runs in terms of magnitude, although visually, the same trend is observed. In the vertical column, small biochar initially is removing As^{+5} at a rate of ~0.01 μg hr^{-1} cm^{-3} followed by a reduction in removal to just above 0.005 μg hr^{-1} cm^{-3} for the next two sample points. Removal appears to increase once again around 300 μg, but a breakthrough is quickly achieved soon after. By 800 μg, the vertical column is predicting leaching of As^{+5}, however by approximately 1300 μg the system appears to reach equilibrium with a removal rate at or near 0.00 μg hr^{-1} cm^{-3}. As mentioned, the horizontal column experiment yielded similar results only at smaller magnitudes. The same process of reducing removal rate, followed by a slight increase in removal rate then leaching is observed for the horizontal column, although results stay between just below 0.00 μg hr^{-1} cm^{-3} and 0.0025 μg hr^{-1} cm^{-3}. This range is also applicable to the horizontal control column which is also shown and constitutes no source of As^{+5} removal to the system.

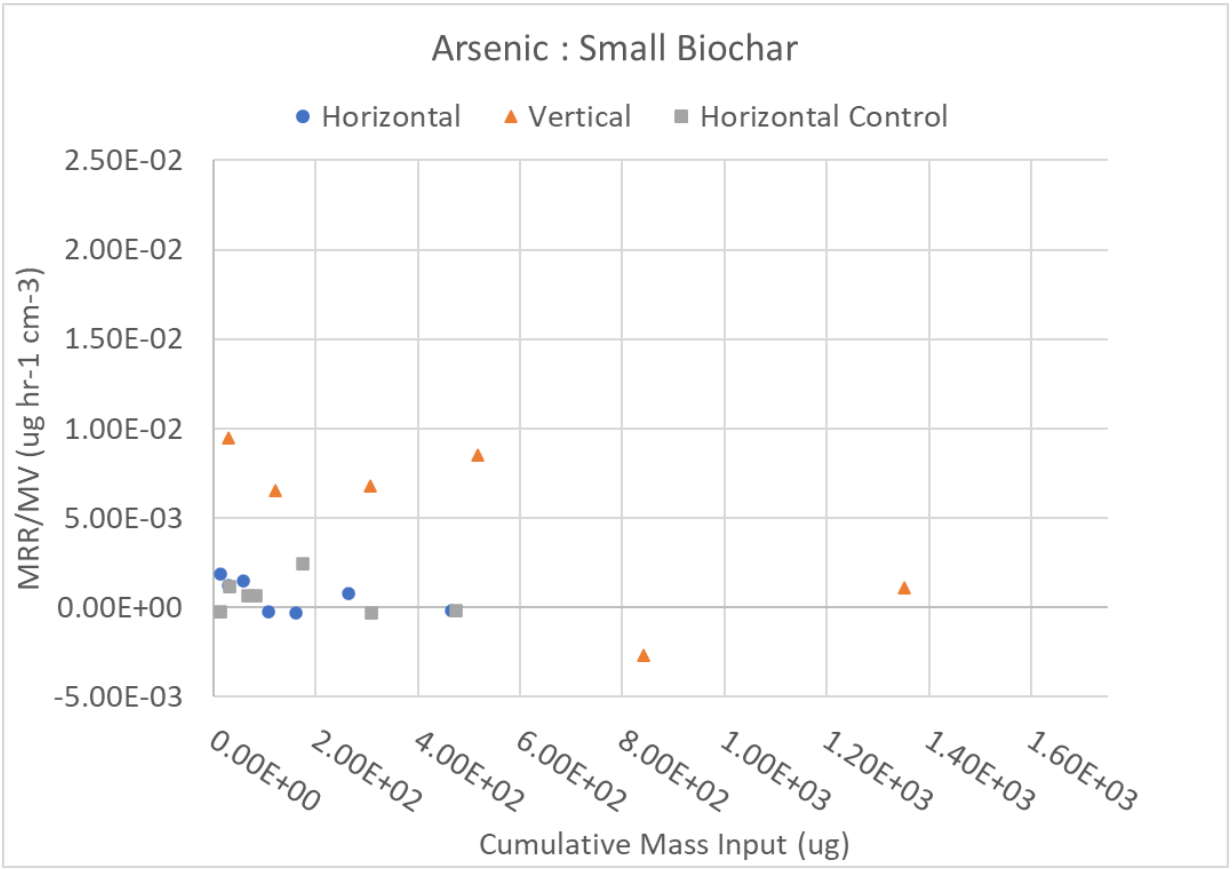

Figure 3-24 Comparison of column orientation on the mass removal rate (MRR) of As^{+5} per media volume (MV) of small biochar against cumulative As^{+5} input.

3.4.5.2 Phosphorus

Small steel slag results in the vertical column experiment yielded a similar analysis as was shown in the As^{+5} removal analysis. In early portions of the experiment when not much P had been passed into the column, small steel slag removed P at the highest rate (just below 0.5 µg hr^{-1} cm^{-3}). The removal rate then steadily declined as more P was passed into the system. Interestingly however, the final point in the vertical column experiment yielded a removal rate that was higher than the removal rate previously measured. Without further data provided, determining this point as an outlier, natural variation in the data, or representing a potential trend is unknown. The horizontal column experiment yielded a MRR MV^{-1} trend that demonstrated an increase in removal with an increase in P passed into the system. The horizontal control column shows a trend with a moderate initial removal (0.18 µg hr^{-1} cm^{-3}) and the removal rate quickly dropping off to 0 µg hr^{-1} cm^{-3} by the time 3 µg P has been passed through the system. In comparison, as the horizontal control column declines in removal rate, the horizontal column increases.

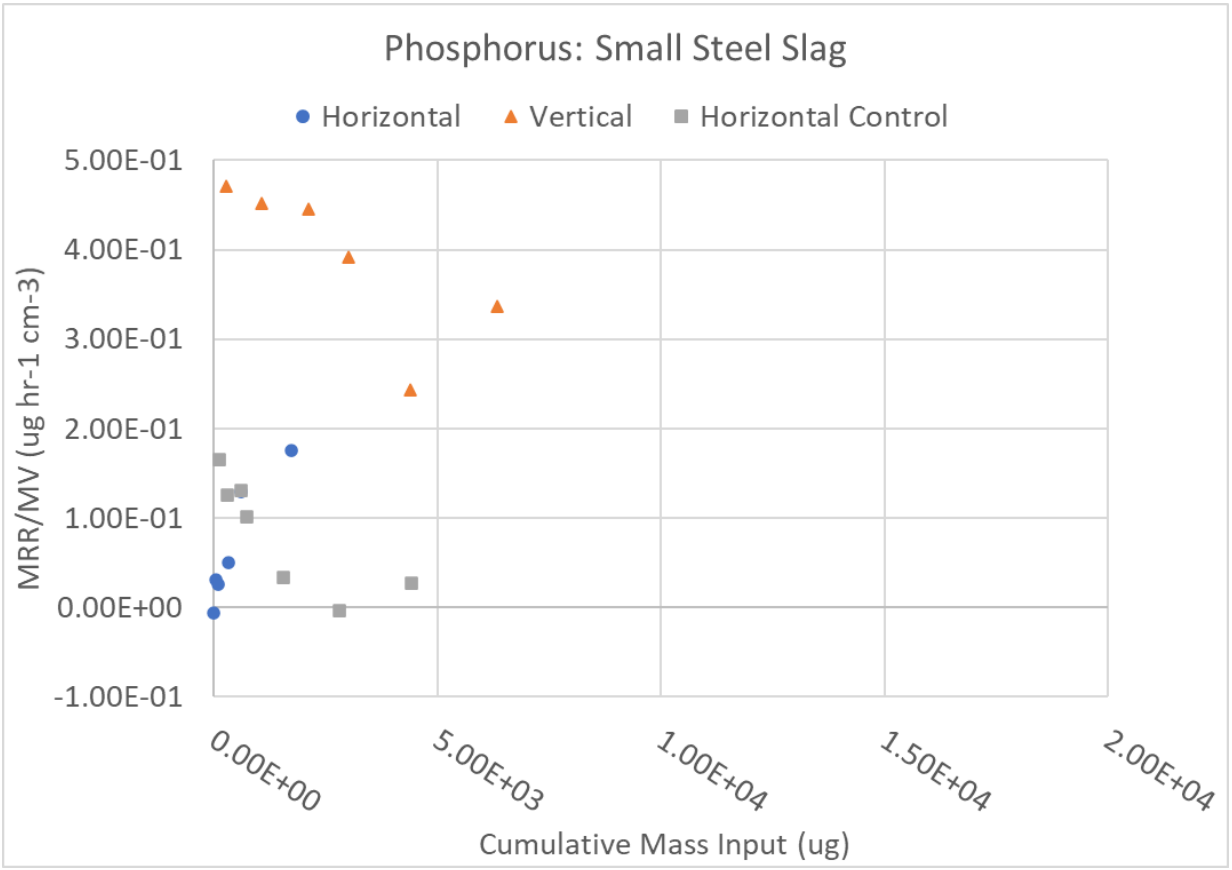

Figure 3-25 Comparison of column orientation on the mass removal rate (MRR) of P per media volume (MV) of small steel slag against cumulative P input.

Small aggregated fly ash yielded vertical column analysis results demonstrating a maximum removal rate (~0.38 μg hr^{-1} cm^{-3}) at the lowest cumulative mass input and the removal rate steadily declining. The media was unable to remove any more P at around 1000 μg P flushed into the system and the analysis demonstrated the small aggregated fly ash began to leach P back into solution (-0.1 μg hr^{-1} cm^{-3}). The horizontal control column results yielded an initial removal in the control column of approximately 0.18 μg hr^{-1} cm^{-3} with a steady decline to 0 μg hr^{-1} cm^{-3} by approximately 300 μg P passed through. Conversely, the horizontal column yielded no P removal initially with the removal rate increasing as more P was passed into the system. After 100 μg P passed, the horizontal column peaked at a removal rate just below 0.1 μg hr^{-1} cm^{-3} then began to decline at a rate similar to the trend in the vertical column. Exhaustion of the media to remove P in the horizontal experiment was reached right at the termination of the experiment with approximately 400 μg P passed through.

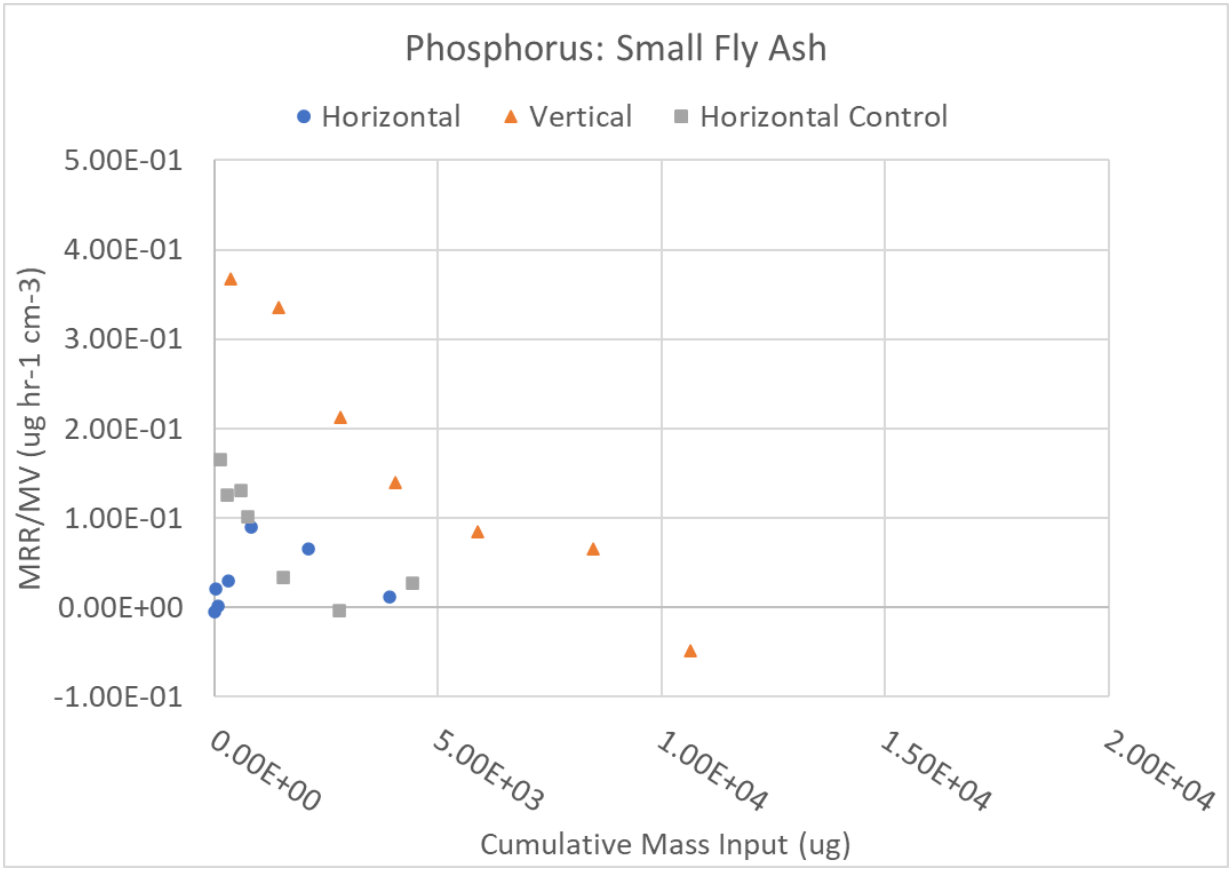

Figure 3-26 Comparison of column orientation on the mass removal rate (MRR) of P per media volume (MV) of small aggregated fly ash against cumulative P input.

Finally, as was demonstrated with Figure 3-14 and Figure 3-21, biochar has not demonstrated a strong tendency to remove P from solution. The vertical column experiment further corroborated this observation by demonstrating a fluctuation between leaching and removal of P from/into solution at rates between -0.03 μg hr^{-1} cm^{-3} and 0.5 μg hr^{-1} cm^{-3}, effectively representing no substantial source or sink of P to/from solution. Once again, the horizontal control results yielded an initial removal in the control column of approximately 0.18 μg hr^{-1} cm^{-3} with a steady decline to 0 μg hr^{-1} cm^{-3} by approximately 300 μg P passed through. Horizontal column results initially demonstrated leaching of P into solution represented by a removal rate of approximately -0.04 μg hr^{-1} cm^{-3}. As the control column's removal rate declined, the horizontal column's removal rate spiked to just under 0.1 μg hr^{-1} cm^{-3} with a rapid decline resulting in media exhaustion by the final point of the experiment (approximately 400 μg P passed through).

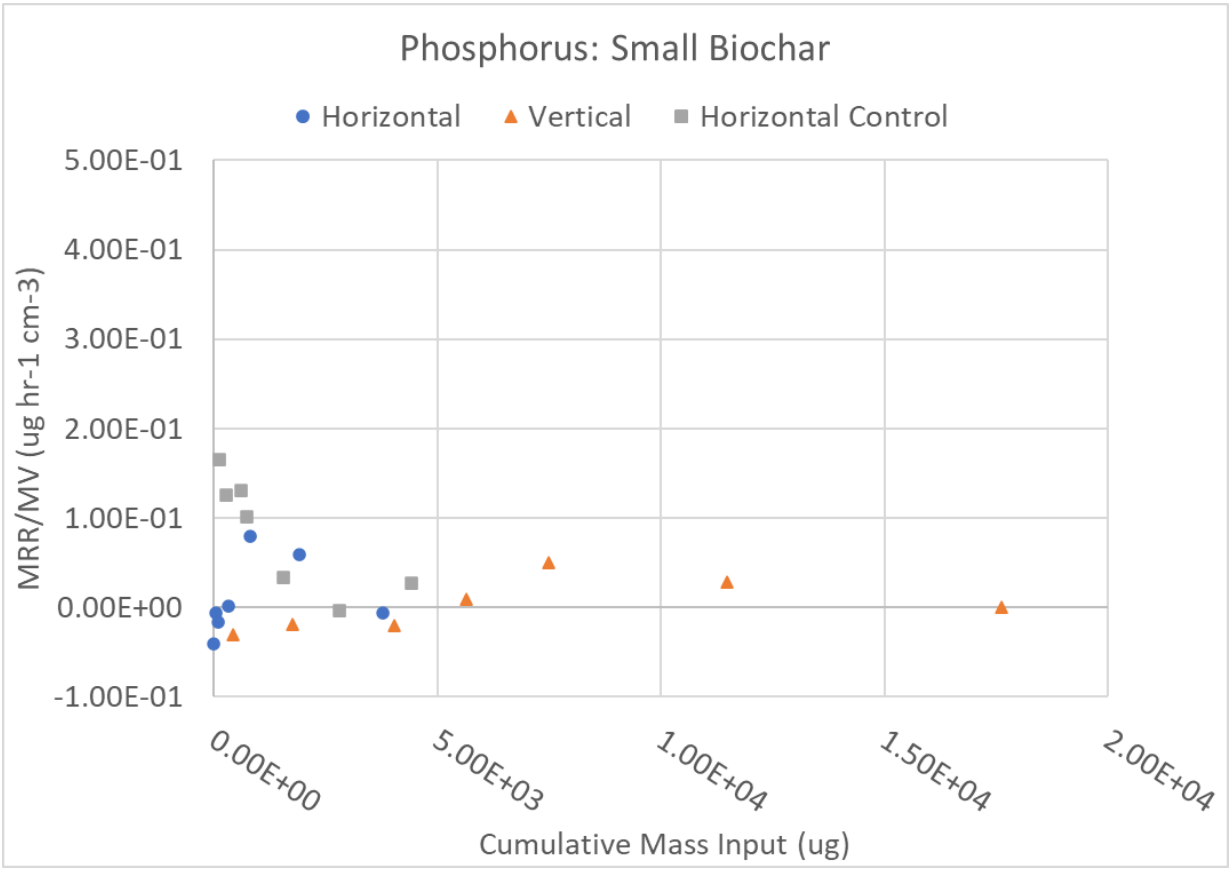

Figure 3-27 Comparison of column orientation on the mass removal rate (MRR) of P per media volume (MV) of small biochar against cumulative P input.

4 Discussion

4.1 Media Dissolution Impacts on pH and Specific Conductivity

Dissolution of -oxide species into solution is of major consideration regarding effluent pH and specific conductivity (SpC). For undersaturated mineral and elemental species, each compositional -oxide species in the treatment media will tend to dissolve into solution (Agyei et al., 2002; Ahmaruzzaman, 2010). Generalized forms of these reactions are shown in Equation 4-1 and demonstrate how metal-oxides will react with water to release ions into solution and form hydroxide ions.

Equation 4-1 Generalized dissolution reactions which contribute to solution pH increase.

$$X_2O + H_2O \rightarrow 2X^{1+}_{(aq)} + 2(OH^-)_{aq}$$

$$XO + H_2O \rightarrow X^{2+}_{(aq)} + 2\,(OH^-)_{aq}$$

Increased ions in solution will increase the solution's ability to conduct current and therefore result in an overall increase in SpC. Furthermore, an increase in OH^- in solution will correspond to an increase in solution pH. Table 2-3 highlights the compositions of each medium used with most metal components expressed in their metal-oxide form. The aggregated fly ash and steel slag used were reported to contain large metal-oxide concentrations with particularly high concentrations of Al_2O_3, Fe_2O_3, CaO, and MgO. Furthermore, biochar was not demonstrated to contain high levels of metal-oxides, but rather had an overwhelming composition of organic carbon (87.4%). Studies have demonstrated fly ash and steel slag (Agyei et al., 2002) yield higher pH and SpC values due to this metal-oxide dissolution.

4.2 Leaching

As was demonstrated in the previous section, both aggregated fly ash and steel slag possess a high potential to leach cations (such as Ca^{+2}, Mg^{+2}, Na^{+}, K^{+}, Fe^{+3}, and Al) into solution. This was demonstrated by reviewing Ca, Mg, Na, K, and Fe ratio data in Table 10-4, Table 10-5, Table 10-6in the appendix. Leaching of a material is of concern to the quality of the water that is flowing into the environment and into various waterbodies. Major cations such as Ca^{+2}, Mg^{+2}, Na^{+}, and K^{+} alone are not considered as substantial threats to aquatic life. However, these elements typically combine to constitute total dissolved solids (TDS) which is a measure that is considered impactful to aquatic life. *Water Quality Standards | Oklahoma Water Resources Board* (n.d.) defines "general use groundwater" as a groundwater that can be used for human consumption or otherwise without adverse impacts and is defined by a TDS value below 3,000 mg L^{-1}. The standards go on to define water sufficient for water supply purposes to be below 5,000 mg L^{-1} and sets a secondary drinking water standard at 500 mg L^{-1} (for more aesthetic purposes). Even in the most extreme of cases, combined Ca^{+2}, Mg^{+2}, Na^{+}, and K^{+} experiment results would not exceed a TDS of more than 150 mg L^{-1}, meaning major cation leaching is not of environmental concern in this study.

Aluminum is another element that was generally leached in aggregated fly ash and steel slag experiments which may pose an environmental concern. The aquatic life criteria is dependent on the hardness of the water, but generally is given in the range of thousands to tens of thousands of µg L^{-1} (US EPA, 2015b). An exceedance of 1,000 µg L^{-1} was generally observed in experiments run with aggregated fly ash with effluent Al concentrations ranging between 615 µg L^{-1} and 21,845 µg L^{-1}. Understandably, the use of aggregated fly ash would constitute a cause for concern and therefore may not be suitable in all situations. All other media were found to leach below 1,000 µg L^{-1}.

Lastly, Fe is designated to be toxic at levels above 1,000 µg L^{-1} (US EPA, 2015b). All results from this study yielded Fe values below 100 µg L^{-1} indicating that the use of this media for the improvement of water quality provides no meaningful environmental concern for Fe.

4.3 Below Detection Limits (BDLs) and Control-Experimental Separation

One potential explanation for results being below detection limits (BDL) is when influent values are measured BDL, therefore so long as the media is not a source of the measured contaminant, then the effluent will also be BDL. This essentially represents the influent concentration for a contaminant being too low to properly quantify in this study. Another explanation is when influent concentrations were above the lower detection limit (LDL) and the media removed the contaminant thoroughly enough throughout the duration of the experiment to yield consistent BDL values. This case would indicate ideal contaminant removal; however, it does not yield a curve appropriate for analysis. Table 4-1 below outlines which contaminant-media-orientation combination yielded which result.

Table 4-1 Media-contaminant-orientation combinations that yielded results below detection limit (BDL).

Column Orientation	*Metals*
Vertical	Cd, Co, Ni
Horizontal	Be, Cd, Co, Fe, Ni, Zn
Influent BDL	Cu, Pb, Se

The second major category in the data is where there is no noticeable separation between the control column and the experimental column in removing contaminants in horizontal column experiments. This could mean that both the control column and the experimental columns are BDL, therefore no separation is able to be determined. Furthermore, removal could be observed in horizontal columns, however, there may be no noticeable separation between the control column and the experimental columns. Where this does indicate that removal took place, it also demonstrates that the bioretention simulation tube was the primary driver of removal and not the experimental media. These media-contaminant-orientation combinations can be found in Table 3-1 above classified as category 2. These results are important to understanding the processes within an augmented bioretention system as suggested, however these specific results are beyond the scope of this study and are suggested for further investigation in future studies.

4.4 Metals

In vertical column experiments, no specific media proved to be statistically different from the rest with results highly clustered between 0% and 50% As^{+5} removal. Horizontal column results however, produced one unique curve in small steel slag ($p = 0.04$). Akter et al. (2005) shows an Eh/pH diagram for As^{-5} speciation in an aqueous system at 25˚C and 1 bar of pressure. For the pH range given in our effluent results (7 – 12) and an assumed Eh between 200 mV and 600 mV (*Characterization of Solutions by pH and Eh*, 2006) results in an expected As species of $HAsO_4^{2-}$

, which is an As^{5-} species. In a study by Liem-Nguyen et al. (2020) a steel slag was used to treat a solution spiked with As^{5-} across a variety of pH conditions. At an initial pH of 7.0, the resultant pH was 12.0 and just over 40% of As^{5-} was reported to be removed from solution by the steel slag. This was also observed in the horizontal column experiments where results initially yielded nearly 100% As^{5-} removal, but eventually reached equilibrium at a removal rate between 40% and 50%. Akter et al. (2005) goes on to explain that As^{5-} removal is due to a combination of precipitation and adsorption. Precipitation is predicted as $Ca_3(AsO_4)_2 \bullet 4H_2O_{(s)}$ and therefore is predicted to Ca dependent. However, with a similar resultant pH to steel slag and a higher Ca content, aggregated fly ash should be expected to also result in a similar removal of As^{5-} from solution, although the horizontal column data did not result in a large quantity of As^{5-} being removed from solution. Therefore, adsorption is likely a more likely mechanism. The composition of media sorption site compositions is beyond the scope of this study, however sorption sites that are associated with compounds at high concentrations in steel slag as compared to the other media are expected to be the key in understanding As^{5-} removal in this case. The most likely of these compounds are Fe- and Mn-oxides.

Manganese (Mn) results show a strong dependence on pH. Steel slag and aggregated fly ash have shown to noticeably increase solution pH to a range of 10 – 12. In an Eh/pH diagram of Mn^{+2} speciation in an aqueous solution by Gabelich et al. (2006) demonstrates that for a resultant pH between 10 and 12 and an Eh between 200 mV and 600 mV, either $MnOOH_{(s)}$ or $Mn_3O_{4\,(s)}$ is predicted to form and precipitate. Conversely, with biochar not noticeably impacting solution pH (pH = 7.0-7.5), Mn is predicted to remain in solution as Mn^{+2}, hence not demonstrating any significant removal from solution.

Although the Gompertz model was not statistically significant, Be^{+2} removal from solution visually appeared to be best with small steel slag. All others remained just below an IE ratio of 1.0. Tokarčíková et al. (2021) did not investigate the removal of Be^{+2} from solution using fly ash or steel slag, but the authors did indicate that charged sites on biochar surfaces was the most likely point of sorption. If the assumption is made that both aggregated fly ash and steel slag have charged surfaces, then Be^{+2} removal from solution via this mechanism is also possible. More likely, however, is the removal of Be^{+2} via complexation as $Be(OH)_2$ at a pH above 4. This was the primary mechanism of removal reported by Tokarčíková et al. (2021) at high pH and is a likely method of removal in this study as well. Curiously, however, a constant removal rate was not observed through the duration of the experiment as was demonstrated with Mn^{+2}. With pH remaining relatively constant throughout the duration of all experiments but Be^{+2} removal declining over time, sorption appears to be the primary method of removal in this study. Further research would need to be conducted to investigate the exact mechanism of removal in this study.

Generally, metals removal from solution is expected when treated with aggregated fly ash (Apak et al., 1998; Ayala et al., 1998; Bayat, 2002a, 2002b; Chandra Srivastava et al., 2006; Diamadopoulos et al., 1993; G. Gupta & Torres, 1998, 1998; V. K. Gupta et al., 2003; V. K. Gupta & Ali, 2000, 2004; V. K. Gupta & Sharma, 2003; Hsu et al., 2008; Lin & Chang, 2001; S.-C. Pan et al., 2003; Panday et al., 1985; Rao et al., 2003; Ricou et al., 1999; Rio et al., 2002; S. Wang et al., 2008; Yadava et al., 1987) and steel slag (Kim et al., 2008; Wu et al., 2014). This study demonstrated both aggregated fly ash and steel slag as effective in removing metals from solution. However, despite the overwhelming body of literature, this study supports steel slag as a more effective and safer option to removal metals from solution as opposed to aggregated fly ash. As this study and the body of literature further demonstrated, biochar is expect to have little to no

significant impact on metals removal from solution without some type of pretreatment (Ding et al., 2016; Reddy et al., 2014a, 2014b; Zhou et al., 2016).

4.5 Phosphorus

Biochar was not shown to remove P from solution, likely due to the lacking charged surface sorption sites and deficient capacity to raise solution pH via metal-oxide dissolution. Conversely, aggregated fly ash and steel slag results demonstrated the P removal capability that charged media surfaces and high solution pH can provide. Both aggregated fly ash sizes in vertical column experiments yielded highly similar results. Due to the high secondary porosity observed between the large and small fractions of the aggregated fly ash, grain size is not anticipated to have a noticeable impact on contaminant removal with the internal crystalline structure being the primary factor. Contrarily, steel slag did not show such secondary porosity and therefore the grain size had a noticeable effect as was demonstrated with P removal. Literature suggests that the Ca content of the treatment media is the primary predictor of how well a media removes P from solution, typically allowing for the formation of hydroxyapatite ($Ca_{10}(PO_4)_5(OH)_2$) (Drizo et al., 2006; Kim et al., 2008; Piatak et al., 2019; Scott & Penn, 2021). In general, fly ash is known to contain ~23% CaO (W. Zhang et al., 2008), where steel slag only contains ~10% (Bowen, 2021), yet small steel slag removed P at a better rate than both aggregated fly ash sizes. While not entirely known based on the results of this study, one potential explanation is regarding steel slag's much higher density than aggregated fly ash, meaning steel slag is able to make available more Ca mass per unit volume than aggregated fly ash. Horizontal column experiments demonstrated the control sand to have a measurable removal of P from solution, however the capacity was exhausted quickly necessitating the use of an amendment to help retain more P. Both biochar and aggregated fly ash removed P

well during the initial stages of the experiment likely as a result of the control sand rather than the media itself removing P. As the control sand's removal capacity tapered off, as did the removal rates for aggregated fly ash and biochar, demonstrating these media to not be effect treatments for removing P from solution. Steel slag however was measured to remove >90% of P from solution for the duration of the experiment. Again, the Ca mechanism of removal is expected, yet the absence of aggregated fly ash to be a reasonable sink of solution P calls that mechanism into question. Instead, Scott & Penn (2021) in a study of steel slags removing P from solution suggest that Fe-oxides could also play a role in P removal. The authors suggest that at a high pH, such as what was observed in this thesis, this mechanism is not as likely. However, with the Ca mechanism of removal in question, it could be possible that this reaction plays an important role in removal despite the high pH of the solution. This is supported by the observed difference in removal and differing Fe-oxide compositions of the steel slag and aggregated fly ash.

4.6 Neonicotinoids

Neonicotinoids in this study showed uniform results across all three sub species (acetamiprid, dinotefuran, and imidacloprid). Vertical column experiments were spiked at the higher neonicotinoid level (1 mg L^{-1}), which is believed to be the source of some unexpected results. Steel slag was not anticipated to be a reasonable source of pesticide removal from solution with atrazine (a herbicide) only removed at 0.3% (Gonzalez et al., 2016) and 2,4-D and carbofuran (pesticides) reported to have a "negligible" removal from solution using steel slag (V. K. Gupta et al., 2006). Therefore, it was unexpected to see small steel slag as the best performer (acetamiprid, $p = 0.01$; dinotefuran, $p = 0.12$; imidacloprid, $p = 0.30$) in the vertical columns. The literature did support fly ash as a potential for the removal of herbicides and pesticides (V. Gupta et al., 2002;

V. K. Gupta & Ali, 2001; Nollet et al., 2003) and vertical column experiments from this study also demonstrated some neonicotinoid removal, albeit not with a modeled fit that was significantly unique as compared to the other modeled fits (all sub species, $p > 0.65$). Biochar was projected to be the best at removing neonicotinoids with mechanisms such as pi-pi, cation-pi, and hydrophobic effects as the primary driver of removal (Shi et al., 2022; P. Zhang et al., 2018). By referring to Table 2-3 these properties are provided by the organic carbon structures of biochar but is not provided by metal-oxide structures such as the primary composition of fly ash and steel slag. In vertical column experiments, excluding large biochar in imidacloprid and dinotefuran results ($p = 0.06$ and 0.50, respectively), all biochar results yielded unique models which demonstrated removal quantities between 25 and 75% tapering to removals between 0 and 10%. Although biochars in the high neonicotinoid spiked vertical column experiments did not provide the highest removal rates, when the neonicotinoid concentration was adjusted and the bioretention simulation horizontal column experiments were run, biochar was the standout media removing nearly all neonicotinoids from solution. Biochar models in all three sub species yielded $p < 0.05$, with acetamiprid and imidacloprid yielding $p << 0.01$. The aromatic structure of the organic C, which is the overwhelming component of biochar, yielded greater than 90% removal of acetamiprid and dinotefuran through the duration of the experiment. Dinotefuran demonstrated greater than 90% removal with biochar in horizontal column experiments, however unlike the others, the removal tapered off to around 60% removal by the end of the experiment. Shi et al. (2022) shows that neonicotinoid sorption is highly selective, despite solution pH and ionic strength, which is likely demonstrated in the difference between acetamiprid/imidacloprid results and the dinotefuran results. Table 1-1 amended from (Morrissey et al., 2015) demonstrates a soil sorptive capacity (log K_{oc}) for dinotefuran that is lower (less sorbent) than the equally matched, higher log K_{oc} (more

sorbent) acetamiprid and imidacloprid. As sites begin to exhaust, dinotefuran is likely the first of the three to yield lower sorption rates. The control column in horizontal column experiments demonstrated 0% (dinotefuran) to ~10% (acetamiprid and imidacloprid) removal from solution, therefore justifying the need for some form of water quality finishing for neonicotinoids. Both aggregated fly ash and steel slag had no statistically unique results with both demonstrating little to no additional removal beyond the control column. Based on the understanding of preferred neonicotinoid removal pathways (pi-pi, cation-pi, and hydrophobicity), combined with previous studies, it is no surprise that steel slag did not yield much removal. Fly ash was potentially expected to remove pesticides (V. Gupta et al., 2002; V. K. Gupta & Ali, 2001; Nollet et al., 2003) albeit no evidence suggested the effective removal of neonicotinoids specifically. Given our predicted proffered neonicotinoid removal mechanisms and our understanding that aggregated fly ash lacks these qualities, the results from horizontal column experiments are no surprise.

4.7 Mass Removal Rate

Small steel slag demonstrated uniform results in removing As^{+5} between the horizontal and vertical experiments which is ideal in comparing the two datasets. Aggregated fly ash results for As^{+5} and P between horizontal and vertical column experiments demonstrated similar trends with different magnitudes. This supports the mechanism of removal being constant between the two experiments, however some difference between the two experimental designs is impacting the effectiveness of aggregated fly ash to remove both contaminants at the same rate as the vertical column. The most likely is the introduction of the bioretention simulation sand in the horizontal column experiment. This impact is suggested as a point of further study; however, this study has demonstrated the potential of negative impacts of bioretention prior to being treated with a

aggregated fly ash to remove arsenic from solution. For arsenic, biochar demonstrated little to no removal in horizontal column experiments, where vertical column experiments showed a mild removal rate between 0.005 and 0.01 $\mu g\ hr^{-1}\ cm^{-3}$. The impact of the overlaying bioretention simulation sand could have a similar impact on As^{+5} removal using biochar as well. In IE ratio graphs, biochar was not shown to remove considerable amounts of P from solution, a trend that was also observed in the mass removal rate analysis. For small steel slag and small aggregated fly ash, P results demonstrated some curious trends between the vertical and horizontal column experiments. Vertical columns demonstrated a high removal rate ($0.3 – 0.5\ \mu g\ hr^{-1}\ cm^{-3}$) early on when low quantities of P have been passed through, with the rate declining over time as more P is passed through, indicating the exhaustion of sorption sites. However, for small steel slag and small aggregated fly ash (and biochar to some degree) in horizontal column experiments, a relationship between media removal and control column removal appeared. The control column as was demonstrated in Figure 3-21 to initially remove some P but breakthrough relatively quickly. This same trend was observed in the mass removal rate analysis with an initial removal rate near 0.18 $\mu g\ hr^{-1}\ cm^{-3}$ and reaching exhaustion by around 300 µg P passed through. Media results however demonstrated that as long as the control column was removing P, the removal rate was low or nonexistent. Intuitively, if the control column is removing large quantities of P from solution, the rate of removal is going to be a function of how much P is left available in solution to remove, so long as that value is not larger than the maximum removal rate capacity of the media. As the control column's removal rate begins to decline with time, there is consequently more P in solution for the media to remove and therefore the removal rate of the media begins to increase. In the aggregated fly ash horizontal column, after the media P removal rate superseded the control

column removal rate, the media removal rate trend began to decline ultimately matching the trend of the vertical column experiment which showed a declining removal rate over time.

5 Considerations

As a contribution to the body of scientific literature, it is important for assumptions, limitation, and potential areas for concern to be clearly divulged to properly contextualize the research being conducted. This section will review these disclosures in order to properly frame this study in the broader scientific discussion around LID modification, contaminant fate and transport, and aqueous geochemistry.

5.1 Gompertz Function and Influent-Effluent Graphs

Chu (2020) makes a strong case the use of the Gompertz function to fit data such as fixed bed adsorption studies similar to what was studied in this thesis. This curve is applicable to this study due to its ability to model asymmetric breakthrough curves well, which was largely the case for the study covered in this thesis. Often, the data analyzed here showed only the decaying tail (concave down) of an S-curve, while other data only showed the exponential growth (concave up) portion of an S-curve, while yet others showed both. The Gompertz function allows for showing one or both of these while also allowing for asymmetry in all cases.

However, there are several considerations with how the Gompertz function was utilized to analyze the data in this study. First, this model is strictly a diagnostic model *not* a predictive one. This meaning, points that fall outside the domain of the experiment are not able to be appropriately characterized by the curve fit *within* the domain of the data. The Gompertz curve would often predict elements outside the domain of the data, however without further data points to confirm the model, these elements cannot be fully relied on. Instead, when elements such as the upper IE asymptote fell outside the domain of the data, the resultant elements are treated as merely speculative rather than predictive. Furthermore, in instances where the model did not reach an

upper IE ratio asymptote of at least 0.95, overriding the asymptote to be fixed at 1.00 was an attempt to calculate a coarse speculation as to where breakthrough *might* occur. Overall, where the key parameters were not measured within the domain of the data collected, further data is needed in order to better calibrate the model to reflect the interactions and processes studied. Conversely, many datasets in this study predicted key parameters of the Gompertz curve within the data domain as collected and therefore this model represents an effective characterization of the interactions and processes occurring.

Another consideration are the underlying assumptions for the proper application of the Gompertz function. Originally, this function was intended to model populations in biological sciences. One of the foundations of the Gompertz function because of this is that relationships are intended to be studied as binary; either a being (person, microbe, animal, etc.) is alive or dead. Furthermore, once a being is alive, it stays alive and once it is dead, it stays dead. What this implies for the use of the Gompertz model for this study is that the contaminant should react, then at some point the reaction stops and nothing further happens. However, it is well known that this is not the case with sorbed contaminants often exchanging for other contaminants and for varying precipitation/dissolution reactions continuously occurring (Attard & Barnes, 1998). Although the study in this thesis is highly complex and is likely to be composed of large quantities of sorption/desorption and dissolution/precipitation reactions, generalizing reactions can help to create a more binary system which is appropriate for Gompertz modeling. Generally, by observing a trend of removing a contaminant followed by an exhaustion of the media to remove a contaminant produces a system that is well modeled by the Gompertz equation.

Overall, the use of the Gompertz function in this study is not necessarily inappropriate and often is descriptive and effective, however, several factors in its utilization should be considered when interpreting results.

5.2 Study Design: Proof of Concept

As has been referenced multiple times through this thesis, the used study design involves highly intricate interactions with a complex influent which underwent complex reactions under a continuously flowing system. This allows for many things to play a role in understanding the removal of contaminants such as kinetics, multi-layer sorption, chemical sorption, competitive sorption, and precipitation/dissolution reactions to name a few.

Furthermore, the experiments performed were only conducted once and had no replicate studies to confirm the reproducibility of what was observed. Therefore, it should be clearly noted that these results apply strictly to the experiments that were conducted and cannot be statistically applied to the wholistic behavior of the studied media in treating the studied contaminants.

This study was designed the way it was in order to serve as a proof of concept for these media to treat a complex mix of contaminants to further inform future, larger-scaled projects. The conclusions from this study will help to better design effluent treatment systems for bioretention which is actively an area of research within the Oklahoma Water Survey. More detailed studies are suggested in “Future Studies” which could help to understand specific mechanisms at play and could overall benefit the final design for bioretention effluent treatment systems.

5.3 Environmental Safety Considerations

Scott & Penn (2021) conclude their study with an excellent mention of the "environmental safety of steel slags." Furthermore, in a review of fly ash, Ahmaruzzaman (2010) was sure to include mention of the safety and proper application of fly ash in environmental settings. Considerations should include a medium's leaching ability, reuse potential, proper disposal, variability of source material, and potential impacts to LID hydraulics. The biochar used in this study has been approved by the US EPA as safe to use in the environment (J. Gaspard, personal communication, October 10, 2022).

Fly ash and steel or iron slags are not homogeneous and as demonstrated by this study, these media possess the potential to leach elements into the environment. The selection of the used media is very important, with source media coming from industries or sources that commonly contain higher concentrations of more harmful metals can be of particular concern. Furthermore, obtaining biochar from a source which produces biochar, and not charcoal is very important to maintain the carbon structures which give biochar its beneficial properties. Likewise, the proper application of media is incredibly important. Generally, deploying a media with a high metal content into a highly acidic environment considerably increases the risk of metals leaching from the media. Although fly ash and steel slag have been shown to buffer solutions well, in doing so, these media may leach metals rather than retaining them.

Lastly, using a porous media in a system designed to capture and distribute water can pose an issue to the hydraulics for said system. Considerations would need to be taken into account to determine if inserting media into a bioretention underdrain would negatively impact the hydraulics of the system and potentially reduce the efficacy of the bioretention as designed. Likewise, impacts

of media interactions with the treated solution (mostly precipitation) would need to be monitored to assess the impacts to bioretention hydraulics.

6 Future Studies

This thesis has highlighted many areas where the proof of concept from this study could be expanded upon to maximize LID design and to further understand the mechanisms in aqueous contaminant removal.

One such approach is aqueous geochemical modeling (AGM) to better understand what specific geochemical processes are factoring into changes in component concentrations. For instance, the SSW solution could be modeled based on measured sample concentrations. This AGM would help in understanding the equilibrium state of the influent solution to predict the contaminant phase (dissolved or complexed) as well as what elements are under or over saturated. Based on the properties of the media used in this study, transport modeling would allow a model to predict the precipitation or dissolution of various components as well as likely sorption (physical or chemical) of different contaminants. Model results could then be compared to measured results to determine any discrepancies between the measured and thermodynamically preferred concentrations/states. With known influent and effluent chemistries, inverse modeling would also provide insight to the likely reactions taking place within the sample column itself.

The Oklahoma Water Survey has ongoing research whose goal it is to scale up the research from this thesis and to apply on a real-life scale. Experimental bioretention cells at the Grand Lake Dam Authority (GRDA) in Langley, OK, USA are outfitted such that both influent and effluent water (quantity and quality) can be controlled as well as the variables within the cells themselves. An initial scaling up has been conducted using the media from this study in columns attached to the underdrains of these cells. Results from this study are outside the scope of this thesis but will illuminate the representativeness of this study to a scaled-up version which could have implications for further use.

This study as a proof of concept has helped to broadly identify the applicability of these media in water quality LID and has helped identify potential future areas of study in terms of the overall sorptive capacity for the contaminants that were used. Beaker experiments would be more appropriate to determine the mass and the rate of sorption of these contaminants onto these treatment media. Furthermore, this would allow for the Langmiur isotherm to apply which is a better statistical model to determine sorption rates and media exhaustion points (W. Zhang et al., 2008). By slowly building a more complex solution mixture, the impact of competitive sorption can also be studied by observing the decrease in sorption efficiency as the overall solution becomes more and more complex. This will also help to develop specific sorption coefficient (K_d) values for each neonicotinoid and medium combination which could be useful for applications outside of LID improvement.

The final suggested future study would be to investigate the media to confirm the sorbed contaminants and to determine the structures that are formed during said sorption. This can be accomplished by performing digestions on the media after it has been used to remove contaminants from solution. If previous leaching studies have been performed on the media as was suggested, then digestions would further confirm the sorbed partition of contaminants to the media in the column experiments. To determine the specific structure that is formed during sorption, x-ray diffraction or as Qin et al. (2018) used, K-edge X-ray absorption near-edge structure (XANES) analysis. This would give further insight to the mechanism of removal and further understanding of the mobility of contaminants once retained in a treatment system. For instance, some sorbed or precipitated molecules can aggregate and form more stable mineral species, where others are amorphous and are easily re-dissolved. This evaluation would help to determine the longevity and long-lasting impacts of these media as LID enhancements.

7 Conclusions

In vertical column experiments, media size appeared to have varying effects on contaminant removal from solution. With columns containing aggregated fly ash, seemingly no meaningful affect was seen between the large and small fractions. In fact, some instances saw large aggregated fly ash performing better than the small fraction. Steel slag, however, saw a major impact between the small and large fractions with the smaller size performing better than the large portion. This relationship was so extreme that in several cases, large steel slag was the least efficient of the media combinations with small steel slag being the most efficient. Biochar showed mixed results with some contaminants being removed equally between the large and small fraction. However, where a separation was observed, the smaller fraction was always the more efficient.

Overall, where removal was seen, small steel slag was the best performer in vertical column experiments. However, where the media was shown to be leaching a contaminant, steel slag was often a, if not, *the* culprit of leaching. Small steel slag was notably the best performer in removing P from solution and also performed well at removing acetamiprid and imidacloprid.

After small steel slag, no distinctive ordering of media emerged with biochars, aggregated fly ashes, and large steel slag ordering differently when treating different contaminants. Where contaminants were leached from aggregated fly ash and steel slag, biochar either leached less of the contaminant, didn't leach at all, or actually removed some of the contaminant.

In horizontal column experiments small steel slag yet again performed best for As^{+5} removal. Moreover, steel slag removed P from solution that no exhaustion point could be interpolated within the bounds of the experiments. In the case of elements that were leached into the effluent, aggregated fly ash and steel slag were most commonly the culprits due to metal-oxide dissolution.

The most impactful results from horizontal column experiments came in the neonicotinoid results. Both aggregated fly ash and steel slag were not far enough removed from the control column for them to be suggested as a treatment for neonicotinoids in bioretention effluent. However, biochar proved to be the ideal treatment removing most, if not all of neonicotinoids from solution.

Overall, media selection for a bioretention underdrain amendment would largely be dependent on what the primary contaminant of concern is for the user and what the environmental conditions are for application. Highly acidic environments such as acid mine drainage may not be applicable due to fly ash and steel slag's ability to leach heavy metals. Furthermore, waters with high dissolved solids may not favor fly ash and steel slag due to their further contribution to solution total solids as well as the media's reliance on the metal-oxide dissolution as a potential mechanism of contaminant removal. However, under the proper conditions, if phosphorus or metals are of primary concern, small steel slag appears to be the best choice. However, if organic contaminants, specifically neonicotinoid pesticides, are the primary concern, small biochar is the standout choice.

Each experiment was run only once per media/contaminant/orientation combination. For this reason, the experiments conducted in this thesis should strictly speak for themselves and not represent a statistical correlation between the various combinations. This data is intended as a catalyst for other studies to draw from to provide more statistically robust results to inform the use of these media for environmental purposes. Such studies would include repeating this study to confirm original results, scaling up this research to a field scale, and further examining the sorption and precipitation mechanisms. The latter can be investigated via beaker studies, leaching studies (pre- and post-media use), and XRD or XANES analysis. Likewise, AGM of this study and future

studies would help to understand the thermodynamically predicted results and could help identify mechanisms that affect any departure from the modeled results.

8 Acknowledgements

This material is based on work supported by the National Science Foundation under Grant No. OIA-1946093. Any opinions, findings, and conclusions or recommendations expressed in this material are those of the author(s) and do not necessarily reflect the views of the National Science Foundation or Oklahoma State Regents for Higher Education.

This grant was awarded through the Oklahoma Established Program to Stimulate Competitive Research (EPSCOR) under the "Variable and Marginal Quality Water Supplies" focus area. This grant was supported and facilitated by the Oklahoma Water Survey (OWS), a research consortium as a part of the University of Oklahoma.

Special thanks to my committee, Dr. Jason Vogel, Dr. Kato Dee, and Dr. Caitlin Hodges, as well as non-committee advisors, Grant Graves and Rishabh Shukla for their countless hours of help, support, and advice in making this project possible. Additionally, thanks to the OWS student staff for their assistance in preparing experiments and collecting and processing samples.

Steel slag used in this research was provided by Michael Wood, TMS International Corporation©. Biochar was purchased from Biochar Now. Supplies, procurement, and research advice was provided by the staff at the University of Oklahoma Chemistry Stockroom, DeAnna Stone and Krissy Griffin.

Help on curve fitting in R was provided by Dr. Claire Curry (University of Oklahoma Science Librarian) and Dr. Wesley Honeycutt (transdisciplinary Postdoctoral Research Associate).

9 Sources

Agyei, N. M., Strydom, C. A., & Potgieter, J. H. (2002). The removal of phosphate ions from aqueous solution by fly ash, slag, ordinary Portland cement and related blends. *Cement and Concrete Research*, *32*(12), 1889–1897. https://doi.org/10.1016/S0008-8846(02)00888-8

Ahmad Zubairi, N. A., Takaijudin, H., Ab Ghani, A., Goh, H. W., & Day, W. A. (2022). Assessment of imidacloprid removal from agricultural runoff by the bioretention treatment train system. *Environmental Advances*, *7*, 100156. https://doi.org/10.1016/j.envadv.2021.100156

Ahmaruzzaman, M. (2010). A review on the utilization of fly ash. *Progress in Energy and Combustion Science*, *36*(3), 327–363. https://doi.org/10.1016/j.pecs.2009.11.003

Akter, K. F., Owens, G., Davey, D. E., & Naidu, R. (2005). Arsenic Speciation and Toxicity in Biological Systems. In G. W. Ware, L. A. Albert, D. G. Crosby, P. de Voogt, O. Hutzinger, J. B. Knaak, F. L. Mayer, D. P. Morgan, D. L. Park, R. S. Tjeerdema, D. M. Whitacre, R. S. H. Yang, & F. A. Gunther (Eds.), *Reviews of Environmental Contamination and Toxicology* (Vol. 184, pp. 97–149). Springer New York. https://doi.org/10.1007/0-387-27565-7_3

Ali, M. T., & Shahram, S. H. (2007). *Converter Slag as a Liming Agent in the Amelioration of Acidic Soils*. *9*(5), 7.

Al-Wabel, M. I., Al-Omran, A., El-Naggar, A. H., Nadeem, M., & Usman, A. R. A. (2013). Pyrolysis temperature induced changes in characteristics and chemical composition of biochar produced from conocarpus wastes. *Bioresource Technology*, *131*, 374–379. https://doi.org/10.1016/j.biortech.2012.12.165

Apak, R., Tütem, E., Hügül, M., & Hizal, J. (1998). Heavy metal cation retention by unconventional sorbents (red muds and fly ashes). *Water Research*, *32*(2), 430–440. https://doi.org/10.1016/S0043-1354(97)00204-2

Arias, C. A., Del Bubba, M., & Brix, H. (2001). Phosphorus removal by sands for use as media in subsurface flow constructed reed beds. *Water Research*, *35*(5), 1159–1168. https://doi.org/10.1016/S0043-1354(00)00368-7

Armbrust, K. L., & Peeler, H. B. (2002). Effects of formulation on the run-off of imidacloprid from turf. *Pest Management Science*, *58*(7), 702–706. https://doi.org/10.1002/ps.518

Ashoori, N., Teixido, M., Spahr, S., LeFevre, G. H., Sedlak, D. L., & Luthy, R. G. (2019). Evaluation of pilot-scale biochar-amended woodchip bioreactors to remove nitrate, metals, and trace organic contaminants from urban stormwater runoff. *Water Research*, *154*, 1–11. https://doi.org/10.1016/j.watres.2019.01.040

ASTM standard specification for coal fly ash and raw or calcined natural pozzolan for use in concrete (No. C618-05; Annual Book of ASTM Standards, Concrete and Aggregates). (2005). American Society for Testing Materials.

Attard, G., & Barnes, C. (1998). *Surfaces*. Oxford University Press.

Ayala, J., Blanco, F., García, P., Rodriguez, P., & Sancho, J. (1998). Asturian fly ash as a heavy metals removal material. *Fuel*, *77*(11), 1147–1154. https://doi.org/10.1016/S0016-2361(98)00027-1

Baby, J., Raj, J., Biby, E., Sankarganesh, P., Jeevitha, M., Ajisha, S., & Rajan, S. (2011). Toxic effect of heavy metals on aquatic environment. *International Journal of Biological and Chemical Sciences*, *4*(4). https://doi.org/10.4314/ijbcs.v4i4.62976

Baciocchi, R., Costa, G., Polettini, A., & Pomi, R. (2015). Effects of thin-film accelerated carbonation on steel slag leaching. *Journal of Hazardous Materials*, *286*, 369–378. https://doi.org/10.1016/j.jhazmat.2014.12.059

Bal, R., Türk, G., Tuzcu, M., Yilmaz, O., Kuloglu, T., Gundogdu, R., Gür, S., Agca, A., Ulas, M., Çambay, Z., Tuzcu, Z., Gencoglu, H., Guvenc, M., Ozsahin, A. D., Kocaman, N., Aslan, A., & Etem, E. (2012). Assessment of imidacloprid toxicity on reproductive organ system of adult male rats. *Journal of Environmental Science and Health, Part B*, *47*(5), 434–444. https://doi.org/10.1080/03601234.2012.663311

Barrett, M. E. (2003). Performance, Cost, and Maintenance Requirements of Austin Sand Filters. *Journal of Water Resources Planning and Management*, *129*(3), 234–242. https://doi.org/10.1061/(ASCE)0733-9496(2003)129:3(234)

Bayat, B. (2002a). Combined Removal of Zinc (II) and Cadmium (II) from Aqueous Solutions by Adsorption onto High-Calcium Turkish Fly Ash. *Water, Air and Soil Pollution*, *136*, 69–92.

Bayat, B. (2002b). Comparative study of adsorption properties of Turkish fly ashes. *Journal of Hazardous Materials*, *95*(3), 275–290. https://doi.org/10.1016/S0304-3894(02)00141-3

Biskri, Y., Achoura, D., Chelghoum, N., & Mouret, M. (2017). Mechanical and durability characteristics of High Performance Concrete containing steel slag and crystalized slag as aggregates. *Construction and Building Materials*, *150*, 167–178. https://doi.org/10.1016/j.conbuildmat.2017.05.083

BMP Statistical Analysis Tool. (n.d.). INT'L STORMWATER BMP DBASE. Retrieved November 18, 2021, from https://bmpdatabase.org/bmp-statistical-analysis-tool

Borsuah, J. F., Messer, T. L., Snow, D. D., Comfort, S. D., & Mittelstet, A. R. (2020). Literature Review: Global Neonicotinoid Insecticide Occurrence in Aquatic Environments. *Water*, *12*(12), 3388. https://doi.org/10.3390/w12123388

Bowden, L. I., Jarvis, A. P., Younger, P. L., & Johnson, K. L. (2009). Phosphorus Removal from Waste Waters Using Basic Oxygen Steel Slag. *Environmental Science & Technology*, *43*(7), 2476–2481. https://doi.org/10.1021/es801626d

Bowen, D. (2021). *Steel Slag TCLP* (Analytical Report No. 180-118695–1). Eurofins.

Brown, G. (2017). *The Application of Fly Ash to Treat Stormwater around Poultry Houses*. Oklahoma State University.

Cairns, S., Robertson, I., Holliman, P., & Street-Perrott, A. (2022). Treatments of wood ash amended biochar to reduce nutrient leaching and immobilise lead, copper, zinc and cadmium in aqueous solution: Column experiments. *Environmental Science: Water Research & Technology*, 10.1039.D1EW00962A. https://doi.org/10.1039/D1EW00962A

Canadian Council of Ministers of the Environment. (2007). *Canadian water quality guidelines: Imidacloprid scientific supporting document*. Canadian Council of Ministers of the Environment. https://www.deslibris.ca/ID/251252

Carleton, J. N., Grizzard, T. J., Godrej, A. N., & Post, H. E. (2001). Factors affecting the performance of stormwater treatment wetlands. *Water Research*, *35*(6), 1552–1562. https://doi.org/10.1016/S0043-1354(00)00416-4

Chandra Srivastava, V., Deo Mall, I., & Mani Mishra, I. (2006). Modelling Individual and Competitive Adsorption of Cadmium(II) and Zinc(II) Metal Ions from Aqueous Solution onto Bagasse Fly Ash. *Separation Science and Technology*, *41*(12), 2685–2710. https://doi.org/10.1080/01496390600725687

Characterization of Solutions by pH and Eh. (2006, October). Railsback's Some Fundaments of Mineralogy and Geochemistry. http://railsback.org/Fundamentals/8150RedoxPlot07LS.pdf

Chen, J., Kong, H., Wu, D., Chen, X., Zhang, D., & Sun, Z. (2007). Phosphate immobilization from aqueous solution by fly ashes in relation to their composition. *Journal of Hazardous Materials*, *139*(2), 293–300. https://doi.org/10.1016/j.jhazmat.2006.06.034

Cheung, K. C., & Venkitachalam, T. H. (2000). Improving phosphate removal of sand infiltration system using alkaline fly ash. *Chemosphere*, *41*(1–2), 243–249. https://doi.org/10.1016/S0045-6535(99)00417-8

Cheung, K. C., Venkitachalam, T. H., & Scott, W. D. (1994). Selecting soil amendment materials for removal of phosphorus. *Water Science and Technology*, *30*(6), 247–256. https://doi.org/10.2166/wst.1994.0275

Chu, K. H. (2020). Fitting the Gompertz equation to asymmetric breakthrough curves. *Journal of Environmental Chemical Engineering*, *8*(3), 103713. https://doi.org/10.1016/j.jece.2020.103713

Cosgrove, S., Jefferson, B., & Jarvis, P. (2019). Pesticide removal from drinking water sources by adsorption: A review. *Environmental Technology Reviews*, *8*(1), 1–24. https://doi.org/10.1080/21622515.2019.1593514

Cox, L., Hermosin, M. C., Koskinen, W. C., & Cornejo, J. (2000). *Interactions of imidacloprid with organicand inorganic-exchanged smectites*. 8.

Davis, A. P., Shokouhian, M., Sharma, H., & Minami, C. (2001). Laboratory Study of Biological Retention for Urban Stormwater Management. *Water Environment Research*, *73*(1), 5–14. https://doi.org/10.2175/106143001X138624

Davis, A. P., Shokouhian, M., Sharma, H., & Minami, C. (2006). Water Quality Improvement through Bioretention Media: Nitrogen and Phosphorus Removal. *Water Environment Research*, *78*(3), 284–293. https://doi.org/10.2175/106143005X94376

December 2021 crude steel production and 2021 global crude steel production totals. (n.d.). *Worldsteel.Org*. Retrieved September 1, 2022, from https://worldsteel.org/media-centre/press-releases/2022/december-2021-crude-steel-production-and-2021-global-totals/

Diamadopoulos, E., Ioannidis, S., & Sakellaropoulos, G. P. (1993). As(V) removal from aqueous solutions by fly ash. *Water Research*, *27*(12), 1773–1777. https://doi.org/10.1016/0043-1354(93)90116-Y

Ding, Z., Hu, X., Wan, Y., Wang, S., & Gao, B. (2016). Removal of lead, copper, cadmium, zinc, and nickel from aqueous solutions by alkali-modified biochar: Batch and column tests. *Journal of Industrial and Engineering Chemistry*, *33*, 239–245. https://doi.org/10.1016/j.jiec.2015.10.007

Drizo, A., Forget, C., Chapuis, R. P., & Comeau, Y. (2006). Phosphorus removal by electric arc furnace steel slag and serpentinite. *Water Research*, *40*(8), 1547–1554. https://doi.org/10.1016/j.watres.2006.02.001

Dzombak, D. A., & Morel, F. M. M. (1990). *Surface complexation modeling: Hydrous ferric oxide*. Wiley.

European Food Safety Authority (EFSA). (2008). Conclusion regarding the peer review of the pesticide risk assessment of the active substance imidacloprid. *EFSA Journal*, *6*(7). https://doi.org/10.2903/j.efsa.2008.148r

Ferreira, V. J., Sáez-De-Guinoa Vilaplana, A., García-Armingol, T., Aranda-Usón, A., Lausín-González, C., López-Sabirón, A. M., & Ferreira, G. (2016). Evaluation of the steel slag incorporation as coarse aggregate for road construction: Technical requirements and environmental impact assessment. *Journal of Cleaner Production*, *130*, 175–186. https://doi.org/10.1016/j.jclepro.2015.08.094

Gabelich, C. J., Gerringer, F. W., Lee, C. C., & Knocke, W. R. (2006). Sequential Manganese Desorption and Sequestration in Anthracite Coal and Silica Sand Filter Media. *Journal - American Water Works Association*, *98*(5), 116–127. https://doi.org/10.1002/j.1551-8833.2006.tb07665.x

Gaspard, J. (2022, October 10). *Personal Communications* [Phone Call].

Genç-Fuhrman, H., Mikkelsen, P. S., & Ledin, A. (2007). Simultaneous removal of As, Cd, Cr, Cu, Ni and Zn from stormwater: Experimental comparison of 11 different sorbents. *Water Research*, *41*(3), 591–602. https://doi.org/10.1016/j.watres.2006.10.024

Goetz, E. R., & Riefler, R. G. (2014). Performance of steel slag leach beds in acid mine drainage treatment. *Chemical Engineering Journal*, *240*, 579–588. https://doi.org/10.1016/j.cej.2013.10.080

Gomes, J. F. P., & Pinto, C. G. (2006). Leaching of heavy metals from steelmaking slags. *Revista de Metalurgia*, *42*(6), 409–416. https://doi.org/10.3989/revmetalm.2006.v42.i6.39

Gonzalez, J. M., Shipitalo, M. J., Smith, D. R., Warnemuende-Pappas, E., & Livingston, S. J. (2016). Atrazine Sorption by Biochar, Tire Chips, and Steel Slag as Media for Blind Inlets: A Kinetic and Isotherm Sorption Approach. *Journal of Water Resource and Protection*, *08*(13), 1266–1282. https://doi.org/10.4236/jwarp.2016.813097

González-Pradas, E., Villafranca-Sánchez, M., Socías-Viciana, M., Fernández-Pérez, M., & Ureña-Amate, M. D. (1999). Preliminary studies in removing atrazine, isoproturon and imidacloprid from water by natural sepiolite. *Journal of Chemical Technology & Biotechnology*, *74*(5), 417–422. https://doi.org/10.1002/(SICI)1097-4660(199905)74:5<417::AID-JCTB58>3.0.CO;2-Q

Grosjean, P. (2022). *SciViews-R*. UMONS. http://www.sciviews.org/SciViews-R

Gunawardana, C., Egodawatta, P., & Goonetilleke, A. (2015). Adsorption and mobility of metals in build-up on road surfaces. *Chemosphere*, *119*, 1391–1398. https://doi.org/10.1016/j.chemosphere.2014.02.048

Guppy, C. N., Menzies, N. W., Blamey, F. P. C., & Moody, P. W. (2005). Do Decomposing Organic Matter Residues Reduce Phosphorus Sorption in Highly Weathered Soils? *Soil Science Society of America Journal*, *69*(5), 1405–1411. https://doi.org/10.2136/sssaj2004.0266

Gupta, G., & Torres, N. (1998). Use of fly ash in reducing toxicity of and heavy metals in wastewater effluent. *Journal of Hazardous Materials*, *57*(1–3), 243–248. https://doi.org/10.1016/S0304-3894(97)00093-9

Gupta, V., Jain, C. K., Ali, I., Chandra, S., & Agarwal, S. (2002). Removal of lindane and malathion from wastewater using bagasse fly ash—A sugar industry waste. *Water Research*, *36*(10), 2483–2490. https://doi.org/10.1016/S0043-1354(01)00474-2

Gupta, V. K., & Ali, I. (2000). Utilisation of bagasse fly ash (a sugar industry waste) for the removal of copper and zinc from wastewater. *Separation and Purification Technology*, *18*(2), 131–140. https://doi.org/10.1016/S1383-5866(99)00058-1

Gupta, V. K., & Ali, I. (2001). Removal of DDD and DDE from wastewater using bagasse fly ash, a sugar industry waste. *Water Research*, *35*(1), 33–40. https://doi.org/10.1016/S0043-1354(00)00232-3

Gupta, V. K., & Ali, I. (2004). Removal of lead and chromium from wastewater using bagasse fly ash—A sugar industry waste. *Journal of Colloid and Interface Science*, *271*(2), 321–328. https://doi.org/10.1016/j.jcis.2003.11.007

Gupta, V. K., Ali, I., Suhas, & Saini, V. K. (2006). Adsorption of 2,4-D and carbofuran pesticides using fertilizer and steel industry wastes. *Journal of Colloid and Interface Science*, *299*(2), 556–563. https://doi.org/10.1016/j.jcis.2006.02.017

Gupta, V. K., Jain, C. K., Ali, I., Sharma, M., & Saini, V. K. (2003). Removal of cadmium and nickel from wastewater using bagasse fly ash—A sugar industry waste. *Water Research*, *37*(16), 4038–4044. https://doi.org/10.1016/S0043-1354(03)00292-6

Gupta, V. K., Mohan, D., Sharma, S., & Park, K. T. (1998). Removal of chromium(VI) from electroplating industry wastewater using bagasse fly ash—A sugar industry waste material. *The Environmentalist*, *19*(2), 129–136. https://doi.org/10.1023/A:1006693017711

Gupta, V. K., & Sharma, S. (2003). Removal of Zinc from Aqueous Solutions Using Bagasse Fly Ash − a Low Cost Adsorbent. *Industrial & Engineering Chemistry Research*, *42*(25), 6619–6624. https://doi.org/10.1021/ie0303146

Gwenzi, W., Chaukura, N., Noubactep, C., & Mukome, F. N. D. (2017). Biochar-based water treatment systems as a potential low-cost and sustainable technology for clean water provision. *Journal of Environmental Management*, *197*, 732–749. https://doi.org/10.1016/j.jenvman.2017.03.087

Han, W., Tian, Y., & Shen, X. (2018). Human exposure to neonicotinoid insecticides and the evaluation of their potential toxicity: An overview. *Chemosphere*, *192*, 59–65. https://doi.org/10.1016/j.chemosphere.2017.10.149

Hladik, M. L., & Kolpin, D. W. (2016). First national-scale reconnaissance of neonicotinoid insecticides in streams across the USA. *Environmental Chemistry*, *13*(1), 12. https://doi.org/10.1071/EN15061

Hladik, M. L., Kolpin, D. W., & Kuivila, K. M. (2014). Widespread occurrence of neonicotinoid insecticides in streams in a high corn and soybean producing region, USA. *Environmental Pollution*, *193*, 189–196. https://doi.org/10.1016/j.envpol.2014.06.033

Hsieh, C., Davis, A. P., & Needelman, B. A. (2007). Bioretention Column Studies of Phosphorus Removal from Urban Stormwater Runoff. *Water Environment Research*, *79*(2), 177–184. https://doi.org/10.2175/106143006X111745

Hsu, T.-C., Yu, C.-C., & Yeh, C.-M. (2008). Adsorption of Cu2+ from water using raw and modified coal fly ashes. *Fuel*, *87*(7), 1355–1359. https://doi.org/10.1016/j.fuel.2007.05.055

Huber, M., Welker, A., & Helmreich, B. (2016). Critical review of heavy metal pollution of traffic area runoff: Occurrence, influencing factors, and partitioning. *Science of The Total Environment*, *541*, 895–919. https://doi.org/10.1016/j.scitotenv.2015.09.033

Imidacloprid Technical Fact Sheet. (n.d.). Retrieved October 17, 2022, from http://npic.orst.edu/factsheets/archive/imidacloprid.html

Ippolito, J. A., Barbarick, K. A., Heil, D. M., Chandler, J. P., & Redente, E. F. (2003). Phosphorus Retention Mechanisms of a Water Treatment Residual. *Journal of Environmental Quality*, *32*(5), 1857–1864. https://doi.org/10.2134/jeq2003.1857

Jain, S. K., Shakil, N. A., Dutta, A., Kumar, J., & Saini, M. K. (2017). Sorption kinetics and isotherm modelling of imidacloprid on bentonite and organobentonites. *Journal of Environmental Science and Health, Part B*, *52*(5), 326–337. https://doi.org/10.1080/03601234.2017.1281653

Jeschke, P., & Nauen, R. (2008). Neonicotinoids—From zero to hero in insecticide chemistry. *Pest Management Science*, *64*(11), 1084–1098. https://doi.org/10.1002/ps.1631

Jeschke, P., Nauen, R., Schindler, M., & Elbert, A. (2011). Overview of the Status and Global Strategy for Neonicotinoids. *Journal of Agricultural and Food Chemistry*, *59*(7), 2897–2908. https://doi.org/10.1021/jf101303g

Kandel, S., Vogel, J., Penn, C., & Brown, G. (2017). Phosphorus Retention by Fly Ash Amended Filter Media in Aged Bioretention Cells. *Water*, *9*(10), 746. https://doi.org/10.3390/w9100746

Kayhanian, M., Fruchtman, B. D., Gulliver, J. S., Montanaro, C., Ranieri, E., & Wuertz, S. (2012). Review of highway runoff characteristics: Comparative analysis and universal implications. *Water Research*, *46*(20), 6609–6624. https://doi.org/10.1016/j.watres.2012.07.026

Kim, D.-H., Shin, M.-C., Choi, H.-D., Seo, C.-I., & Baek, K. (2008). Removal mechanisms of copper using steel-making slag: Adsorption and precipitation. *Desalination*, *223*(1–3), 283–289. https://doi.org/10.1016/j.desal.2007.01.226

Kimura-Kuroda, J., Komuta, Y., Kuroda, Y., Hayashi, M., & Kawano, H. (2012). Nicotine-Like Effects of the Neonicotinoid Insecticides Acetamiprid and Imidacloprid on Cerebellar Neurons from Neonatal Rats. *PLoS ONE*, *7*(2), e32432. https://doi.org/10.1371/journal.pone.0032432

Klarich, K. L., Pflug, N. C., DeWald, E. M., Hladik, M. L., Kolpin, D. W., Cwiertny, D. M., & LeFevre, G. H. (2017). Occurrence of Neonicotinoid Insecticides in Finished Drinking Water and Fate during Drinking Water Treatment. *Environmental Science & Technology Letters*, *4*(5), 168–173. https://doi.org/10.1021/acs.estlett.7b00081

Kumari, K., Singh, R. P., & Saxena, S. K. (1988). Adsorption thermodynamics of carbofuran on fly ash. *Colloids and Surfaces*, *33*, 55–61. https://doi.org/10.1016/0166-6622(88)80048-9

Lan, Y., Liu, Q., Meng, F., Niu, D., & Zhao, H. (2017). Optimization of magnetic separation process for iron recovery from steel slag. *Journal of Iron and Steel Research International*, *24*(2), 165–170. https://doi.org/10.1016/S1006-706X(17)30023-7

Langmuir, D., Chrostowski, P., Vigneault, B., & Chaney, R. (2004). *ISSUE PAPER ON THE ENVIRONMENTAL CHEMISTRY OF METALS*. 113.

Li, S., Cooke, R. A., Wang, L., Ma, F., & Bhattarai, R. (2017). Characterization of fly ash ceramic pellet for phosphorus removal. *Journal of Environmental Management*, *189*, 67–74. https://doi.org/10.1016/j.jenvman.2016.12.042

Li, Y., & Dai, W.-B. (2018). Modifying hot slag and converting it into value-added materials: A review. *Journal of Cleaner Production*, *175*, 176–189. https://doi.org/10.1016/j.jclepro.2017.11.171

Liem-Nguyen, V., Sjöberg, V., Dinh, N. P., Huy, D. H., & Karlsson, S. (2020). Removal mechanism of arsenic (V) by stainless steel slags obtained from scrap metal recycling. *Journal of Environmental Chemical Engineering*, *8*(4), 103833. https://doi.org/10.1016/j.jece.2020.103833

Lin, C.-J., & Chang, J.-E. (2001). Effect of fly ash characteristics on the removal of Cu(II) from aqueous solution. *Chemosphere*, *44*(5), 1185–1192. https://doi.org/10.1016/S0045-6535(00)00494-X

Lobato, N. C. C., Villegas, E. A., & Mansur, M. B. (2015). Management of solid wastes from steelmaking and galvanizing processes: A brief review. *Resources, Conservation and Recycling*, *102*, 49–57. https://doi.org/10.1016/j.resconrec.2015.05.025

Lyngsie, G., Borggaard, O. K., & Hansen, H. C. B. (2014). A three-step test of phosphate sorption efficiency of potential agricultural drainage filter materials. *Water Research*, *51*, 256–265. https://doi.org/10.1016/j.watres.2013.10.061

Magalhaes, L. C., Hunt, T. E., & Siegfried, B. D. (2009). Efficacy of Neonicotinoid Seed Treatments to Reduce Soybean Aphid Populations Under Field and Controlled Conditions in Nebraska. *Journal of Economic Entomology*, *102*(1), 187–195. https://doi.org/10.1603/029.102.0127

Main, A. R., Headley, J. V., Peru, K. M., Michel, N. L., Cessna, A. J., & Morrissey, C. A. (2014). Widespread Use and Frequent Detection of Neonicotinoid Insecticides in Wetlands of Canada's Prairie Pothole Region. *PLoS ONE*, *9*(3), e92821. https://doi.org/10.1371/journal.pone.0092821

Marsh, H., & Reinoso, F. R. (2006). *Activated Carbon*. Elsevier.

Martin, T. D., Brockhoff, C. A., Creed, J. T., Kopp, J. F., Martin, E. R., & EMMC Methods Work Group. (1996). *DETERMINATION OF METALS AND TRACE ELEMENTS IN WATER AND WASTES BY INDUCTIVELY COUPLED PLASMA-ATOMIC EMISSION SPECTROMETRY* (Method 200.7). https://doi.org/10.1016/B978-0-8155-1398-8.50010-0

Method 3120 B. (2005). *Standard Methods for the Examination of Water and Wastewater*, *21th Edition*, 3–39 to 3–44.

Mineau, P., & Palmer, C. (2013). *The Impact of the Nation's Most Windly used Insecticides on Birds*. American Bird Conservancy.

Mohanty, S. K., Valenca, R., Berger, A. W., Yu, I. K. M., Xiong, X., Saunders, T. M., & Tsang, D. C. W. (2018). Plenty of room for carbon on the ground: Potential applications of biochar for stormwater treatment. *Science of The Total Environment*, *625*, 1644–1658. https://doi.org/10.1016/j.scitotenv.2018.01.037

Moodley, I., Sheridan, C. M., Kappelmeyer, U., & Akcil, A. (2018). Environmentally sustainable acid mine drainage remediation: Research developments with a focus on waste/by-products. *Minerals Engineering*, *126*, 207–220. https://doi.org/10.1016/j.mineng.2017.08.008

Morrissey, C. A., Mineau, P., Devries, J. H., Sanchez-Bayo, F., Liess, M., Cavallaro, M. C., & Liber, K. (2015). Neonicotinoid contamination of global surface waters and associated risk to aquatic invertebrates: A review. *Environment International*, *74*, 291–303. https://doi.org/10.1016/j.envint.2014.10.024

Mukherjee, A., Zimmerman, A. R., & Harris, W. (2011). Surface chemistry variations among a series of laboratory-produced biochars. *Geoderma*, *163*(3–4), 247–255. https://doi.org/10.1016/j.geoderma.2011.04.021

Negro, C., Martínez Pérez-Cejuela, H., Simó-Alfonso, E. F., Herrero-Martínez, J. M., Bruno, R., Armentano, D., Ferrando-Soria, J., & Pardo, E. (2021). Highly Efficient Removal of Neonicotinoid Insecticides by Thioether-Based (Multivariate) Metal–Organic

Frameworks. *ACS Applied Materials & Interfaces*, *13*(24), 28424–28432. https://doi.org/10.1021/acsami.1c08833

Nollet, H., Roels, M., Lutgen, P., Van der Meeren, P., & Verstraete, W. (2003). Removal of PCBs from wastewater using fly ash. *Chemosphere*, *53*(6), 655–665. https://doi.org/10.1016/S0045-6535(03)00517-4

Norton, G. A. (2004). *Cleaning of Equipment for Water Sampling* (Manual Book 9, Chapter A3; National Field Manual for the Collection of Water-Quality Data, p. 83). U.S. Geologic Survey.

Okochi, N. C., & McMartin, D. W. (2012). A Laboratory Study of the Treatability of Synthetic Stormwater Under Varying Conditions Using Electric Arc Furnace Steel Slag. *Water*, *4*(2), 321–344. https://doi.org/10.3390/w4020321

OSHA. (2004). *Toxic Metals—Overview | Occupational Safety and Health Administration*. https://www.osha.gov/toxic-metals

Pan, S.-C., Lin, C.-C., & Tseng, D.-H. (2003). Reusing sewage sludge ash as adsorbent for copper removal from wastewater. *Resources, Conservation and Recycling*, *39*(1), 79–90. https://doi.org/10.1016/S0921-3449(02)00122-2

Pan, S.-Y., Adhikari, R., Chen, Y.-H., Li, P., & Chiang, P.-C. (2016). Integrated and innovative steel slag utilization for iron reclamation, green material production and CO2 fixation via accelerated carbonation. *Journal of Cleaner Production*, *137*, 617–631. https://doi.org/10.1016/j.jclepro.2016.07.112

Panday, K. K., Prasad, G., & Singh, V. N. (1985). Copper(II) removal from aqueous solutions by fly ash. *Water Research*, *19*(7), 869–873. https://doi.org/10.1016/0043-1354(85)90145-9

Pasetto, M., Baliello, A., Giacomello, G., & Pasquini, E. (2017). Sustainable solutions for road pavements: A multi-scale characterization of warm mix asphalts containing steel slags. *Journal of Cleaner Production*, *166*, 835–843. https://doi.org/10.1016/j.jclepro.2017.07.212

Paus, K. H., Morgan, J., Gulliver, J. S., & Hozalski, R. M. (2014). Effects of Bioretention Media Compost Volume Fraction on Toxic Metals Removal, Hydraulic Conductivity, and Phosphorous Release. *Journal of Environmental Engineering*, *140*(10), 04014033. https://doi.org/10.1061/(ASCE)EE.1943-7870.0000846

Pesticide Fact Sheet: Acetamiprid. (2002). US EPA.

Pesticide Fact Sheet: Dinotefuran. (2004). US EPA.

Piatak, Ii, Hoppe, Green, & Buszka. (2019). Geochemical Characterization of Iron and Steel Slag and Its Potential to Remove Phosphate and Neutralize Acid. *Minerals*, *9*(8), 468. https://doi.org/10.3390/min9080468

Posthuma-Doodeman, C. J. A. M. (2008). *Environmental risk limits for imidacloprid* (No. 601716018/2008). National Institute for Public Health and the Environment (RIVM).

Procedures Used by OSU Soil, Water, and Forage Analytical Laboratory—Oklahoma State University. (2018, May 1). https://extension.okstate.edu/fact-sheets/procedures-used-by-osu-soil-water-and-forage-analytical-laboratory.html

Qin, Z., Shober, A. L., Scheckel, K. G., Penn, C. J., & Turner, K. C. (2018). Mechanisms of Phosphorus Removal by Phosphorus Sorbing Materials. *Journal of Environmental Quality*, *47*(5), 1232–1241. https://doi.org/10.2134/jeq2018.02.0064

R Core Team. (2022). *R: A language and environment for statistical computing.* (4.2.1) [R]. R Foundation for Statistical Computing. https://R-project.org/

Rao, M., Parwate, A. V., Kadu, P. A., & Bhole, A. G. (2003). Performance of low-cost adsorbents for the removal of copper and lead. *Journal of Water Supply: Research and Technology-Aqua*, *52*(1), 49–58. https://doi.org/10.2166/aqua.2003.0005

Rebek, Dr. E. (2021, September 13). *Personal Communications* [Phone Call].

Reddy, K. R., Xie, T., & Dastgheibi, S. (2014a). Removal of heavy metals from urban stormwater runoff using different filter materials. *Journal of Environmental Chemical Engineering*, *2*(1), 282–292. https://doi.org/10.1016/j.jece.2013.12.020

Reddy, K. R., Xie, T., & Dastgheibi, S. (2014b). Evaluation of Biochar as a Potential Filter Media for the Removal of Mixed Contaminants from Urban Storm Water Runoff. *Journal of Environmental Engineering*, *140*(12), 04014043. https://doi.org/10.1061/(ASCE)EE.1943-7870.0000872

Results for the Spring 2022 Inter-laboratory Comparison Study. (n.d.). Standard Reference Sample Project. Retrieved December 8, 2022, from https://bqs.usgs.gov/srs_study/reports/round_details.php?fy=2022&season=1

Ricci, M., Vos, E. de, & Oostra, A. (2010). *Certification of the mass concentrations of ammonium, chloride, fluoride, magnesium, nitrate, ortho-phosphate, sulfate, and of pH and conductivity in simulated rainwater: Certified reference material ERM-CA408*. Publications Office. https://data.europa.eu/doi/10.2787/28626

Ricou, P., Lecuyer, I., & Le Cloirec, P. (1999). *Removal of Cu2+, Zn2+ and Pb2+ by Adsorption Onto Fly Ash and Fly Ash/Lime Mixing*. *39*(10–11), 239–247.

Rio, S., Delebarre, A., Héquet, V., Cloirec, P. L., & Blondin, J. (2002). Metallic ion removal from aqueous solutions by fly ashes: Multicomponent studies: Metallic ion removal from

aqueous solutions by fly ashes. *Journal of Chemical Technology & Biotechnology*, *77*(3), 382–388. https://doi.org/10.1002/jctb.573

Ritz, C., Baty, F., Streibig, J. C., & Gerhard, D. (2015). Dose-Response Analysis Using R. *PLOS ONE*, *10*(12), e0146021. https://doi.org/10.1371/journal.pone.0146021

Roccamante, M., Miralles-Cuevas, S., Cabrera-Reina, A., Oller, I., & Malato, S. (2022). Evaluation of commercial zerovalent iron sources in combination with solar energy to remove microcontaminants from natural water at circumneutral pH. *Chemosphere*, *286*, 131557. https://doi.org/10.1016/j.chemosphere.2021.131557

Rommel, S. H., Stinshoff, P., & Helmreich, B. (2021). Sequential extraction of heavy metals from sorptive filter media and sediments trapped in stormwater quality improvement devices for road runoff. *Science of The Total Environment*, *782*, 146875. https://doi.org/10.1016/j.scitotenv.2021.146875

Samson-Robert, O., Labrie, G., Chagnon, M., & Fournier, V. (2014). Neonicotinoid-Contaminated Puddles of Water Represent a Risk of Intoxication for Honey Bees. *PLoS ONE*, *9*(12), e108443. https://doi.org/10.1371/journal.pone.0108443

Sánchez-Bayo, F., Goka, K., & Hayasaka, D. (2016). Contamination of the Aquatic Environment with Neonicotinoids and its Implication for Ecosystems. *Frontiers in Environmental Science*, *4*, 71. https://doi.org/10.3389/fenvs.2016.00071

Sánchez-Bayo, F., & Hyne, R. V. (2014). Detection and analysis of neonicotinoids in river waters – Development of a passive sampler for three commonly used insecticides. *Chemosphere*, *99*, 143–151. https://doi.org/10.1016/j.chemosphere.2013.10.051

Sarkhot, D. V., Ghezzehei, T. A., & Berhe, A. A. (2013). Effectiveness of Biochar for Sorption of Ammonium and Phosphate from Dairy Effluent. *Journal of Environmental Quality*, *42*(5), 1545–1554. https://doi.org/10.2134/jeq2012.0482

Schlesinger, W. H., & Bernhardt, E. S. (2013). Biogeochemistry: An Analysis of Global Change. In *Biogeochemistry* (3rd ed.). Elsevier. https://doi.org/10.1016/B978-0-12-385874-0.09985-4

Scott, I. S. P. C., & Penn, C. J. (2021). Estimating the variability of steel slag properties and their influence in phosphorus removal ability. *Chemosphere*, *276*, 130205. https://doi.org/10.1016/j.chemosphere.2021.130205

Shi, Y., Wang, S., Xu, M., Yan, X., Huang, J., & Wang, H. (2022). Removal of neonicotinoid pesticides by adsorption on modified Tenebrio molitor frass biochar: Kinetics and mechanism. *Separation and Purification Technology*, 12.

Smit, C. E. (2014). *Water quality standards for imidacloprid*. 94.

Socías-Viciana, M., González-Pradas, E., Saifi, M., Ureña-Amate, M., Flores-Céspedes, F., & Fernández-Pérez, M. (2003). The potential removal of imidacloprid from water by heat-treated kerolites: Removal of imidacloprid from water using kerolites. *Pest Management Science*, *59*(10), 1162–1168. https://doi.org/10.1002/ps.745

Starner, K., & Goh, K. S. (2012). Detections of the Neonicotinoid Insecticide Imidacloprid in Surface Waters of Three Agricultural Regions of California, USA, 2010–2011. *Bulletin of Environmental Contamination and Toxicology*, *88*(3), 316–321. https://doi.org/10.1007/s00128-011-0515-5

Struger, J., Grabuski, J., Cagampan, S., Sverko, E., McGoldrick, D., & Marvin, C. H. (2017). Factors influencing the occurrence and distribution of neonicotinoid insecticides in surface

waters of southern Ontario, Canada. *Chemosphere*, *169*, 516–523. https://doi.org/10.1016/j.chemosphere.2016.11.036

Suliman, W., Harsh, J. B., Fortuna, A.-M., Garcia-Pérez, M., & Abu-Lail, N. I. (2017). Quantitative Effects of Biochar Oxidation and Pyrolysis Temperature on the Transport of Pathogenic and Nonpathogenic *Escherichia coli* in Biochar-Amended Sand Columns. *Environmental Science & Technology*, *51*(9), 5071–5081. https://doi.org/10.1021/acs.est.6b04535

Tan, G., Sun, W., Xu, Y., Wang, H., & Xu, N. (2016). Sorption of mercury (II) and atrazine by biochar, modified biochars and biochar based activated carbon in aqueous solution. *Bioresource Technology*, *211*, 727–735. https://doi.org/10.1016/j.biortech.2016.03.147

Tang, Z., & Nairn, R. W. (2021). Recovered mine drainage passive treatment residuals address legacy sediment pollution: A field mesocosm study at Grand Lake o' the Cherokees, Oklahoma. *Ecological Engineering*, *170*, 106358. https://doi.org/10.1016/j.ecoleng.2021.106358

Tokarčíková, M., Motyka, O., Peikertová, P., Gabor, R., & Seidlerová, J. (2021). Magnetically Modified Biosorbent for Rapid Beryllium Elimination from the Aqueous Environment. *Materials*, *14*(21), 6610. https://doi.org/10.3390/ma14216610

Trace Metals ICP Calibration/Quality Control Standard Certificate. (n.d.). Inorganic Ventures. https://www.inorganicventures.com/icp-cal-std-trace-metals-125ml

Trenouth, W. R., & Gharabaghi, B. (2015). Soil amendments for heavy metals removal from stormwater runoff discharging to environmentally sensitive areas. *Journal of Hydrology*, *529*, 1478–1487. https://doi.org/10.1016/j.jhydrol.2015.08.034

Tsitouridou, R., & Georgiou, J. (1988). A contribution to the study of phosphate sorption by three Greek fly ashes. *Toxicological & Environmental Chemistry*, *17*(2), 129–138. https://doi.org/10.1080/02772248809357285

Ugurlu, A., & Salam, B. (1998). Phosphorus removal by fly ash. *Environment International*, *24*(8), 911–918. https://doi.org/10.1016/S0160-4120(98)00079-8

Ulén, B., Bechmann, M., Fölster, J., Jarvie, H. P., & Tunney, H. (2007). Agriculture as a phosphorus source for eutrophication in the north-west European countries, Norway, Sweden, United Kingdom and Ireland: A review. *Soil Use and Management*, *23*(s1), 5–15. https://doi.org/10.1111/j.1475-2743.2007.00115.x

US EPA, O. (2013, February 1). *Nutrient Pollution Policy and Data* [Collections and Lists]. https://www.epa.gov/nutrient-policy-data

US EPA, O. (2015a, April 13). *Aquatic Life Benchmarks and Ecological Risk Assessments for Registered Pesticides* [Data and Tools]. https://www.epa.gov/pesticide-science-and-assessing-pesticide-risks/aquatic-life-benchmarks-and-ecological-risk

US EPA, O. (2015b, September 3). *National Recommended Water Quality Criteria—Aquatic Life Criteria Table* [Data and Tools]. https://www.epa.gov/wqc/national-recommended-water-quality-criteria-aquatic-life-criteria-table

US EPA, O. (2015c, November 4). *Metals* [Data and Tools]. https://www.epa.gov/caddis-vol2/metals

US EPA, O. (2015d, November 4). *Nutrients* [Data and Tools]. https://www.epa.gov/caddis-vol2/nutrients

Van Dijk, T. C., Van Staalduinen, M. A., & Van der Sluijs, J. P. (2013). Macro-Invertebrate Decline in Surface Water Polluted with Imidacloprid. *PLoS ONE*, *8*(5), e62374. https://doi.org/10.1371/journal.pone.0062374

Vijayaraghavan, J., Jude, A. B., & Thivya, J. (2017). Effect of copper slag, iron slag and recycled concrete aggregate on the mechanical properties of concrete. *Resources Policy*, *53*, 219–225. https://doi.org/10.1016/j.resourpol.2017.06.012

Vogel, J. (2022, February). *Bioretention* [Lecture].

von Wandruszka, R. (2006). Phosphorus retention in calcareous soils and the effect of organic matter on its mobility. *Geochemical Transactions*, *7*(1), 6. https://doi.org/10.1186/1467-4866-7-6

Voorhees, J. P., Anderson, B. S., Phillips, B. M., & Tjeerdema, R. S. (2017). Carbon Treatment as a Method to Remove Imidacloprid from Agriculture Runoff. *Bulletin of Environmental Contamination and Toxicology*, *99*(2), 200–202. https://doi.org/10.1007/s00128-017-2074-x

Vordonis, L., Koutsoukos, P. G., Tzannini, A., & Lycourghiotis, A. (1988). Uptake of inorganic orthophosphate by greek fly ashes characterized using various techniques. *Colloids and Surfaces*, *34*(1), 55–68. https://doi.org/10.1016/0166-6622(88)80081-7

Wang, S., Terdkiatburana, T., & Tadé, M. O. (2008). Single and co-adsorption of heavy metals and humic acid on fly ash. *Separation and Purification Technology*, *58*(3), 353–358. https://doi.org/10.1016/j.seppur.2007.05.009

Wang, X., & Cai, Q.-S. (2006). Steel Slag as an Iron Fertilizer for Corn Growth and Soil Improvement in a Pot Experiment. *Pedosphere*, *16*(4), 519–524. https://doi.org/10.1016/S1002-0160(06)60083-0

Water Quality Standards | Oklahoma Water Resources Board. (n.d.). Retrieved November 3, 2021, from https://www.owrb.ok.gov/quality/standards/standards.php

Wickham, H., François, R., Henry, L., & Müller, K. (2022). *dplyr: A Grammar of Data Manipulation* (1.0.10). https://CRAN.R-project.org/package=dplyr

Wu, Q., You, R., Clark, M., & Yu, Y. (2014). Pb(II) removal from aqueous solution by a low-cost adsorbent dry desulfurization slag. *Applied Surface Science*, *314*, 129–137. https://doi.org/10.1016/j.apsusc.2014.06.154

Yadava, K. P., Tyagi, B. S., Panday, K. K., & Singh, V. N. (1987). Fly ash for the treatment of Cd(II) rich effluents. *Environmental Technology Letters*, *8*(1–12), 225–234. https://doi.org/10.1080/09593338709384482

Yamamoto, I., Yabuta, G., Tomizawa, M., Saito, T., Miyamoto, T., & Kagabu, S. (1995). Molecular Mechanism for Selective Toxicity of Nicotinoids and Neonicotinoids. *Journal of Pesticide Science*, *20*(1), 33–40. https://doi.org/10.1584/jpestics.20.33

Yang, Y., Sun, K., Han, L., Jin, J., Sun, H., Yang, Y., & Xing, B. (2018). Effect of minerals on the stability of biochar. *Chemosphere*, *204*, 310–317. https://doi.org/10.1016/j.chemosphere.2018.04.057

Yao, Y., Gao, B., Inyang, M., Zimmerman, A. R., Cao, X., Pullammanappallil, P., & Yang, L. (2011). Removal of phosphate from aqueous solution by biochar derived from anaerobically digested sugar beet tailings. *Journal of Hazardous Materials*, *190*(1–3), 501–507. https://doi.org/10.1016/j.jhazmat.2011.03.083

You, X., Jiang, H., Zhao, M., Suo, F., Zhang, C., Zheng, H., Sun, K., Zhang, G., Li, F., & Li, Y. (2020). Biochar reduced Chinese chive (Allium tuberosum) uptake and dissipation of

thiamethoxam in an agricultural soil. *Journal of Hazardous Materials*, *390*, 121749. https://doi.org/10.1016/j.jhazmat.2019.121749

Zhang, F.-S., & Itoh, H. (2006). Photocatalytic oxidation and removal of arsenite from water using slag-iron oxide-TiO2 adsorbent. *Chemosphere*, *65*(1), 125–131. https://doi.org/10.1016/j.chemosphere.2006.02.027

Zhang, P., Sun, H., Ren, C., Min, L., & Zhang, H. (2018). Sorption mechanisms of neonicotinoids on biochars and the impact of deashing treatments on biochar structure and neonicotinoids sorption. *Environmental Pollution*, *234*, 812–820. https://doi.org/10.1016/j.envpol.2017.12.013

Zhang, W., Brown, G. O., Storm, D. E., & Zhang, H. (2008). Fly-Ash-Amended Sand as Filter Media in Bioretention Cells to Improve Phosphorus Removal. *Water Environment Research*, *80*(6), 507–516. https://doi.org/10.2175/106143008X266823

Zhang, X., Chen, J., Jiang, J., Li, J., Tyagi, R. D., & Surampalli, R. Y. (2020). The potential utilization of slag generated from iron- and steelmaking industries: A review. *Environ Geochem Health*, *42*, 1321–1334. https://doi.org/10.1007/s10653-019-00419-y

Zhou, D., Ghosh, S., Zhang, D., Liang, N., Dong, X., Wu, M., & Pan, B. (2016). Role of Ash Content in Biochar for Copper Immobilization. *Environmental Engineering Science*, *33*(12), 962–969. https://doi.org/10.1089/ees.2016.0042

Zuo, M., Renman, G., Gustafsson, J. P., & Klysubun, W. (2018). Phosphorus removal by slag depends on its mineralogical composition: A comparative study of AOD and EAF slags. *Journal of Water Process Engineering*, *25*, 105–112. https://doi.org/10.1016/j.jwpe.2018.07.003

10 Appendix

Table 10-1 Run and media combinations

Run	*Column*	*Media Type*	*Media Size*	*Sand?*
1	A	Aggregated fly Ash	Large	N
1	B	Aggregated fly Ash	Small	N
1	C	Steel Slag	Small	N
1	I	Influent	Influent	N
2	A	Biochar	Small	N
2	B	Biochar	Large	N
2	C	Steel Slag	Large	N
2	I	Influent	Influent	N
10	A	Steel Slag	Small	Y
10	B	Biochar	Small	Y
10	C	Aggregated fly Ash	Small	Y
10	D	Control	Control	Y
10	I	Influent	Influent	N

Table 10-2 Sample collection information

Sample ID	*Run*	*Column*	*Representative Sample Point*	*Actual Sample Point*	*Pore Volume*	*Start Date/Time*	*QA Code*	*Sample Date/Time*	*Flow Rate*
1-A-010-1	1	A	10	10.0	149.23	10/6/21 6:30	1	10/6/21 10:38	6
1-A-040-1	1	A	40	40.0	149.23	10/6/21 6:30	1	10/6/21 23:04	6
1-A-090-1	1	A	90	90.0	149.23	10/6/21 6:30	1	10/7/21 19:48	6
1-A-090-2	1	A	90	90.0	149.23	10/6/21 6:30	2	10/7/21 19:48	6
1-A-160-1	1	A	160	160.0	149.23	10/6/21 6:30	1	10/9/21 0:49	6
1-A-160-2	1	A	160	160.0	149.23	10/6/21 6:30	2	10/9/21 0:49	6
1-A-270-1	1	A	270	270.0	149.23	10/6/21 6:30	1	10/10/21 22:25	6
1-A-430-1	1	A	430	430.0	149.23	10/6/21 6:30	1	10/13/21 16:44	6
1-A-670-1	1	A	670	677.9	149.23	10/6/21 6:30	1	10/17/21 23:30	6
1-B-010-1	1	B	10	10.0	131.45	10/6/21 6:30	1	10/6/21 10:09	6
1-B-040-1	1	B	40	40.0	131.45	10/6/21 6:30	1	10/6/21 21:06	6
1-B-040-2	1	B	40	40.0	131.45	10/6/21 6:30	2	10/6/21 21:06	6
1-B-090-1	1	B	90	90.1	131.45	10/6/21 6:30	1	10/7/21 15:23	6
1-B-160-1	1	B	160	160.0	131.45	10/6/21 6:30	1	10/8/21 16:55	6
1-B-270-1	1	B	270	270.0	131.45	10/6/21 6:30	1	10/10/21 9:05	6
1-B-270-2	1	B	270	270.0	131.45	10/6/21 6:30	2	10/10/21 9:05	6
1-B-430-1	1	B	430	430.0	131.45	10/6/21 6:30	1	10/12/21 19:30	6
1-B-670-1	1	B	670	670.0	131.45	10/6/21 6:30	1	10/16/21 11:08	6
1-C-010-1	1	C	10	10.0	97.97	10/6/21 6:30	1	10/6/21 9:13	6
1-C-040-1	1	C	40	40.0	97.97	10/6/21 6:30	1	10/6/21 17:23	6
1-C-040-2	1	C	40	40.0	97.97	10/6/21 6:30	2	10/6/21 17:23	6
1-C-090-1	1	C	90	90.2	97.97	10/6/21 6:30	1	10/7/21 7:03	6
1-C-090-2	1	C	90	90.2	97.97	10/6/21 6:30	2	10/7/21 7:03	6
1-C-160-1	1	C	160	160.1	97.97	10/6/21 6:30	1	10/8/21 2:04	6
1-C-270-1	1	C	270	270.0	97.97	10/6/21 6:30	1	10/9/21 7:58	6

1-C-430-1	1	C	430	430.8	97.97	10/6/21 6:30	1	10/11/21 3:45	6
1-C-430-2	1	C	430	430.8	97.97	10/6/21 6:30	2	10/11/21 3:45	6
1-C-670-1	1	C	670	669.9	97.97	10/6/21 6:30	1	10/13/21 20:49	6
1-I-000-3	1	I	0	0.0		10/6/21 6:30	3	10/6/21 6:30	6
1-I-160-3	1	I	160	23.3		10/6/21 6:30	3	10/8/21 23:09	6
1-I-670-3	1	I	670	100.2		10/6/21 6:30	3	10/17/21 20:51	6
2-A-010-1	2	A	10	8.9	164.28	11/10/21 16:00	1	11/10/21 20:05	6
2-A-040-1	2	A	40	36.3	164.28	11/10/21 16:00	1	11/11/21 8:35	6
2-A-090-1	2	A	90	92.8	164.28	11/10/21 16:00	1	11/12/21 10:22	6
2-A-090-2	2	A	90	92.8	164.28	11/10/21 16:00	2	11/12/21 10:22	6
2-A-160-1	2	A	160	156.4	164.28	11/10/21 16:00	1	11/13/21 15:22	6
2-A-270-1	2	A	270	255.4	164.28	11/10/21 16:00	1	11/15/21 12:32	6
2-A-430-1	2	A	430	412.2	164.28	11/10/21 16:00	1	11/18/21 12:05	6
2-A-430-2	2	A	430	412.2	164.28	11/10/21 16:00	2	11/18/21 12:05	6
2-A-670-1	2	A	670	668.6	164.28	11/10/21 16:00	1	11/23/21 9:05	6
2-B-010-1	2	B	10	9.0	164.03	11/10/21 16:00	1	11/10/21 20:05	6
2-B-040-1	2	B	40	36.4	164.03	11/10/21 16:00	1	11/11/21 8:35	6
2-B-090-1	2	B	90	93.0	164.03	11/10/21 16:00	1	11/12/21 10:22	6
2-B-090-2	2	B	90	93.0	164.03	11/10/21 16:00	2	11/12/21 10:22	6
2-B-160-1	2	B	160	156.6	164.03	11/10/21 16:00	1	11/13/21 15:22	6
2-B-160-2	2	B	160	156.6	164.03	11/10/21 16:00	2	11/13/21 15:22	6
2-B-270-1	2	B	270	255.8	164.03	11/10/21 16:00	1	11/15/21 12:32	6
2-B-430-1	2	B	430	412.8	164.03	11/10/21 16:00	1	11/18/21 12:05	6
2-B-670-1	2	B	670	669.6	164.03	11/10/21 16:00	1	11/23/21 9:05	6
2-C-010-1	2	C	10	10.0	111.16	11/10/21 16:00	1	11/10/21 19:05	6
2-C-040-1	2	C	40	42.1	111.16	11/10/21 16:00	1	11/11/21 5:00	6
2-C-090-1	2	C	90	83.4	111.16	11/10/21 16:00	1	11/11/21 17:45	6
2-C-160-1	2	C	160	151.4	111.16	11/10/21 16:00	1	11/12/21 14:45	6
2-C-270-1	2	C	270	285.0	111.16	11/10/21 16:00	1	11/14/21 8:01	6

2-C-270-2	2	C	270	285.0	111.16	11/10/21 16:00	2	11/14/21 8:01	6
2-C-430-1	2	C	430	453.4	111.16	11/10/21 16:00	1	11/16/21 12:00	6
2-C-670-1	2	C	670	681.8	111.16	11/10/21 16:00	1	11/19/21 10:32	6
2-C-670-2	2	C	670	681.8	111.16	11/10/21 16:00	2	11/19/21 10:32	6
2-I-000-3	2	I	0	0.5		11/10/21 16:00	3	11/10/21 17:20	6
2-I-160-3	2	I	160	27.1		11/10/21 16:00	3	11/13/21 19:20	6
2-I-670-3	2	I	670	111.1		11/10/21 16:00	3	11/23/21 12:29	6
10-A-0-1	10	A	0	0.3		6/24/22 7:05	1	6/24/22 7:58	5.4
10-A-1-1	10	A	1	1.0		6/24/22 7:05	1	6/24/22 10:10	5.4
10-A-1-2	10	A	1	1.0		6/24/22 7:05	2	6/24/22 10:10	5.4
10-A-2-1	10	A	2	2.0		6/24/22 7:05	1	6/24/22 13:15	5.4
10-A-4-1	10	A	4	4.0		6/24/22 7:05	1	6/24/22 19:25	5.4
10-A-6-1	10	A	6	7.7		6/24/22 7:05	1	6/25/22 7:00	5.4
10-A-10-1	10	A	10	10.0		6/24/22 7:05	1	6/25/22 13:56	5.4
10-A-17-1	10	A	17	16.9		6/24/22 7:05	1	6/26/22 11:13	5.4
10-A-17-2	10	A	17	16.9		6/24/22 7:05	2	6/26/22 11:13	5.4
10-A-27-1	10	A	27	27.0		6/24/22 7:05	1	6/27/22 18:25	5.4
10-B-0-1	10	B	0	0.2		6/24/22 7:05	1	6/24/22 7:58	4.6
10-B-1-1	10	B	1	1.0		6/24/22 7:05	1	6/24/22 10:42	4.6
10-B-1-2	10	B	1	1.0		6/24/22 7:05	2	6/24/22 10:42	4.6
10-B-2-1	10	B	2	2.0		6/24/22 7:05	1	6/24/22 14:19	4.6
10-B-4-1	10	B	4	3.6		6/24/22 7:05	1	6/24/22 20:00	4.6
10-B-6-1	10	B	6	6.6		6/24/22 7:05	1	6/25/22 7:00	4.6
10-B-10-1	10	B	10	10.0		6/24/22 7:05	1	6/25/22 19:18	4.6
10-B-17-1	10	B	17	15.7		6/24/22 7:05	1	6/26/22 16:00	4.6
10-B-27-1	10	B	27	27.0		6/24/22 7:05	1	6/28/22 8:54	4.6
10-B-27-2	10	B	27	27.0		6/24/22 7:05	2	6/28/22 8:54	4.6
10-C-0-1	10	C	0	0.3		6/24/22 7:05	1	6/24/22 8:08	4.5
10-C-1-1	10	C	1	1.1		6/24/22 7:05	1	6/24/22 11:09	4.5

10-C-1-2	10	C	1	1.1	6/24/22 7:05	2	6/24/22 11:09	4.5
10-C-2-1	10	C	2	2.0	6/24/22 7:05	1	6/24/22 14:29	4.5
10-C-4-1	10	C	4	3.5	6/24/22 7:05	1	6/24/22 20:00	4.5
10-C-6-1	10	C	6	6.5	6/24/22 7:05	1	6/25/22 7:10	4.5
10-C-10-1	10	C	10	10.0	6/24/22 7:05	1	6/25/22 20:07	4.5
10-C-17-1	10	C	17	22.9	6/24/22 7:05	1	6/27/22 20:00	4.5
10-C-27-1	10	C	27	27.1	6/24/22 7:05	1	6/28/22 11:35	4.5
10-C-27-2	10	C	27	27.1	6/24/22 7:05	2	6/28/22 11:35	4.5
10-D-0-1	10	D	0	0.2	6/24/22 7:05	1	6/24/22 7:35	6
10-D-1-1	10	D	1	1.0	6/24/22 7:05	1	6/24/22 9:51	6
10-D-1-2	10	D	1	1.0	6/24/22 7:05	2	6/24/22 9:51	6
10-D-2-1	10	D	2	2.0	6/24/22 7:05	1	6/24/22 12:38	6
10-D-4-1	10	D	4	4.0	6/24/22 7:05	1	6/24/22 18:11	6
10-D-6-1	10	D	6	4.8	6/24/22 7:05	1	6/24/22 20:30	6
10-D-10-1	10	D	10	10.0	6/24/22 7:05	1	6/25/22 10:51	6
10-D-17-1	10	D	17	17.6	6/24/22 7:05	1	6/26/22 8:00	6
10-D-17-2	10	D	17	17.6	6/24/22 7:05	2	6/26/22 8:00	6
10-D-27-1	10	D	27	27.0	6/24/22 7:05	1	6/27/22 10:05	6
10-D-27-2	10	D	27	27.0	6/24/22 7:05	2	6/27/22 10:05	6
10-I-0-3	10	I	0	0.9	6/24/22 7:05	3	6/24/22 10:15	4.6
10-I-1-3	10	I	1	1.0	6/24/22 7:05	3	6/24/22 10:42	4.6
10-I-2-3	10	I	2	2.0	6/24/22 7:05	3	6/24/22 14:19	4.6
10-I-4-3	10	I	4	3.6	6/24/22 7:05	3	6/24/22 20:00	4.6
10-I-6-3	10	I	6	7.3	6/24/22 7:05	3	6/25/22 9:25	4.6
10-I-10-3	10	I	10	10.0	6/24/22 7:05	3	6/25/22 19:18	4.6
10-I-17-3	10	I	17	15.7	6/24/22 7:05	3	6/26/22 16:00	4.6
10-I-27-3	10	I	27	27.0	6/24/22 7:05	3	6/28/22 8:54	4.6
10-I-999-4	10	I	999	BLANK	6/24/22 7:05	4	6/28/22 11:35	4.6

Table 10-3 pH, specific conductivity, and temperature results.

Sample ID	*Sand?*	*Flow Rate*	*pH*	*Sp. Cond (µS cm^{-1})*	*Temp (°C)*
1-A-010-1	N	6	10.4		19
1-A-040-1	N	6	10.4		22
1-A-090-1	N	6	10.25		22
1-A-090-2	N	6	10.25		22
1-A-160-1	N	6	10.2		21
1-A-160-2	N	6	10.2		21
1-A-270-1	N	6	10.1		21
1-A-430-1	N	6	10		21
1-A-670-1	N	6	9.8		21
1-B-010-1	N	6	10.4		20
1-B-040-1	N	6	10.4		21
1-B-040-2	N	6	10.4		21
1-B-090-1	N	6			22
1-B-160-1	N	6	10.1		22
1-B-270-1	N	6	10.1		22
1-B-270-2	N	6	10.1		22
1-B-430-1	N	6	9.8		22
1-B-670-1	N	6	9.8		21
1-C-010-1	N	6	10.8		20
1-C-040-1	N	6	10.8		21
1-C-040-2	N	6	10.8		21
1-C-090-1	N	6	10.7		23
1-C-090-2	N	6	10.7		23
1-C-160-1	N	6	10.7		21
1-C-270-1	N	6	10.6		22
1-C-430-1	N	6	10.6		21
1-C-430-2	N	6	10.6		21
1-C-670-1	N	6	10.5		21
1-I-000-3	N	6	7.5		21
1-I-160-3	N	6	7		22
1-I-670-3	N	6	6.7		21
2-A-010-1	N	6	7.9	58.25	20.9
2-A-040-1	N	6	7.3	51.67	20.6
2-A-090-1	N	6	7.1	52.4	20.3
2-A-090-2	N	6	7.1	52.4	20.3
2-A-160-1	N	6	6.9	51.96	19.8
2-A-270-1	N	6	7	52.85	19.9

2-A-430-1	N	6	6.7	53.46	20.7
2-A-430-2	N	6	6.7	53.46	20.7
2-A-670-1	N	6	6.7	50.2	11.7
2-B-010-1	N	6	7.2	51.8	21.1
2-B-040-1	N	6	7.7	51.83	20.6
2-B-090-1	N	6	7.5	52.28	20.3
2-B-090-2	N	6	7.5	52.28	20.3
2-B-160-1	N	6	7.6	52.33	19.8
2-B-160-2	N	6	7.6	52.33	19.8
2-B-270-1	N	6	7.3	51.88	19.8
2-B-430-1	N	6	6.7	51.78	20.6
2-B-670-1	N	6	6.6	50.61	11.5
2-C-010-1	N	6	10.2	155.8	20.3
2-C-040-1	N	6	10.2	146	21
2-C-090-1	N	6	10.2	120.1	20.5
2-C-160-1	N	6	10	108	20
2-C-270-1	N	6	9.9	105	20.1
2-C-270-2	N	6	9.9	105	20.1
2-C-430-1	N	6	9.7	93.89	20.2
2-C-670-1	N	6	9.8	90.84	6.7
2-C-670-2	N	6	9.8	90.84	6.7
2-I-000-3	N	6	7.4	79.21	21.4
2-I-160-3	N	6	7	58.39	20.6
2-I-670-3	N	6	6.6	49.96	12.2
10-A-0-1	Y	5.4	11.91	775	23.6
10-A-1-1	Y	5.4	11.15	578	22.5
10-A-1-2	Y	5.4	11.15	578	22.5
10-A-2-1	Y	5.4	11.49	468	21.9
10-A-4-1	Y	5.4	11.66	351	14.5
10-A-6-1	Y	5.4	11.42	256	12.7
10-A-10-1	Y	5.4	11.27	325	21.5
10-A-17-1	Y	5.4	11.18	308	22.3
10-A-17-2	Y	5.4	11.18	308	22.3
10-A-27-1	Y	5.4	11.2	274	22.2
10-B-0-1	Y	4.6	8.07		23
10-B-1-1	Y	4.6	8.73	731	22.1
10-B-1-2	Y	4.6	8.73	731	22.1
10-B-2-1	Y	4.6	7.58	65.4	21.9
10-B-4-1	Y	4.6	8.36	76.4	12.5
10-B-6-1	Y	4.6	7.69	93.5	14.4
10-B-10-1	Y	4.6	8.25	71.6	14.1

10-B-17-1	Y	4.6	7.5	76.2	16.2
10-B-27-1	Y	4.6	8.14	77.3	21.9
10-B-27-2	Y	4.6	8.14	77.3	21.9
10-C-0-1	Y	4.5	11.3	480	22.9
10-C-1-1	Y	4.5	11.33	435	22.1
10-C-1-2	Y	4.5	11.33	435	22.1
10-C-2-1	Y	4.5	11.27	486	21.9
10-C-4-1	Y	4.5	11.6	320	11.8
10-C-6-1	Y	4.5	9.77	256	13.8
10-C-10-1	Y	4.5	11.75	351	11.5
10-C-17-1	Y	4.5	11.2	222	15.3
10-C-27-1	Y	4.5	10.72	185	22.1
10-C-27-2	Y	4.5	10.72	185	22.1
10-D-0-1	Y	6	10.22	114	23.9
10-D-1-1	Y	6	10.34	69.6	22.4
10-D-1-2	Y	6	10.34	69.6	22.4
10-D-2-1	Y	6	9.92	90.9	22.1
10-D-4-1	Y	6	9.9	98.3	22
10-D-6-1	Y	6	7.85	166.2	15.4
10-D-10-1	Y	6	9.43	84.5	10.3
10-D-17-1	Y	6	9.46	81.3	21.7
10-D-17-2	Y	6	9.46	81.3	21.7
10-D-27-1	Y	6	9.82	80.5	22.3
10-D-27-2	Y	6	9.82	80.5	22.3
10-I-0-3	N	4.6	7.73	50.8	23.9
10-I-1-3	N	4.6	8.01	47.3	21.9
10-I-2-3	N	4.6	7.5	52.3	21.9
10-I-4-3	N	4.6	8.03	50.6	22.2
10-I-6-3	N	4.6	7.43	63	21.3
10-I-10-3	N	4.6	6.97	45	21.8
10-I-17-3	N	4.6	7.7	49.1	13.7
10-I-27-3	N	4.6	7.19	80.6	21.9
10-I-999-4	N	BLANK	7	0	20

Table 10-4 Dissolved metals sample results for Arsenic, beryllium, and calcium. All results in ug L^{-1}.

Sample ID	*Al*	*Al Ratio*	*As*	*As Ratio*	*Be*	*Be Ratio*	*Ca*	*Ca Ratio*
1-A-010-1	6360.73	83.31	13.05	0.68	5.93	0.66	18251.83	50.36
1-A-040-1	614.83	8.41	14.15	0.74	2.12	0.24	31961.22	87.72
1-A-090-1	4523.06	66.71	13.67	0.72	6.41	0.75	13871.85	37.73
1-A-090-2	4542.11	66.99	15.08	0.79	5.12	0.60	14077.61	38.29
1-A-160-1	5333.33	81.71	14.84	0.78	5.79	0.81	16248.27	44.48
1-A-160-2	5128.23	78.56	14.15	0.75	5.64	0.79	15880.78	43.47
1-A-270-1	3452.82	71.08	15.51	0.83	6.06	0.80	11814.09	31.14
1-A-430-1	2619.97	123.29	13.85	0.76	6.29	0.93	9746.07	25.01
1-A-670-1	1718.83	80.88	15.17	0.86	7.01	1.22	7333.18	18.02
1-B-010-1	7469.17	97.83	10.92	0.57	5.24	0.58	21074.90	58.15
1-B-040-1	7166.80	97.98	13.11	0.68	4.96	0.56	19307.81	52.99
1-B-040-2	7078.23	96.77	12.12	0.63	3.67	0.42	19288.28	52.94
1-B-090-1	5238.09	77.26	15.01	0.79	6.55	0.77	14845.35	40.38
1-B-160-1	4163.58	63.79	16.16	0.85	6.98	0.98	12947.47	35.44
1-B-270-1	4002.40	82.39	16.33	0.88	6.12	0.81	11791.23	31.08
1-B-270-2	3893.31	80.15	15.00	0.80	4.15	0.55	11621.32	30.64
1-B-430-1	2176.25	102.41	17.12	0.94	6.10	0.90	7815.73	20.05
1-B-670-1	1806.54	85.01	16.19	0.92	6.44	1.12	7041.77	17.30
1-C-010-1	696.74	9.13	8.96	0.46	1.69	0.19	32998.62	91.05
1-C-040-1	637.57	8.72	13.80	0.72	2.20	0.25	31699.09	87.00
1-C-040-2	632.57	8.65	12.88	0.67	1.16	0.13	32160.11	88.26
1-C-090-1	145.82	2.15	9.85	0.52	0.72	0.08	31410.31	85.44
1-C-090-2	586.34	8.65	14.51	0.76	2.37	0.28	30825.45	83.85
1-C-160-1	560.24	8.58	13.81	0.73	2.56	0.36	31025.24	84.93
1-C-270-1	470.13	9.68	16.34	0.88	3.08	0.40	27649.59	72.89
1-C-430-1	419.64	19.75	14.38	0.79	3.40	0.50	25288.04	64.88

1-C-430-2	420.67	19.80	14.86	0.82	2.00	0.30	25492.91	65.41
1-C-670-1	365.59	17.20	15.07	0.86	4.05	0.70	22441.22	55.13
1-I-000-3	73.64	1.00	19.34	1.00	9.85	1.00	367.01	1.00
1-I-160-3	65.27	1.00	18.92	1.00	7.12	1.00	365.30	1.00
1-I-670-3	BDL	1.00	17.60	1.00	5.76	1.00	407.02	1.00
2-A-010-1	BDL	0.38	15.25	0.75	7.52	0.57	780.43	1.98
2-A-040-1	BDL	0.39	16.76	0.83	9.11	0.70	652.17	1.65
2-A-090-1	52.67	0.99	16.58	0.82	10.46	0.81	542.03	1.37
2-A-090-2	51.38	0.96	15.86	0.79	10.73	0.84	531.18	1.34
2-A-160-1	BDL	1.00	15.60	0.78	6.19	0.63	546.59	1.24
2-A-270-1	57.25	1.21	21.38	1.07	10.51	0.86	684.90	1.70
2-A-430-1	BDL	1.00	19.23	0.97	9.32	0.80	585.41	1.44
2-A-430-2	43.57	2.05	19.61	0.99	9.60	0.82	589.99	1.45
2-A-670-1	BDL	1.00	19.59	1.00	7.41	0.65	496.65	1.23
2-B-010-1	BDL	0.38	16.96	0.84	9.55	0.73	660.26	1.68
2-B-040-1	52.43	0.95	17.19	0.85	10.70	0.82	661.09	1.67
2-B-090-1	54.48	1.02	17.65	0.88	11.81	0.92	504.72	1.27
2-B-090-2	61.77	1.16	16.62	0.83	11.86	0.92	500.78	1.26
2-B-160-1	44.91	2.11	15.46	0.77	9.22	0.93	495.06	1.13
2-B-160-2	65.00	3.06	16.68	0.83	11.16	1.13	484.02	1.10
2-B-270-1	BDL	0.45	19.18	0.96	10.32	0.85	495.20	1.23
2-B-430-1	49.83	2.34	19.40	0.98	11.48	0.99	524.51	1.29
2-B-670-1	BDL	1.00	19.22	0.98	8.79	0.77	483.67	1.20
2-C-010-1	170.37	3.05	11.55	0.57	5.85	0.45	13679.96	34.71
2-C-040-1	147.39	2.68	11.67	0.58	6.53	0.50	11173.10	28.28
2-C-090-1	142.60	2.68	15.60	0.77	7.33	0.57	10190.13	25.70
2-C-160-1	140.04	6.59	14.83	0.74	8.09	0.82	8969.82	20.42
2-C-270-1	136.62	2.89	18.71	0.94	9.41	0.77	8644.66	21.51
2-C-270-2	155.66	3.29	18.98	0.95	9.21	0.75	8690.21	21.62

2-C-430-1	134.48	6.33	19.61	0.99	10.28	0.88	7789.65	19.15
2-C-670-1	130.29	6.13	18.89	0.97	8.54	0.75	6836.26	16.91
2-C-670-2	135.87	6.39	18.63	0.95	9.35	0.82	6938.59	17.16
2-I-000-3	76.58	1.00	20.24	1.00	15.22	1.00	362.96	1.00
2-I-160-3	BDL	1.00	20.08	1.00	9.87	1.00	439.26	1.00
2-I-670-3	BDL	1.00	19.56	1.00	11.43	1.00	404.29	1.00
10-A-0-1	420.15	19.77	BDL	0.02	BDL	0.00	52650.07	121.11
10-A-1-1	383.26	18.03	0.84	0.05	BDL	0.00	52379.89	131.02
10-A-1-2	403.90	19.01	BDL	0.02	BDL	0.00	52271.87	130.75
10-A-2-1	345.67	16.27	0.86	0.05	BDL	0.00	36292.52	88.87
10-A-4-1	310.32	14.60	BDL	0.02	BDL	0.00	30534.25	81.56
10-A-6-1	259.74	12.22	1.75	0.10	BDL	0.00	31744.23	81.87
10-A-10-1	255.74	12.03	3.93	0.22	BDL	0.00	31067.34	67.95
10-A-17-1	242.70	11.42	8.92	0.50	BDL	0.00	28514.91	64.42
10-A-17-2	249.37	11.73	9.25	0.52	BDL	0.00	28188.07	63.68
10-A-27-1	224.79	10.58	10.73	0.61	BDL	0.00	27065.41	59.96
10-B-0-1	BDL	1.00	13.89	0.77	BDL	0.00	4579.35	10.53
10-B-1-1	BDL	1.00	15.59	0.90	BDL	0.00	4997.58	12.50
10-B-1-2	BDL	1.00	15.44	0.89	BDL	0.00	4991.59	12.49
10-B-2-1	BDL	1.00	15.41	0.86	BDL	0.00	4831.21	11.83
10-B-4-1	BDL	1.00	15.65	0.88	BDL	0.00	5058.91	13.51
10-B-6-1	126.74	5.96	16.58	0.98	BDL	0.00	5301.73	13.67
10-B-10-1	BDL	1.00	16.11	0.89	BDL	0.00	5560.84	12.16
10-B-17-1	203.71	9.59	17.18	0.97	BDL	0.00	5797.80	13.10
10-B-27-1	189.99	8.94	17.85	1.02	BDL	0.00	5965.25	13.22
10-B-27-2	195.22	9.19	16.99	0.97	BDL	0.00	5980.85	13.25
10-C-0-1	20894.29	983.20	9.44	0.53	BDL	0.00	35624.93	81.94
10-C-1-1	19259.60	906.28	11.62	0.67	BDL	0.00	27852.73	69.67
10-C-1-2	19209.51	903.92	12.20	0.70	BDL	0.00	27839.70	69.64

10-C-2-1	21846.61	1028.01	11.99	0.67	BDL	0.00	30070.25	73.63
10-C-4-1	16315.49	767.74	12.53	0.70	BDL	0.00	28550.26	76.26
10-C-6-1	13680.37	643.74	12.74	0.75	BDL	0.00	27977.93	72.16
10-C-10-1	15492.05	728.99	13.17	0.73	BDL	0.00	32132.98	70.28
10-C-17-1	6591.53	310.17	13.73	0.78	BDL	0.00	20922.46	47.27
10-C-27-1	5347.63	251.64	15.30	0.87	BDL	0.00	19485.77	43.17
10-C-27-2	5342.95	251.42	14.63	0.84	BDL	0.00	19169.72	42.47
10-D-0-1	111.63	5.25	13.58	0.76	BDL	0.00	11832.90	27.22
10-D-1-1	149.86	7.05	17.57	1.01	BDL	0.00	9704.47	24.27
10-D-1-2	160.33	7.54	17.02	0.98	BDL	0.00	9663.26	24.17
10-D-2-1	184.92	8.70	16.74	0.94	BDL	0.00	8366.51	20.49
10-D-4-1	222.06	10.45	17.19	0.97	BDL	0.00	8155.07	21.78
10-D-6-1	233.30	10.98	16.30	0.96	BDL	0.00	10224.65	26.37
10-D-10-1	218.98	10.30	15.76	0.87	BDL	0.00	7260.26	15.88
10-D-17-1	190.41	8.96	17.98	1.02	BDL	0.00	7021.45	15.86
10-D-17-2	197.08	9.27	17.04	0.96	BDL	0.00	6990.33	15.79
10-D-27-1	165.54	7.79	17.69	1.01	BDL	0.00	6755.01	14.97
10-D-27-2	168.12	7.91	16.59	0.95	BDL	0.00	6750.19	14.96
10-I-0-3	BDL	1.00	17.95	1.00	9.29	1.00	434.74	1.00
10-I-1-3	BDL	1.00	17.36	1.00	9.01	1.00	399.78	1.00
10-I-2-3	BDL	1.00	17.86	1.00	9.13	1.00	408.40	1.00
10-I-4-3	BDL	1.00	17.80	1.00	9.16	1.00	374.37	1.00
10-I-6-3	BDL	1.00	16.91	1.00	9.18	1.00	387.74	1.00
10-I-10-3	BDL	1.00	18.11	1.00	9.32	1.00	457.24	1.00
10-I-17-3	BDL	1.00	17.68	1.00	8.75	1.00	442.66	1.00
10-I-27-3	BDL	1.00	17.49	1.00	9.07	1.00	451.36	1.00
10-I-999-4	BDL	BLANK	BDL	BLANK	BDL	BLANK	50.27	BLANK

Table 10-5 Dissolved metals sample results for cobalt, copper, iron, and potassium. All results in ug L^{-1}.

Sample ID	*Co*	*Co Ratio*	*Cu*	*Cu Ratio*	*Fe*	*Fe Ratio*	*K*	*K Ratio*
1-A-010-1	BDL	0.02	BDL	1.00	4.58	0.13	1548.44	1.24
1-A-040-1	BDL	0.02	BDL	1.00	BDL	0.05	1320.79	1.06
1-A-090-1	BDL	0.02	BDL	1.00	6.17	0.19	1433.59	1.15
1-A-090-2	BDL	0.02	BDL	1.00	5.28	0.17	1446.90	1.16
1-A-160-1	BDL	0.02	BDL	1.00	5.62	0.26	1465.56	1.18
1-A-160-2	BDL	0.02	BDL	1.00	4.52	0.21	1458.29	1.18
1-A-270-1	BDL	0.02	BDL	1.00	8.37	0.37	1363.60	1.09
1-A-430-1	0.93	0.06	BDL	1.00	10.11	0.68	1324.23	1.06
1-A-670-1	2.18	0.13	BDL	1.00	18.63	3.85	1325.27	1.05
1-B-010-1	BDL	0.02	BDL	1.00	5.65	0.16	1525.48	1.22
1-B-040-1	BDL	0.02	BDL	1.00	4.11	0.12	1540.55	1.23
1-B-040-2	BDL	0.02	BDL	1.00	BDL	0.05	1510.31	1.21
1-B-090-1	BDL	0.02	BDL	1.00	8.45	0.27	1464.76	1.17
1-B-160-1	BDL	0.02	BDL	1.00	10.93	0.51	1490.82	1.20
1-B-270-1	BDL	0.02	BDL	1.00	7.34	0.32	1416.79	1.13
1-B-270-2	BDL	0.02	BDL	1.00	BDL	0.07	1372.04	1.10
1-B-430-1	1.68	0.10	BDL	1.00	15.54	1.04	1344.85	1.07
1-B-670-1	1.95	0.12	BDL	1.00	15.60	3.22	1312.16	1.04
1-C-010-1	BDL	0.02	BDL	1.00	BDL	0.05	1267.75	1.02
1-C-040-1	BDL	0.02	BDL	1.00	5.88	0.17	1285.58	1.03
1-C-040-2	BDL	0.02	BDL	1.00	BDL	0.05	1292.81	1.04
1-C-090-1	BDL	0.02	BDL	1.00	BDL	0.05	1331.50	1.07
1-C-090-2	BDL	0.02	BDL	1.00	4.23	0.13	1283.39	1.03
1-C-160-1	BDL	0.02	BDL	1.00	5.89	0.27	1300.89	1.05
1-C-270-1	BDL	0.02	BDL	1.00	7.11	0.31	1303.30	1.04
1-C-430-1	BDL	0.02	BDL	1.00	5.92	0.40	1291.16	1.03

1-C-430-2	BDL	0.02	BDL	1.00	BDL	0.11	1312.02	1.05
1-C-670-1	BDL	0.02	BDL	1.00	6.30	1.30	1290.38	1.03
1-I-000-3	15.50	1.00	BDL	1.00	41.13	1.00	1254.52	1.00
1-I-160-3	16.10	1.00	BDL	1.00	21.54	1.00	1239.39	1.00
1-I-670-3	16.72	1.00	BDL	1.00	4.84	1.00	1256.88	1.00
2-A-010-1	1.39	0.08	BDL	0.35	55.75	1.57	2415.81	1.83
2-A-040-1	2.23	0.12	BDL	0.36	57.28	1.68	2001.00	1.51
2-A-090-1	3.29	0.18	BDL	0.37	62.41	1.97	1682.06	1.26
2-A-090-2	3.46	0.19	BDL	0.37	64.16	2.03	1648.14	1.24
2-A-160-1	4.53	0.23	BDL	1.00	34.46	1.08	1631.04	1.11
2-A-270-1	8.92	0.48	6.54	0.95	54.69	2.40	1704.95	1.25
2-A-430-1	10.82	0.57	BDL	1.00	45.37	3.03	1485.10	1.07
2-A-430-2	11.05	0.58	BDL	1.00	46.25	3.09	1507.96	1.08
2-A-670-1	10.80	0.56	BDL	1.00	30.86	0.84	1431.13	1.02
2-B-010-1	5.91	0.32	BDL	0.35	54.21	1.52	2004.73	1.52
2-B-040-1	7.95	0.43	BDL	0.36	58.35	1.71	1770.58	1.34
2-B-090-1	9.95	0.54	6.02	0.75	61.74	1.95	1638.93	1.23
2-B-090-2	9.99	0.54	6.29	0.79	62.12	1.96	1611.49	1.21
2-B-160-1	9.98	0.50	BDL	1.00	46.33	1.45	1535.74	1.05
2-B-160-2	10.03	0.50	BDL	1.00	57.84	1.81	1472.86	1.01
2-B-270-1	13.42	0.72	6.22	0.91	45.70	2.00	1557.89	1.14
2-B-430-1	14.86	0.78	7.11	2.37	52.75	3.52	1533.36	1.10
2-B-670-1	14.77	0.77	BDL	1.00	32.76	0.89	1461.34	1.04
2-C-010-1	4.87	0.27	BDL	0.35	32.74	0.92	1337.37	1.01
2-C-040-1	4.59	0.25	BDL	0.36	35.66	1.05	1308.27	0.99
2-C-090-1	4.52	0.25	BDL	0.37	38.07	1.20	1254.71	0.94
2-C-160-1	4.41	0.22	BDL	1.00	42.64	1.33	1261.58	0.86
2-C-270-1	5.91	0.32	6.46	0.94	48.49	2.13	1435.99	1.05
2-C-270-2	5.25	0.28	6.06	0.89	45.52	1.99	1437.50	1.05

2-C-430-1	5.88	0.31	7.24	2.42	53.81	3.59	1472.98	1.06
2-C-670-1	4.89	0.25	6.20	2.07	49.05	1.34	1384.30	0.99
2-C-670-2	5.49	0.29	7.30	2.44	55.23	1.50	1406.94	1.00
2-I-000-3	17.12	1.00	10.18	1.00	67.59	1.00	1224.99	1.00
2-I-160-3	19.96	1.00	BDL	1.00	31.98	1.00	1465.04	1.00
2-I-670-3	19.23	1.00	BDL	1.00	36.74	1.00	1402.87	1.00
10-A-0-1	BDL	0.02	BDL	1.00	BDL	1.00	3871.57	13.31
10-A-1-1	BDL	0.02	BDL	1.00	BDL	0.38	2781.17	9.50
10-A-1-2	BDL	0.02	BDL	1.00	BDL	0.38	2751.81	9.40
10-A-2-1	BDL	0.02	BDL	1.00	BDL	1.00	1611.94	5.87
10-A-4-1	BDL	0.02	BDL	1.00	BDL	1.00	897.96	3.16
10-A-6-1	BDL	0.02	BDL	1.00	BDL	1.00	521.74	1.67
10-A-10-1	BDL	0.02	BDL	1.00	BDL	1.00	507.02	1.62
10-A-17-1	BDL	0.02	BDL	0.21	BDL	1.00	403.17	1.56
10-A-17-2	BDL	0.02	BDL	0.21	BDL	1.00	375.95	1.45
10-A-27-1	BDL	0.02	BDL	1.00	BDL	1.00	358.68	1.44
10-B-0-1	BDL	0.02	BDL	1.00	BDL	1.00	7841.25	26.95
10-B-1-1	BDL	0.02	BDL	1.00	BDL	0.38	5933.95	20.27
10-B-1-2	BDL	0.02	BDL	1.00	BDL	0.38	5971.22	20.39
10-B-2-1	BDL	0.02	BDL	1.00	BDL	1.00	4700.12	17.13
10-B-4-1	0.77	0.04	BDL	1.00	BDL	1.00	3621.26	12.76
10-B-6-1	BDL	0.02	BDL	1.00	BDL	1.00	2472.17	7.92
10-B-10-1	BDL	0.02	BDL	1.00	3.64	2.15	2014.52	6.45
10-B-17-1	BDL	0.02	BDL	0.21	BDL	1.00	1376.29	5.32
10-B-27-1	BDL	0.02	BDL	1.00	BDL	1.00	1093.27	4.38
10-B-27-2	BDL	0.02	BDL	1.00	BDL	1.00	1091.67	4.37
10-C-0-1	BDL	0.02	BDL	1.00	3.86	2.28	10882.94	37.40
10-C-1-1	BDL	0.02	BDL	1.00	4.96	1.12	7496.92	25.60
10-C-1-2	BDL	0.02	BDL	1.00	5.15	1.17	7475.81	25.53

10-C-2-1	BDL	0.02	BDL	1.00	6.45	3.81	7540.65	27.48
10-C-4-1	BDL	0.02	BDL	1.00	BDL	1.00	4490.34	15.83
10-C-6-1	BDL	0.02	BDL	1.00	16.23	9.58	2645.81	8.47
10-C-10-1	BDL	0.02	BDL	1.00	BDL	1.00	2121.74	6.80
10-C-17-1	BDL	0.02	BDL	0.21	BDL	1.00	724.09	2.80
10-C-27-1	BDL	0.02	BDL	1.00	BDL	1.00	703.51	2.82
10-C-27-2	BDL	0.02	BDL	1.00	BDL	1.00	707.22	2.83
10-D-0-1	BDL	0.02	BDL	1.00	77.68	45.86	2647.17	9.10
10-D-1-1	BDL	0.02	BDL	1.00	BDL	0.38	1618.09	5.53
10-D-1-2	BDL	0.02	BDL	1.00	BDL	0.38	1622.92	5.54
10-D-2-1	BDL	0.02	BDL	1.00	BDL	1.00	979.02	3.57
10-D-4-1	BDL	0.02	BDL	1.00	BDL	1.00	574.95	2.03
10-D-6-1	0.86	0.05	BDL	1.00	BDL	1.00	504.45	1.62
10-D-10-1	0.71	0.04	BDL	1.00	BDL	1.00	343.12	1.10
10-D-17-1	BDL	0.02	BDL	0.21	6.54	3.86	345.09	1.33
10-D-17-2	BDL	0.02	BDL	0.21	BDL	1.00	358.32	1.39
10-D-27-1	BDL	0.02	BDL	1.00	BDL	1.00	304.58	1.22
10-D-27-2	BDL	0.02	BDL	1.00	BDL	1.00	306.59	1.23
10-I-0-3	16.33	1.00	BDL	1.00	BDL	1.00	290.96	1.00
10-I-1-3	17.22	1.00	BDL	1.00	4.42	1.00	292.81	1.00
10-I-2-3	17.12	1.00	BDL	1.00	BDL	1.00	274.45	1.00
10-I-4-3	17.58	1.00	BDL	1.00	BDL	1.00	283.74	1.00
10-I-6-3	17.99	1.00	BDL	1.00	BDL	1.00	312.22	1.00
10-I-10-3	17.53	1.00	BDL	1.00	BDL	1.00	312.24	1.00
10-I-17-3	17.97	1.00	13.99	1.00	BDL	1.00	258.50	1.00
10-I-27-3	17.59	1.00	BDL	1.00	BDL	1.00	249.85	1.00
10-I-999-4	BDL	BLANK	BDL	BLANK	BDL	BLANK	99.38	BLANK

Table 10-6 Dissolved metals sample results for magnesium, manganese, sodium, and nickel. All results in ug L^{-1} .

Sample ID	*Mg*	*Mg Ratio*	*Mn*	*Mn Ratio*	*Na*	*Na Ratio*	*Ni*	*Ni Ratio*
1-A-010-1	180.22	1.11	1.69	0.10	7326.62	1.11	BDL	0.07
1-A-040-1	160.42	0.98	0.42	0.02	7076.65	1.07	BDL	0.07
1-A-090-1	197.89	1.21	1.59	0.09	7085.91	1.07	BDL	0.07
1-A-090-2	200.29	1.22	0.53	0.03	7227.26	1.10	BDL	0.07
1-A-160-1	201.56	1.21	1.70	0.10	7234.28	1.09	BDL	0.07
1-A-160-2	206.06	1.24	1.63	0.09	7300.71	1.10	BDL	0.07
1-A-270-1	217.58	1.32	2.16	0.12	6973.85	1.05	BDL	0.07
1-A-430-1	224.42	1.35	2.76	0.16	6978.58	1.05	BDL	0.07
1-A-670-1	254.13	1.51	4.48	0.25	7038.72	1.05	2.51	0.15
1-B-010-1	238.31	1.46	1.34	0.08	7344.19	1.12	BDL	0.07
1-B-040-1	233.64	1.43	1.16	0.07	7327.98	1.11	BDL	0.07
1-B-040-2	152.12	0.93	0.18	0.01	7292.79	1.11	BDL	0.07
1-B-090-1	247.51	1.51	2.46	0.14	7220.60	1.09	BDL	0.07
1-B-160-1	261.41	1.57	2.64	0.15	7349.54	1.11	BDL	0.07
1-B-270-1	257.37	1.56	1.33	0.08	7134.91	1.08	BDL	0.07
1-B-270-2	248.13	1.50	0.48	0.03	7040.72	1.06	BDL	0.07
1-B-430-1	275.79	1.66	2.36	0.13	6985.46	1.05	BDL	0.07
1-B-670-1	286.06	1.70	3.76	0.21	6935.47	1.03	2.20	0.14
1-C-010-1	155.45	0.95	0.38	0.02	7060.73	1.07	BDL	0.07
1-C-040-1	158.22	0.97	0.64	0.04	6940.34	1.05	BDL	0.07
1-C-040-2	159.82	0.98	BDL	0.00	7019.46	1.07	BDL	0.07
1-C-090-1	158.64	0.97	0.34	0.02	7044.56	1.07	BDL	0.07
1-C-090-2	160.14	0.98	0.51	0.03	6896.12	1.05	BDL	0.07
1-C-160-1	163.92	0.98	0.67	0.04	6913.50	1.05	BDL	0.07
1-C-270-1	175.85	1.06	1.10	0.06	6878.11	1.04	BDL	0.07
1-C-430-1	180.04	1.08	1.05	0.06	6829.47	1.03	BDL	0.07

1-C-430-2	183.31	1.10	0.27	0.02	6923.62	1.04	BDL	0.07
1-C-670-1	182.62	1.09	1.13	0.06	6957.33	1.04	BDL	0.07
1-I-000-3	161.20	1.00	16.82	1.00	6583.15	1.00	16.67	1.00
1-I-160-3	166.48	1.00	17.42	1.00	6608.28	1.00	15.41	1.00
1-I-670-3	168.10	1.00	17.84	1.00	6704.78	1.00	16.24	1.00
2-A-010-1	235.55	1.31	20.97	1.14	5738.51	0.65	BDL	0.14
2-A-040-1	204.24	1.14	16.91	0.92	6289.84	0.71	BDL	0.14
2-A-090-1	192.39	1.07	15.78	0.85	6593.89	0.75	2.44	0.32
2-A-090-2	189.44	1.05	15.64	0.84	6468.53	0.73	2.95	0.39
2-A-160-1	196.74	1.03	15.85	0.81	6482.59	0.74	3.72	0.49
2-A-270-1	237.64	1.31	20.07	1.07	9298.14	1.06	BDL	0.14
2-A-430-1	217.20	1.19	18.96	1.00	8408.75	0.97	BDL	0.14
2-A-430-2	218.93	1.20	19.35	1.02	8486.43	0.98	BDL	0.14
2-A-670-1	191.16	1.05	16.75	0.88	8473.93	0.99	BDL	0.14
2-B-010-1	215.85	1.20	24.54	1.33	6102.13	0.69	5.73	0.76
2-B-040-1	199.38	1.11	21.72	1.18	6388.92	0.72	7.35	0.97
2-B-090-1	186.36	1.04	19.95	1.08	6431.69	0.73	8.52	1.13
2-B-090-2	183.13	1.02	19.62	1.06	6362.09	0.72	9.17	1.21
2-B-160-1	183.71	0.96	19.24	0.99	6420.89	0.73	9.16	1.21
2-B-160-2	178.82	0.94	18.70	0.96	6173.99	0.70	8.66	1.15
2-B-270-1	195.84	1.08	19.93	1.06	8398.45	0.96	BDL	0.14
2-B-430-1	205.75	1.13	20.16	1.06	8612.41	0.99	BDL	0.14
2-B-670-1	190.77	1.05	18.58	0.98	8606.87	1.00	BDL	0.14
2-C-010-1	466.04	2.60	4.91	0.27	6746.00	0.76	4.19	0.55
2-C-040-1	507.15	2.83	5.00	0.27	6806.67	0.77	4.47	0.59
2-C-090-1	554.65	3.09	5.13	0.28	6476.72	0.73	3.79	0.50
2-C-160-1	568.46	2.97	5.31	0.27	6494.04	0.74	3.81	0.50
2-C-270-1	610.95	3.37	5.93	0.32	8505.48	0.97	BDL	0.14
2-C-270-2	614.22	3.39	5.80	0.31	8550.60	0.98	BDL	0.14

2-C-430-1	644.28	3.53	6.57	0.35	8822.02	1.02	BDL	0.14
2-C-670-1	605.10	3.33	5.15	0.27	8370.18	0.97	BDL	0.14
2-C-670-2	614.72	3.38	5.79	0.30	8474.35	0.99	BDL	0.14
2-I-000-3	170.81	1.00	17.72	1.00	8857.80	1.00	7.58	1.00
2-I-160-3	191.19	1.00	19.52	1.00	8793.50	1.00	7.55	1.00
2-I-670-3	181.88	1.00	18.99	1.00	8588.61	1.00	7.43	1.00
10-A-0-1	19.29	0.11	BDL	0.00			BDL	0.07
10-A-1-1	28.22	0.16	0.14	0.01			BDL	0.11
10-A-1-2	29.37	0.17	0.14	0.01			BDL	0.11
10-A-2-1	43.50	0.25	0.48	0.03	6433.80	1.00	BDL	0.09
10-A-4-1	60.42	0.35	BDL	0.00	6572.79	1.02	BDL	0.10
10-A-6-1	118.89	0.69	0.46	0.03	6531.23	1.00	BDL	0.11
10-A-10-1	155.16	0.89	0.47	0.03	6734.92	1.03	BDL	0.10
10-A-17-1	241.52	1.40	0.44	0.02	6510.69	1.02	BDL	0.09
10-A-17-2	239.48	1.39	0.40	0.02	6461.15	1.01	BDL	0.09
10-A-27-1	296.69	1.74	0.50	0.03	6489.33	1.01	BDL	0.14
10-B-0-1	1215.44	6.82	4.32	0.25			BDL	0.07
10-B-1-1	1021.83	5.95	3.08	0.17			BDL	0.11
10-B-1-2	1018.33	5.93	3.21	0.18			BDL	0.11
10-B-2-1	870.58	5.02	2.46	0.14	3502.48	0.54	BDL	0.09
10-B-4-1	742.79	4.36	1.85	0.11	4153.43	0.64	BDL	0.10
10-B-6-1	595.61	3.45	1.12	0.06	4756.61	0.73	BDL	0.11
10-B-10-1	537.63	3.07	1.16	0.07	5310.61	0.81	BDL	0.10
10-B-17-1	461.64	2.68	0.67	0.04	5462.45	0.86	BDL	0.09
10-B-27-1	426.25	2.50	0.65	0.04	5973.82	0.93	BDL	0.14
10-B-27-2	425.37	2.50	0.60	0.03	5982.90	0.94	BDL	0.14
10-C-0-1	111.98	0.63	BDL	0.00			BDL	0.07
10-C-1-1	128.07	0.75	BDL	0.00	27677.90	4.24	BDL	0.11
10-C-1-2	125.86	0.73	BDL	0.00	27615.88	4.23	BDL	0.11

10-C-2-1	137.82	0.79	BDL	0.00	28541.23	4.42	BDL	0.09
10-C-4-1	164.29	0.96	0.30	0.02	18421.21	2.85	BDL	0.10
10-C-6-1	222.36	1.29	6.47	0.36	12625.70	1.93	BDL	0.11
10-C-10-1	223.99	1.28	BDL	0.00	10972.17	1.68	BDL	0.10
10-C-17-1	332.65	1.93	0.21	0.01	7402.36	1.16	BDL	0.09
10-C-27-1	365.52	2.15	0.34	0.02	7524.21	1.18	BDL	0.14
10-C-27-2	357.30	2.10	0.19	0.01	7479.15	1.17	BDL	0.14
10-D-0-1	198.98	1.12	0.50	0.03			BDL	0.07
10-D-1-1	190.56	1.11	0.15	0.01			BDL	0.11
10-D-1-2	185.38	1.08	0.83	0.05			BDL	0.11
10-D-2-1	198.04	1.14	0.36	0.02	6460.53	1.00	BDL	0.09
10-D-4-1	236.77	1.39	0.15	0.01	6491.42	1.00	BDL	0.10
10-D-6-1	319.68	1.85	2.28	0.13	6484.86	0.99	BDL	0.11
10-D-10-1	300.10	1.72	0.23	0.01	6481.41	0.99	BDL	0.10
10-D-17-1	352.88	2.05	0.26	0.01	6700.35	1.05	BDL	0.09
10-D-17-2	348.85	2.03	0.20	0.01	6692.70	1.05	BDL	0.09
10-D-27-1	334.34	1.96	0.20	0.01	6420.27	1.00	BDL	0.14
10-D-27-2	336.95	1.98	0.14	0.01	6450.34	1.01	BDL	0.14
10-I-0-3	178.24	1.00	17.21	1.00			16.08	1.00
10-I-1-3	171.85	1.00	17.71	1.00	6527.22	1.00	9.80	1.00
10-I-2-3	173.49	1.00	17.58	1.00	6462.03	1.00	11.88	1.00
10-I-4-3	170.54	1.00	17.49	1.00	6472.03	1.00	10.57	1.00
10-I-6-3	172.89	1.00	17.92	1.00	6533.06	1.00	9.72	1.00
10-I-10-3	174.93	1.00	17.80	1.00	6547.35	1.00	10.44	1.00
10-I-17-3	171.95	1.00	18.25	1.00	6373.51	1.00	11.95	1.00
10-I-27-3	170.23	1.00	17.77	1.00	6397.77	1.00	7.79	1.00
10-I-999-4	30.54	BLANK	BDL	BLANK	1447.35	BLANK	BDL	BLANK

Table 10-7 Dissolved metals sample results for lead, selenium, silica, and zinc. All results in ug L^{-1} .

Sample ID	*Pb*	*Pb Ratio*	*Se*	*Se Ratio*	*Si*	*Si Ratio*	*Zn*	*Zn Ratio*
1-A-010-1	BDL	0.19	BDL	1.00	395.87	3.07	4.12	0.18
1-A-040-1	BDL	0.20	BDL	1.00	10430.44	80.61	BDL	0.08
1-A-090-1	BDL	0.21	5.87	2.14	391.07	3.01	BDL	0.07
1-A-090-2	BDL	0.21	BDL	1.00	409.27	3.15	14.14	0.51
1-A-160-1	BDL	0.36	BDL	1.00	482.77	3.67	5.63	0.21
1-A-160-2	BDL	0.36	7.34	2.68	497.01	3.78	10.16	0.37
1-A-270-1	BDL	0.32	BDL	1.00	448.88	3.38	4.27	0.11
1-A-430-1	BDL	1.00	BDL	1.00	433.62	3.21	10.24	0.22
1-A-670-1	2.78	2.62	6.76	2.47	412.68	2.98	14.81	0.24
1-B-010-1	BDL	0.19	5.86	2.14	607.82	4.71	BDL	0.09
1-B-040-1	BDL	0.20	7.25	2.65	574.93	4.44	BDL	0.08
1-B-040-2	BDL	0.20	BDL	1.00	591.26	4.57	BDL	0.08
1-B-090-1	BDL	0.21	5.58	2.04	533.66	4.10	6.25	0.23
1-B-160-1	BDL	0.36	5.81	2.12	521.98	3.97	6.52	0.24
1-B-270-1	BDL	0.32	7.49	2.73	491.33	3.70	4.46	0.12
1-B-270-2	BDL	0.32	BDL	1.00	489.12	3.68	BDL	0.05
1-B-430-1	BDL	1.00	6.01	2.20	464.24	3.43	10.12	0.22
1-B-670-1	BDL	1.00	BDL	1.00	443.88	3.20	13.67	0.22
1-C-010-1	BDL	0.19	5.66	2.07	10922.53	84.70	BDL	0.09
1-C-040-1	BDL	0.20	6.05	2.21	10401.60	80.39	BDL	0.08
1-C-040-2	BDL	0.20	5.76	2.10	10500.78	81.15	BDL	0.08
1-C-090-1	BDL	0.21	6.28	2.29	9678.77	74.38	BDL	0.07
1-C-090-2	BDL	0.21	BDL	1.00	10010.60	76.93	BDL	0.07
1-C-160-1	BDL	0.36	BDL	1.00	10032.60	76.21	7.86	0.29
1-C-270-1	BDL	0.32	BDL	1.00	8901.27	67.03	33.86	0.90
1-C-430-1	BDL	1.00	BDL	1.00	7980.96	59.05	4.99	0.11

1-C-430-2	BDL	1.00	BDL	1.00	8011.17	59.27	BDL	0.04
1-C-670-1	BDL	1.00	BDL	1.00	7078.55	51.08	12.73	0.21
1-I-000-3	6.89	1.00	BDL	1.00	128.44	1.00	26.07	1.00
1-I-160-3	2.92	1.00	BDL	1.00	131.64	1.00	27.26	1.00
1-I-670-3	BDL	1.00	BDL	1.00	138.58	1.00	60.80	1.00
2-A-010-1	9.39	0.95	BDL	1.00	265.05	1.69	101.73	1.22
2-A-040-1	9.08	0.93	BDL	1.00	222.90	1.41	43.43	0.52
2-A-090-1	10.80	1.13	6.67	2.43	186.56	1.17	30.14	0.36
2-A-090-2	11.23	1.18	BDL	1.00	174.56	1.09	29.05	0.35
2-A-160-1	5.68	0.93	BDL	1.00	192.36	1.08	32.75	0.41
2-A-270-1	10.06	1.16	BDL	1.00	208.94	1.26	49.47	0.61
2-A-430-1	8.31	1.06	BDL	1.00	191.80	1.12	34.78	0.44
2-A-430-2	8.39	1.07	BDL	1.00	193.03	1.13	40.74	0.51
2-A-670-1	6.06	0.82	BDL	1.00	184.28	1.05	61.44	0.79
2-B-010-1	9.30	0.94	7.39	2.70	256.17	1.63	46.30	0.55
2-B-040-1	11.09	1.14	BDL	1.00	200.76	1.27	59.13	0.71
2-B-090-1	10.83	1.14	BDL	1.00	193.54	1.21	37.02	0.45
2-B-090-2	11.53	1.21	BDL	1.00	187.53	1.18	38.44	0.46
2-B-160-1	8.19	1.33	BDL	1.00	183.20	1.03	63.27	0.79
2-B-160-2	10.51	1.71	5.83	2.13	194.96	1.10	39.43	0.50
2-B-270-1	8.80	1.02	BDL	1.00	190.34	1.15	47.77	0.59
2-B-430-1	9.56	1.22	5.49	2.00	200.20	1.17	114.27	1.44
2-B-670-1	6.47	0.87	BDL	1.00	197.16	1.12	71.50	0.92
2-C-010-1	6.06	0.61	BDL	1.00	4535.09	28.93	22.67	0.27
2-C-040-1	6.98	0.71	BDL	1.00	3996.60	25.33	50.62	0.61
2-C-090-1	7.10	0.75	BDL	1.00	3757.00	23.55	22.20	0.27
2-C-160-1	7.15	1.17	6.40	2.34	3301.99	18.56	19.74	0.25
2-C-270-1	9.26	1.07	5.70	2.08	3351.92	20.21	21.05	0.26
2-C-270-2	8.44	0.98	BDL	1.00	3367.37	20.30	20.69	0.26

2-C-430-1	9.73	1.24	BDL	1.00	2949.05	17.20	27.77	0.35
2-C-670-1	8.99	1.21	BDL	1.00	2616.00	14.85	41.07	0.53
2-C-670-2	10.28	1.39	BDL	1.00	2624.31	14.90	30.05	0.39
2-I-000-3	12.28	1.00	BDL	1.00	144.34	1.00	85.57	1.00
2-I-160-3	6.14	1.00	BDL	1.00	177.87	1.00	79.61	1.00
2-I-670-3	7.40	1.00	BDL	1.00	176.16	1.00	77.83	1.00
10-A-0-1	BDL	1.00	BDL	1.00	7705.47	80.89	BDL	0.05
10-A-1-1	BDL	1.00	BDL	0.46	7834.86	75.25	8.88	0.19
10-A-1-2	BDL	1.00	BDL	0.46	8010.59	76.94	60.15	1.27
10-A-2-1	BDL	1.00	BDL	1.00	8304.29	104.39	BDL	0.04
10-A-4-1	BDL	1.00	5.90	2.16	8877.78	88.49	BDL	0.05
10-A-6-1	BDL	1.00	BDL	1.00	9161.93	71.19	24.10	0.53
10-A-10-1	BDL	1.00	BDL	0.49	9037.99	71.07	BDL	0.04
10-A-17-1	BDL	1.00	BDL	1.00	9109.06	65.33	BDL	0.05
10-A-17-2	BDL	1.00	BDL	1.00	9031.16	64.77	7.60	0.17
10-A-27-1	BDL	1.00	BDL	1.00	8844.73	57.92	BDL	0.05
10-B-0-1	BDL	1.00	BDL	1.00	6615.43	69.45	35.11	0.79
10-B-1-1	BDL	1.00	BDL	0.46	3808.44	36.58	65.56	1.39
10-B-1-2	BDL	1.00	BDL	0.46	3743.93	35.96	139.70	2.96
10-B-2-1	BDL	1.00	BDL	1.00	2590.94	32.57	BDL	0.04
10-B-4-1	BDL	1.00	BDL	1.00	1919.78	19.14	BDL	0.05
10-B-6-1	BDL	1.00	BDL	1.00	1343.89	10.44	35.16	0.78
10-B-10-1	BDL	1.00	BDL	0.49	1122.43	8.83	16.88	0.34
10-B-17-1	BDL	1.00	BDL	1.00	907.22	6.51	BDL	0.05
10-B-27-1	BDL	1.00	BDL	1.00	834.98	5.47	5.94	0.13
10-B-27-2	BDL	1.00	BDL	1.00	835.62	5.47	55.90	1.24
10-C-0-1	BDL	1.00	5.71	2.09	5110.43	53.65	50.44	1.14
10-C-1-1	BDL	1.00	6.61	1.12	2827.42	27.16	12.35	0.26
10-C-1-2	BDL	1.00	6.92	1.17	2824.51	27.13	115.35	2.44

10-C-2-1	BDL	1.00	7.56	2.76	2149.99	27.03	24.22	0.52
10-C-4-1	BDL	1.00	6.39	2.33	1692.33	16.87	BDL	0.05
10-C-6-1	BDL	1.00	BDL	1.00	1280.18	9.95	BDL	0.05
10-C-10-1	BDL	1.00	BDL	0.49	1124.04	8.84	BDL	0.04
10-C-17-1	BDL	1.00	BDL	1.00	959.65	6.88	19.75	0.45
10-C-27-1	BDL	1.00	BDL	1.00	978.57	6.41	BDL	0.05
10-C-27-2	BDL	1.00	BDL	1.00	978.19	6.41	BDL	0.05
10-D-0-1	BDL	1.00	BDL	1.00	5626.72	59.07	BDL	0.05
10-D-1-1	BDL	1.00	BDL	0.46	2815.35	27.04	BDL	0.04
10-D-1-2	BDL	1.00	BDL	0.46	2768.47	26.59	59.16	1.25
10-D-2-1	BDL	1.00	BDL	1.00	1900.59	23.89	7.11	0.15
10-D-4-1	BDL	1.00	BDL	1.00	1393.38	13.89	BDL	0.05
10-D-6-1	BDL	1.00	BDL	1.00	1293.56	10.05	51.71	1.15
10-D-10-1	BDL	1.00	BDL	0.49	937.71	7.37	45.35	0.91
10-D-17-1	BDL	1.00	BDL	1.00	744.94	5.34	BDL	0.05
10-D-17-2	BDL	1.00	BDL	1.00	742.62	5.33	13.92	0.32
10-D-27-1	BDL	1.00	BDL	1.00	715.37	4.68	13.91	0.31
10-D-27-2	BDL	1.00	BDL	1.00	721.66	4.73	96.09	2.13
10-I-0-3	BDL	1.00	BDL	1.00	95.25	1.00	44.20	1.00
10-I-1-3	BDL	1.00	5.92	1.00	104.11	1.00	47.25	1.00
10-I-2-3	BDL	1.00	BDL	1.00	79.55	1.00	47.02	1.00
10-I-4-3	BDL	1.00	BDL	1.00	100.33	1.00	43.42	1.00
10-I-6-3	BDL	1.00	BDL	1.00	128.69	1.00	45.14	1.00
10-I-10-3	BDL	1.00	5.64	1.00	127.17	1.00	49.61	1.00
10-I-17-3	BDL	1.00	BDL	1.00	139.44	1.00	43.70	1.00
10-I-27-3	BDL	1.00	BDL	1.00	152.70	1.00	45.06	1.00
10-I-999-4	BDL	BLANK	BDL	BLANK	74.21	BLANK	BDL	BLANK

Table 10-8 Phosphorus sample results. All results in mg L^{-1} .

Sample ID	*P (mg L^{-1})*	*P Ratio*
1-A-010-1	0.136	0.100
1-A-010-2	0.089	0.324
1-A-040-1	0.039	0.144
1-A-090-1	0.157	0.589
1-A-160-1	0.162	0.648
1-A-160-2	0.152	0.608
1-A-270-1	0.189	0.761
1-A-430-1	0.178	0.766
1-A-670-1	0.222	1.213
1-A-670-2	0.183	1.000
1-B-010-1	0.082	0.299
1-B-040-1	0.096	0.354
1-B-090-1	0.155	0.582
1-B-160-1	0.177	0.708
1-B-160-2	0.166	0.664
1-B-270-1	0.204	0.821
1-B-430-1	0.198	0.852
1-B-670-1	0.208	1.137
1-B-670-2	0.217	1.186
1-C-010-1	0.028	0.102
1-C-040-1	0.035	0.129
1-C-090-1	0.033	0.124
1-C-090-2	0.023	0.086
1-C-160-1	0.045	0.180
1-C-270-1	0.121	0.487
1-C-270-2	0.027	0.109
1-C-430-1	0.056	0.241
1-C-670-1	0.092	0.503
1-C-670-2	0.064	0.350
1-I-000-3	0.278	1.000
1-I-160-3	0.25	1.000
1-I-670-3	0.183	1.000
2-A-010-1	0.314	1.053
2-A-040-1	0.306	1.033
2-A-090-1	0.303	1.036
2-A-160-1	0.276	0.982

2-A-160-2	0.263	0.936
2-A-270-1	0.254	0.907
2-A-270-2	0.254	0.907
2-A-430-1	0.254	0.945
2-A-670-1	0.254	1.000
2-B-010-1	0.311	1.043
2-B-040-1	0.298	1.006
2-B-040-2	0.3	1.013
2-B-090-1	0.298	1.018
2-B-160-1	0.285	1.014
2-B-270-1	0.254	0.907
2-B-430-1	0.254	0.945
2-B-430-2	0.254	0.945
2-B-670-1	0.254	1.000
2-C-010-1	0.162	0.543
2-C-010-2	0.161	0.540
2-C-040-1	0.201	0.679
2-C-090-1	0.214	0.731
2-C-160-1	0.245	0.872
2-C-270-1	0.249	0.889
2-C-430-1	0.254	0.945
2-C-430-2	0.254	0.945
2-C-670-1	0.254	1.000
2-I-000-3	0.304	1.000
2-I-160-3	0.281	1.000
2-I-670-3	0.254	1.000
10-A-0-1	0.029	0.145
10-A-1-1	0.011	0.066
10-A-1-2	0.016	0.096
10-A-2-1	0.008	0.051
10-A-4-1	0.008	0.051
10-A-6-1	0.018	0.112
10-A-10-1	0.007	0.045
10-A-17-1	0.01	0.061
10-A-17-2	0.01	0.061
10-A-27-1	0.01	0.058
10-B-0-1	0.129	0.645
10-B-1-1	0.049	0.295
10-B-1-2	0.057	0.343
10-B-2-1	0.043	0.274
10-B-4-1	0.049	0.310

10-B-6-1	0.062	0.385
10-B-10-1	0.041	0.261
10-B-17-1	0.106	0.642
10-B-27-1	0.152	0.884
10-B-27-2	0.12	0.698
10-C-0-1	0.017	0.085
10-C-1-1	0.011	0.066
10-C-1-2	0.026	0.157
10-C-2-1	0.014	0.089
10-C-4-1	0.03	0.190
10-C-6-1	0.031	0.193
10-C-10-1	0.027	0.172
10-C-17-1	0.098	0.594
10-C-27-1	0.133	0.773
10-C-27-2	0.134	0.779
10-D-0-1	0.006	0.030
10-D-1-1	0.006	0.036
10-D-1-2	0.016	0.096
10-D-2-1	0.036	0.229
10-D-4-1	0.032	0.203
10-D-6-1	0.063	0.391
10-D-10-1	0.125	0.796
10-D-17-1	0.169	1.024
10-D-17-2	0.167	1.012
10-D-27-1	0.146	0.849
10-D-27-2	0.151	0.878
10-I-0-3	0.2	1.000
10-I-1-3	0.166	1.000
10-I-2-3	0.157	1.000
10-I-4-3	0.158	1.000
10-I-6-3	0.161	1.000
10-I-10-3	0.157	1.000
10-I-17-3	0.165	1.000
10-I-27-3	0.172	1.000
10-I-999-4	BRL	BLANK

Table 10-9 Neonicotinoid sample results. All results given in ug L^{-1}.

Sample ID	*Acetamiprid*	*Acetamiprid Ratio*	*Dinotefuran*	*Dinotefuran Ratio*	*Imidacloprid*	*Imidacloprid Ratio*
1-A-010-1	500.237	0.553	729.878	0.765	393.290	0.608
1-A-040-1	200.864	0.224	830.339	0.876	250.256	0.390
1-A-040-2	207.583	0.231	890.426	0.940	272.486	0.425
1-A-090-1	704.690	0.798	965.955	1.030	565.744	0.895
1-A-160-1	493.663	0.563	720.494	0.769	386.613	0.635
1-A-270-1	479.152	0.576	622.130	0.690	363.285	0.606
1-A-270-2	582.616	0.701	753.265	0.835	432.049	0.721
1-A-430-1	537.558	0.684	650.746	0.748	397.172	0.697
1-A-670-1	618.128	0.866	690.232	0.844	436.681	0.826
1-B-010-1	336.740	0.372	753.218	0.790	326.877	0.506
1-B-010-2	440.869	0.487	971.602	1.019	437.363	0.677
1-B-040-1	445.829	0.497	864.795	0.912	395.462	0.617
1-B-090-1	533.863	0.605	855.829	0.913	451.253	0.714
1-B-090-2	542.991	0.615	880.116	0.939	475.486	0.753
1-B-160-1	768.458	0.876	877.817	0.936	562.714	0.924
1-B-270-1	508.002	0.611	637.924	0.708	386.327	0.645
1-B-430-1	628.045	0.799	720.594	0.829	472.290	0.829
1-B-670-1	630.904	0.883	729.911	0.892	463.174	0.876
1-C-010-1	162.612	0.180	723.090	0.758	218.473	0.338
1-C-040-1	228.810	0.255	874.993	0.923	286.258	0.447
1-C-090-1	209.537	0.237	820.535	0.875	242.616	0.384
1-C-090-2	164.581	0.186	694.216	0.740	202.610	0.321
1-C-160-1	260.839	0.297	764.063	0.815	295.654	0.486
1-C-160-2	317.694	0.362	881.041	0.940	346.516	0.569

1-C-270-1	373.028	0.449	756.560	0.839	338.568	0.565
1-C-430-1	437.987	0.557	682.686	0.785	369.724	0.649
1-C-670-1	479.876	0.672	657.915	0.804	375.921	0.711
1-I-000-3	896.732	1.000	945.378	1.000	656.135	1.000
1-I-160-3	877.557	1.000	937.365	1.000	608.720	1.000
1-I-670-3	714.119	1.000	818.144	1.000	528.608	1.000
2-A-010-1	227.491	0.255	504.403	0.528	159.340	0.239
2-A-010-2	231.625	0.260	518.933	0.543	155.803	0.234
2-A-040-1	392.324	0.443	602.227	0.640	257.723	0.390
2-A-040-2	358.644	0.405	577.115	0.613	249.969	0.378
2-A-090-1	462.901	0.529	656.911	0.716	337.291	0.517
2-A-160-1	493.987	0.575	664.283	0.760	374.214	0.564
2-A-270-1	655.701	0.784	817.219	0.984	479.624	0.773
2-A-430-1	655.398	0.818	816.511	1.083	497.007	0.839
2-A-670-1	641.458	0.856	614.217	0.958	451.329	0.828
2-B-010-1	519.938	0.583	709.958	0.743	374.738	0.563
2-B-010-2	487.315	0.546	667.623	0.699	361.722	0.543
2-B-040-1	604.884	0.683	746.420	0.793	411.146	0.622
2-B-090-1	633.743	0.724	746.066	0.813	460.263	0.706
2-B-160-1	668.025	0.778	772.037	0.883	511.221	0.771
2-B-270-1	714.972	0.855	795.831	0.958	527.542	0.850
2-B-430-1	781.516	0.975	894.243	1.186	586.686	0.990
2-B-670-1	690.776	0.921	637.161	0.994	505.219	0.927
2-B-670-2	629.556	0.840	577.498	0.901	445.783	0.818
2-C-010-1	884.999	0.992	954.979	0.999	698.371	1.049
2-C-040-1	812.822	0.918	858.365	0.912	634.049	0.960
2-C-040-2	812.532	0.917	863.792	0.918	604.773	0.916
2-C-090-1	851.355	0.973	861.606	0.939	626.768	0.962
2-C-090-2	843.605	0.964	921.376	1.005	643.232	0.987

2-C-160-1	816.636	0.951	833.688	0.954	617.992	0.932
2-C-270-1	839.684	1.005	860.179	1.035	612.026	0.986
2-C-430-1	888.060	1.108	931.954	1.236	685.713	1.157
2-C-670-1	929.567	1.240	984.732	1.536	707.740	1.299
2-I-000-3	895.252	1.000	967.659	1.000	649.424	1.000
2-I-160-3	858.521	1.000	874.155	1.000	663.364	1.000
2-I-670-3	749.630	1.000	641.066	1.000	544.919	1.000
10-A-0-1	4.568	0.655	5.210	0.924	4.402	0.785
10-A-1-1	4.635	0.746	4.805	0.946	4.589	0.805
10-A-1-2	4.623	0.744	5.000	0.985	4.727	0.829
10-A-2-1	4.807	0.852	5.303	1.053	5.182	0.921
10-A-4-1	4.375	0.729	4.772	0.952	4.699	0.808
10-A-6-1	4.551	0.651	4.860	0.860	4.870	0.767
10-A-10-1	4.943	0.856	4.888	1.013	5.345	0.947
10-A-17-1	5.005	0.801	4.882	0.973	5.499	0.880
10-A-17-2	5.282	0.845	5.080	1.013	5.749	0.920
10-A-27-1	5.024	0.764	4.643	0.903	5.617	0.839
10-B-0-1	0.006	0.072	0.115	0.089	0.006	0.089
10-B-1-1	0.009	0.081	0.296	0.098	0.006	0.088
10-B-1-2	0.009	0.081	0.319	0.098	0.006	0.088
10-B-2-1	0.017	0.089	0.391	0.099	0.011	0.089
10-B-4-1	0.034	0.083	0.617	0.100	0.021	0.086
10-B-6-1	0.083	0.072	0.885	0.089	0.054	0.079
10-B-10-1	0.144	0.087	1.084	0.225	0.095	0.089
10-B-17-1	0.297	0.080	1.272	0.254	0.215	0.080
10-B-27-1	0.487	0.076	1.578	0.307	0.358	0.075
10-B-27-2	0.518	0.076	1.504	0.293	0.375	0.075
10-C-0-1	3.645	0.523	4.897	0.869	4.221	0.753
10-C-1-1	3.981	0.641	4.706	0.927	4.794	0.841

10-C-1-2	4.006	0.645	4.859	0.957	5.087	0.893
10-C-2-1	3.885	0.689	4.740	0.941	4.678	0.832
10-C-4-1	4.090	0.682	4.938	0.985	4.578	0.787
10-C-6-1	4.540	0.650	4.961	0.878	5.012	0.789
10-C-10-1	4.589	0.795	4.645	0.963	5.225	0.926
10-C-17-1	5.068	0.811	4.839	0.965	5.674	0.908
10-C-27-1	5.391	0.819	4.974	0.968	6.013	0.898
10-C-27-2	4.567	0.694	4.591	0.893	5.108	0.763
10-D-0-1	5.342	0.766	6.066	1.076	5.100	0.910
10-D-1-1	5.212	0.839	5.357	1.055	5.162	0.906
10-D-1-2	4.360	0.702	5.047	0.994	4.166	0.731
10-D-2-1	5.715	1.013	5.417	1.076	5.969	1.061
10-D-4-1	5.046	0.841	5.014	1.000	5.478	0.942
10-D-6-1	4.863	0.696	4.928	0.873	5.028	0.792
10-D-10-1	5.393	0.934	5.186	1.075	5.896	1.045
10-D-17-1	4.998	0.800	4.843	0.966	5.381	0.861
10-D-17-2	5.130	0.821	4.651	0.927	5.549	0.888
10-D-27-1	5.521	0.839	5.133	0.999	6.031	0.901
10-D-27-2	5.326	0.809	4.796	0.933	5.649	0.844
10-I-0-3	6.975	1.000	5.636	1.000	5.607	1.000
10-I-1-3	6.210	1.000	5.078	1.000	5.699	1.000
10-I-2-3	5.641	1.000	5.036	1.000	5.624	1.000
10-I-4-3	6.001	1.000	5.014	1.000	5.813	1.000
10-I-6-3	6.987	1.000	5.648	1.000	6.349	1.000
10-I-10-3	5.772	1.000	4.825	1.000	5.642	1.000
10-I-17-3	6.247	1.000	5.016	1.000	6.249	1.000
10-I-27-3	6.580	1.000	5.140	1.000	6.694	1.000
10-I-999-4	0.005	BLANK	0.003	BLANK	0.002	BLANK

Table 10-10 Coefficient of variation (%) for metals samples. A mild variation exceedance is >10% and a substantial exceedance is >20%.

Sample ID	*Al*	*As*	*Be*	*Ca*	*Co*	*Cu*	*Fe*	*K*	*Mg*	*Mn*	*Na*	*Ni*	*Pb*	*Si*	*Zn*
1-A-010															
1-A-040															
1-A-090	0.30	6.91	15.85	1.04			10.94	0.65	0.85	70.67	1.40			3.22	95.05
1-A-160	2.77	3.34	1.84	1.62			15.27	0.35	1.56	2.94	0.65			2.06	40.59
1-A-270															
1-A-670															
1-B-010															
1-B-040	0.88	5.55	21.20	0.07				1.40	29.89	102.42	0.34			1.98	159.06
1-B-090															
1-B-160															
1-B-270	1.95	6.00	27.06	1.03				2.27	2.58	65.87	0.94			0.32	151.88
1-B-670															
1-C-040	0.56	4.90	43.61	1.02				0.40	0.71		0.80			0.67	17.40
1-C-090	85.09	27.04	75.40	1.33				2.60	0.67	27.37	1.51			2.38	38.85
1-C-160															
1-C-270															
1-C-430	0.17	2.34	36.67	0.57				1.13	1.27	83.86	0.97			0.27	44.34
1-C-670															
2-A-010															
2-A-040															
2-A-090	1.75	3.15	1.82	1.43	3.70		1.95	1.44	1.09	0.63	1.36	13.40	2.74	4.70	2.61
2-A-160															
2-A-270															
2-A-430		1.38	2.10	0.55	1.49		1.37	1.08	0.56	1.45	0.65		0.64	0.45	11.16
2-B-010															

2-B-040															
2-B-090	8.88	4.21	0.32	0.56	0.29	3.13	0.44	1.19	1.23	1.17	0.77	5.26	4.40	2.23	2.66
2-B-160	25.85	5.38	13.44	1.59	0.41		15.63	2.96	1.91	1.98	2.77	3.93	17.53	4.39	32.83
2-B-430															
2-B-670															
2-C-010															
2-C-040															
2-C-090															
2-C-270	9.21	1.01	1.52	0.37	8.34	4.42	4.47	0.07	0.38	1.61	0.37		6.51	0.33	1.23
2-C-430															
2-C-670	2.97	0.96	6.42	1.05	8.16	11.54	8.38	1.15	1.12	8.22	0.87		9.47	0.22	21.92
9-A-6	0.65			0.47			52.86	0.01	2.83	12.06	0.05			1.30	9.05
9-A-17	0.34	13.26		0.14			27.02	0.04	0.02	0.13				0.25	
9-B-6	2.59	6.08		0.43			21.28	0.63	0.29	11.30	0.21			0.61	45.05
9-B-17	1.46	10.38		0.76			0.08	0.75	1.03	3.82				1.06	
10-A-1	3.71			0.15				0.75	2.83	3.66				1.57	105.05
10-A-17	1.92	2.54		0.82				4.94	0.60	6.09	0.54			0.61	
10-B-1		0.69		0.08				0.44	0.24	2.75				1.21	51.08
10-B-27	1.92	3.46		0.18				0.10	0.15	5.42	0.11			0.05	114.26
10-C-1	0.18	3.46		0.03				0.20	1.23		0.16			0.07	114.08
10-C-27	0.06	3.14		1.16				0.37	1.61	40.91	0.42			0.03	
10-D-1	4.77	2.26		0.30				0.21	1.95	97.72				1.19	
10-D-17	2.43	3.82		0.31				2.66	0.81	19.86	0.08			0.22	
10-D-27	1.09	4.51		0.05				0.46	0.55	22.88	0.33			0.62	105.65

Table 10-11 Coefficient of variation (%) for phosphorus and all three neonicotinoids. A mild variation exceedance is >10% and a substantial exceedance is >20%.

Sample ID	*P*	*Acetamiprid*	*Dinotefuran*	*Imidacloprid*
1-A-010	29.54			
1-A-040		2.33	4.94	6.01
1-A-090				
1-A-160	4.50			
1-A-270		13.78	13.48	12.23
1-A-670	13.62			
1-B-010		18.94	17.91	20.45
1-B-040				
1-B-090		1.20	1.98	3.70
1-B-160	4.54			
1-B-270				
1-B-670	2.99			
1-C-040				
1-C-090	25.25	16.99	11.79	12.71
1-C-160		13.90	10.06	11.20
1-C-270	89.82			
1-C-430				
1-C-670	25.38			
2-A-010		1.27	2.01	1.59
2-A-040		6.34	3.01	2.16
2-A-090				
2-A-160	3.41			
2-A-270	0.00			
2-A-430				
2-B-010		4.58	4.35	2.50
2-B-040	0.47			
2-B-090				
2-B-160				
2-B-430	0.00			
2-B-670		6.56	6.95	8.84
2-C-010	0.44			
2-C-040		0.03	0.45	3.34
2-C-090		0.65	4.74	1.83
2-C-270				
2-C-430	0.00			

2-C-670				
9-A-6	0.00	0.00	0.00	0.00
9-A-17	9.43	1.14	18.56	21.79
9-B-6	2.57	3.62	3.31	2.39
9-B-17	5.13	33.33	29.24	33.35
10-A-1	26.19	0.18	2.81	2.09
10-A-17	0.00	3.80	2.81	3.15
10-B-1	10.67	3.63	5.39	2.64
10-B-27	16.64	4.44	3.41	3.19
10-C-1	57.33	0.45	2.25	4.20
10-C-27	0.53	11.71	5.67	11.52
10-D-1	64.28	12.59	4.21	15.10
10-D-17	0.84	1.84	2.86	2.16
10-D-27	2.38	2.54	4.80	4.62

Table 10-12 Contaminant front experiment results. Column initially saturated with DI water then an 11,000 µS cm^{-1} NaCl solution poured with 6 in. of ponding at the top of the bioretention simulation sand and effluent SC values measured. One pore volume was ~300 mL.

Start Time	**End Time**	**Flow Rate**	**Specific Conductivity (µS cm^{-1})**	**Total Volume Passed**
1621	1626	6.6	1831	33
1630	1635	6.6	1670	66
1637	1642	6.4	1630	98
1644	1649	6.2	1630	129
1650	1655	6.2	1955	160
1657	1702	6.2	4530	191
1704	1709	6.4	8015	223
1711	1717	6.5	9890	262
1721	1726	5.8	11030	291
1729	1734	5.6	11290	319